

# Groundwater discharge and hydrogeochemistry in a nutrient-rich coastal lagoon

---

A thesis submitted in partial fulfilment of the requirements for the

Degree of Doctor of Philosophy

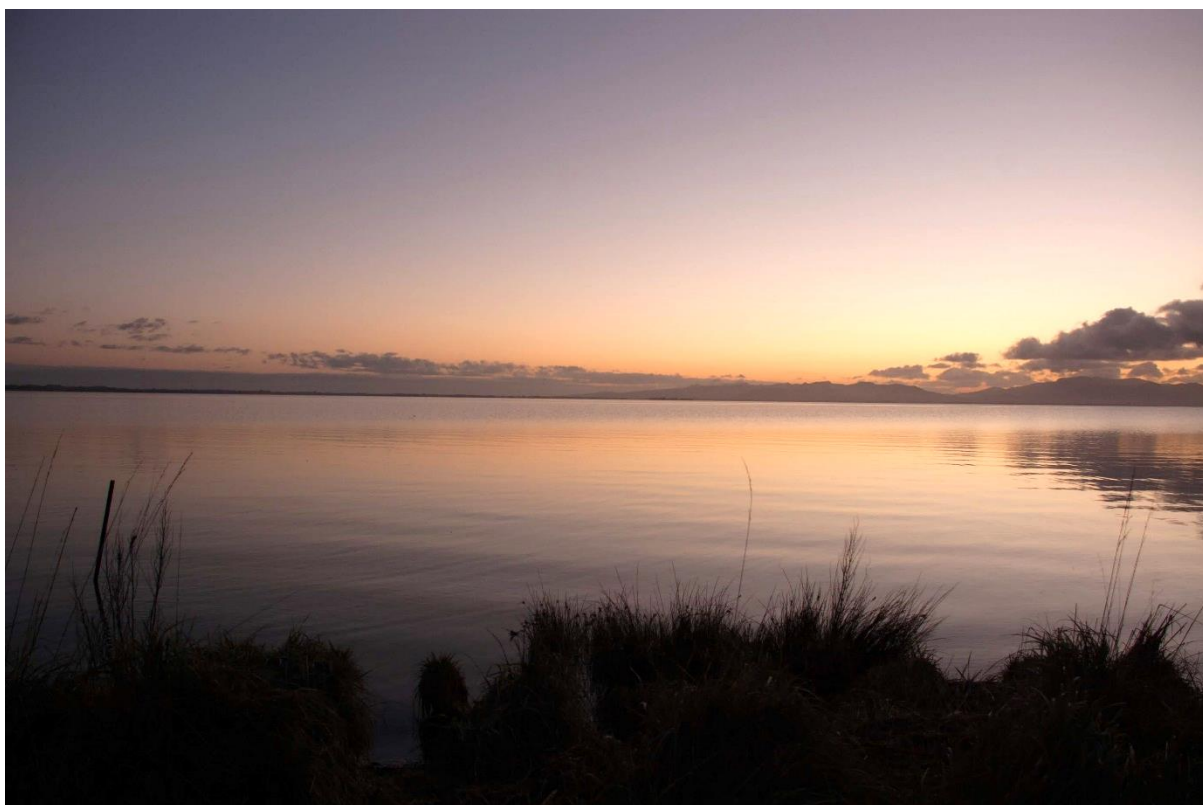
by K. M. Coluccio

Waterways Centre for Freshwater Management

School of Earth and Environment

University of Canterbury

2021



Sunrise at Te Waihora (Lake Ellesmere)

Photo credit: Katie Coluccio

I dedicate this thesis to J. Cannon.

# Table of Contents

Acknowledgements .....	vii
Abstract .....	ix
Contributions and publications .....	xi
1. Groundwater discharge in coastal lagoons: Current literature and key gaps .....	1
1.1 Groundwater discharge into coastal lagoons.....	1
1.2 Coastal lagoon characteristics .....	9
1.3 Identifying areas of groundwater inflow to coastal lake/lagoons .....	12
1.4 Quantifying groundwater discharge .....	15
1.5 Groundwater source characterisation.....	17
1.6 Literature on groundwater discharge to Waituna-type lagoons .....	18
1.7 Research rationale .....	19
1.8 Research aim .....	20
1.9 Structure of thesis.....	20
2. Mapping groundwater discharge to a coastal lagoon using combined spatial airborne thermal imaging, radon ( <sup>222</sup> Rn) and multiple physicochemical variables .....	22
2.1 Abstract .....	22
2.2 Introduction.....	22
2.3 Materials and methods .....	24
2.3.1 Site description.....	24
2.3.2 Sampling and analysis.....	26
2.3.2.1 Airborne thermal infrared imaging .....	27
2.3.2.2 Spatial <sup>222</sup> Rn and physicochemical surveys .....	28
2.3.2.3 Integrated analysis of the full dataset.....	31
2.4 Results .....	31
2.4.1 Thermal infrared imaging .....	31
2.4.2 In-situ water temperature .....	33
2.4.3 Conductivity.....	35
2.4.4 Dissolved Oxygen .....	35
2.4.5 Radon .....	36
2.5 Discussion .....	37
2.5.1 Integrating multiple lines of evidence to detect groundwater seepage .....	37
2.5.2 Method advantages and disadvantages .....	41
2.6 Conclusion .....	45
3. Groundwater discharge rates and uncertainties in a coastal lagoon using a radon mass balance .....	46
3.1 Abstract .....	46

3.2	Introduction.....	46
3.3	Material and methods.....	49
3.3.1	Site description.....	49
3.3.2	Sampling and analysis.....	51
3.4	Results.....	59
3.4.1	Environmental conditions .....	59
3.4.2	Spatial <sup>222</sup> Rn surveys.....	60
3.4.3	Shallow groundwater sampling.....	60
3.4.4	Sediment diffusion .....	61
3.4.5	Radium decay.....	61
3.4.6	Surface water sampling.....	61
3.4.7	Atmospheric evasion.....	61
3.4.8	Lagoon exchange with the sea .....	62
3.4.9	Radon/wind speed time series.....	63
3.4.10	Radon mass balance .....	64
3.5	Discussion .....	65
3.5.1	Quantifying groundwater discharge in coastal lagoons .....	65
3.5.2	Uncertainty analysis.....	68
3.5.3	Mass balance results in context of lagoon water balance.....	73
3.6	Conclusion .....	74
3.7	Appendix: Supplementary data.....	74
4.	Resolving groundwater sources to a coastal lagoon using major ions, nutrients and stable isotopes .....	80
4.1	Abstract .....	80
4.2	Introduction.....	80
4.3	Methods.....	82
4.3.1	Site Description.....	82
4.3.2	Sampling and analysis.....	84
4.4	Results.....	86
4.4.1	Field parameters .....	86
4.4.2	Major ions .....	89
4.4.3	Trace metals .....	90
4.4.4	Nutrients.....	90
4.4.5	Stable Isotopes .....	91
4.5	Discussion .....	92
4.5.1	Groundwater sources to the lagoon.....	92
4.5.2	Implications of groundwater sources for nutrient transport .....	97
4.6	Conclusion .....	102

5. Synthesis and Conclusions.....	104
5.1 Study motivation and objectives .....	104
5.2 Key study findings and contributions .....	104
5.2.1 Mapping the spatial distribution of groundwater seepage in a lagoon.....	104
5.2.2 Quantifying groundwater seepage to a lagoon.....	105
5.2.3 Identifying groundwater seepage sources and their nutrient transport implications in a lagoon .....	106
5.3 Local insights and management implications .....	107
5.4 Directions for future research .....	108
References.....	110

## Acknowledgements

I owe much of my success in this PhD endeavour to the many people that provided support along the way. I am very grateful to my supervisory team—Dr Leanne Morgan, Professor Isaac Santos, Dr Marwan Katurji and Dr Fouad Alkhaier for their assistance and mentorship over the past three years. Leanne, I appreciate that you have been generous with your time and supportive of the various directions this project went in as it evolved. Isaac, your willingness to share your knowledge and resources and be available from afar has been so valuable. Marwan, I am grateful for your willingness to step into the water world and share your expertise and knowledge on thermal imaging and atmospheric processes. Finally, Fouad, your support of the overall aims of this research from the beginning has been very much appreciated.

I would like to express my gratitude to Luke Jeffrey who was integral in helping to collect a large proportion of the data for this thesis during an epic week of field work. Luke, your willingness to take the time to come to New Zealand and share your knowledge is so appreciated. I am not sure whether you realised you were signing up for a multi-year commitment when you signed on to that week of field work. Your help over the past few years in turning this work into journal manuscripts has been so valuable.

I am very grateful to my trusty skipper Renny Bishop for his willingness to spend countless hours in blazing sun, freezing cold and howling winds bobbing around Te Waihora with me. I appreciate your sense of humour in me bringing everything but the kitchen sink out on the boat with me. I owe you big thanks for even allowing me to drill holes in your boat for my equipment. Thank you Renny for your good company and ability to navigate us out of thick fog!

I would like to acknowledge the fantastic support of staff at the Waterways Centre. I extend my considerable thanks to Suellen Knopick for her rock star ability to solve problems and for her endless moral support through this experience. I owe thanks to John Revell who was always available for technical support and accompanied me down more than one rabbit hole of inquiry. I greatly appreciate Warwick Hill and his jack-of-all trades ability to turn rough drawings on scraps of paper into functional field equipment. I also acknowledge Professor Jenny Webster-Brown and Professor James Brasington for their support of my PhD work.

I owe thanks to my various field helpers during the course of this project who helped collect samples. I owe particular thanks to Benjamin Schumacher who took time out of his own PhD to help carry out my thermal imaging survey. I also acknowledge Paul Bealing who supported me in setting up the survey and Jonathan Davidson who helped process the thermal imaging data.

I am thankful for the knowledge and resourcefulness of Hamish Carrad who has a unique ability to problem solve and create useful things in the shed. I thank Hamish for his willingness to take the time to help.

I would like to thank Graeme Horrell for sharing his wealth of knowledge about Te Waihora's hydrology.

I am grateful for my fellow students in the Waterways whānau, in particular, Rachel Teen, Rachel Skews, Irene Setiawan, Linda Robb, Justin Rogers and Amandine Bosserelle. Thank you for being great company over the past several years, providing laughs and support.

I have been very fortunate to receive scholarships and research funding from various sources. I acknowledge the University of Canterbury for awarding me a College of Science Doctoral Scholarship. I am very grateful to Environment Canterbury, particularly Carl Hanson, for supporting the project with funding that allowed for extensive data collection and lab analysis. I am also very grateful to Alex Ring, Tina Bayer and others at Environment Canterbury who graciously fielded my endless requests for data. I would like to acknowledge the New Zealand Hydrological Society for their research grant that supported fieldwork. I am thankful to Southern Cross University for providing equipment and lab analysis. Finally, I am very grateful to the Waterways Centre for Freshwater Management and the School of Earth and Environment for providing funding and resources that made this project a success.

I acknowledge the Taumutu Rūnanga, the kaitiaki of Te Waihora for their support of this project.

I am enormously grateful to my family who provided not just moral support, but in many cases, also played integral roles in pulling off this thesis. To my brothers, Sean and Steve Coluccio, thank goodness you trained as engineers! I am eternally grateful that you are willing to field my basic math questions and dust off your physics knowledge. Steve, you went above and beyond with the coding help you provided. Your patience in helping to de-bug my code and answer endless queries is so appreciated. To my grandmother, Betty Cannon, you have provided such steadfast support through this project. To my parents, Patti Niles and Gary Coluccio, your unwavering support of my endless academic endeavours is so appreciated.

Finally, I am considerably grateful to Peter Joynt, who provided tireless support through this process. I appreciate you entertaining my endless queries and opinion seeking. Your resourcefulness was hugely helpful in pulling off this research successfully. I appreciate your willingness to simply 'get things done' when needed. My long stint in postgraduate studies might not have been possible without your support, so I very much have you to thank for enabling me to achieve this PhD degree.



## Abstract

Coastal lagoons provide important wetland and aquatic habitat and food resources. These valuable cultural and recreational sites are also home to some of the world's most developed coastal communities. Yet they are often significantly influenced by anthropogenic activities and face many pressures such as habitat degradation, eutrophication, draining and land development. Ongoing research has shown that groundwater discharge plays important roles in coastal biogeochemical processes and water quality. However, groundwater input to coastal water bodies has frequently been discounted as an important component of water and nutrient budgets, largely because groundwater seepage is difficult to measure. This thesis addresses this gap by investigating groundwater processes in a large, nutrient-rich coastal lagoon in New Zealand: Te Waihora (Lake Ellesmere).

I first identified where discharge locations occur. Traditional conceptual models of groundwater seepage distribution place most seepage near the margins of lakes and lagoons. The first part of this thesis research set out to test the validity of this model in a geologically heterogeneous lagoon. I carried out an airborne thermal infrared imaging survey and spatial surveys (measuring  $^{222}\text{Rn}$ —a naturally occurring groundwater tracer and other physicochemical parameters) by boat in two seasons. The initial survey concentrated on the margins of the lagoon. I found evidence of diffuse seepage, as well as point-source seepage (i.e., springs) on mudflats and on the lagoon shore. Signs of groundwater seepage were concentrated on the northern and western sides of the lagoon. I later conducted a more comprehensive spatial survey with a high-density sampling grid to identify artesian aquifers discharging to the lagoon. However, I found no significant signs of freshwater inputs away from the lagoon shore. I did find new evidence of freshwater along the lagoon-barrier interface, which I hypothesised is either sourced from upwelling inland-sourced groundwater from underneath the lagoon or seepage from the surface aquifer on the mixed sand and gravel barrier.

Previous work based on seepage meter measurements estimated that groundwater discharge to Te Waihora was a small component of the lagoon's water budget. I built on earlier work using a method at a broader scale than seepage meters—radon mass balances. These models showed that groundwater seepage to the lagoon was 1-2 orders of magnitude greater than previous estimates. Groundwater discharge estimates to the lagoon ranged from  $5.2 \pm 5.8 \text{ m}^3/\text{s}$  to  $18.7 \pm 19.6 \text{ m}^3/\text{s}$  during summer and  $0.9 \pm 2.2 \text{ m}^3/\text{s}$  to  $8.1 \pm 10.5 \text{ m}^3/\text{s}$  during winter. Wind-driven radon degassing to the atmosphere was the most influential variable in the model. I carried out an in-depth uncertainty analysis and found that the most sensitive parameters in the model were radon degassing, as well as lagoon surface area and volume; the radon in groundwater endmember; and the average radon concentration in the lagoon surface water.

Finally, I carried out a hydrogeochemistry survey to distinguish groundwater sources to Te Waihora and shed light on their contribution to nutrient transport to the lagoon. I analysed major ions, stable

water isotopes, trace metals and nutrients in lagoon surface water, porewater (shallow nearshore groundwater), existing groundwater wells and springs. Groundwater seepage split into two groups: (1) Inland samples with low ion concentrations, dominated by  $\text{Ca}^{2+}$  and  $\text{HCO}_3^-$  ions and more negative oxygen-18 and deuterium ratios, and (2) permeable barrier samples with higher ion concentrations, dominated by  $\text{Na}^+$  and  $\text{Cl}^-$  ions and more positive oxygen-18 and deuterium ratios. The ion and stable isotope chemistry imply that inland seepage is sourced primarily from alpine river recharge and inland rainfall recharge, while barrier porewater is comprised of mainly mixing with lagoon surface water and localised rainfall recharge on the barrier. The study did not find evidence in the barrier porewater of freshwater inputs from upwelling artesian groundwater from under the lagoon. Analysis of porewater samples showed evidence of potential denitrification on the lagoon margins attenuating nitrogen inputs. In contrast, dissolved reactive phosphorus was elevated in porewater, suggesting phosphorus mobilisation in nearshore anoxic groundwater. Seepage-derived nitrogen inputs were only 3% of dissolved inorganic nitrogen river inputs, but the phosphorus groundwater load was 30% of river inputs.

While previous studies assumed groundwater discharge played a minor role in the hydrology and water quality of Te Waihora, the results of this thesis highlight that groundwater is an important component of both the water and nutrient budget at this site. This research underscores that groundwater discharge in coastal environments should not be discounted. These results also highlight the value in studying lagoon types that do not feature as prominently in the international literature, such as those in temperate climates with gravel barriers and managed openings to the sea.

## Contributions and publications

This thesis has been written with the intention that, at the time of submission, Chapters 2-4 will be published or submitted in the near future. These submissions are co-authored in recognition of inputs from colleagues and supervisors. My contributions to each are outlined in the co-authorship declarations below.

### Published peer-reviewed articles

Chapter 2: **Coluccio, K.**, Santos, I., Jeffrey, L. C., Katurji, M., Coluccio, S., & Morgan, L. K. (2020). Mapping groundwater discharge to a coastal lagoon using combined spatial airborne thermal imaging, radon ( $^{222}\text{Rn}$ ) and multiple physicochemical variables. *Hydrological Processes*, 34(24), 4592-4608. <https://doi.org/10.1002/hyp.13903>

This article has been included in this thesis with permission from the publisher.

### Accepted peer-reviewed articles

Chapter 3: **Coluccio, K.**, Santos, I. R., Jeffrey, L. C., & Morgan, L. K. (2021). Groundwater discharge rates and uncertainties in a coastal lagoon using a radon mass balance. [In press] *Journal of Hydrology*. <https://doi.org/10.1016/j.jhydrol.2021.126436>

This article has been included in this thesis with permission from the publisher.

### Manuscripts submitted for peer review

Chapter 4: **Coluccio, K.**, Morgan, L. K., Santos, I. R. (2021). Resolving groundwater sources to a coastal lagoon using major ions, nutrients and stable isotopes. *Manuscript submitted to Hydrology and Earth System Sciences*.

Deputy Vice-Chancellor's Office  
Postgraduate Research Office

### Co-Authorship Form

This form is to accompany the submission of any thesis that contains research reported in co-authored work that has been published, accepted for publication, or submitted for publication. A copy of this form should be included for each co-authored work that is included in the thesis. Completed forms should be included at the front (after the thesis abstract) of each copy of the thesis submitted for examination and library deposit.

Please indicate the chapter/section/pages of this thesis that are extracted from co-authored work and provide details of the publication or submission from the extract comes:

***Chapter 2: Mapping groundwater discharge to a coastal lagoon using combined spatial airborne thermal imaging, radon ( $^{222}\text{Rn}$ ) and multiple physicochemical variables***  
***PUBLISHED IN HYDROLOGICAL PROCESSES***

Please detail the nature and extent (%) of contribution by the candidate:

*My contribution was 80%. In collaboration with co-authors, I designed the experiment, conducted field work and data analysis, and wrote the manuscript.*

### Certification by Co-authors:

If there is more than one co-author then a single co-author can sign on behalf of all

The undersigned certifies that:

- The above statement correctly reflects the nature and extent of the Doctoral candidate's contribution to this co-authored work
- In cases where the candidate was the lead author of the co-authored work he or she wrote the text

Name: *Leanne Morgan* Signature:

Date: 6/5/2021

Deputy Vice-Chancellor's Office  
Postgraduate Research Office

### Co-Authorship Form

This form is to accompany the submission of any thesis that contains research reported in co-authored work that has been published, accepted for publication, or submitted for publication. A copy of this form should be included for each co-authored work that is included in the thesis. Completed forms should be included at the front (after the thesis abstract) of each copy of the thesis submitted for examination and library deposit.

Please indicate the chapter/section/pages of this thesis that are extracted from co-authored work and provide details of the publication or submission from the extract comes:

***Chapter 3: Groundwater discharge rates and uncertainties in a coastal lagoon using a radon mass balance.***

***ACCEPTED FOR PUBLICATION IN JOURNAL OF HYDROLOGY***

Please detail the nature and extent (%) of contribution by the candidate:

*My contribution was 90%. In collaboration with co-authors, I designed the experiment, conducted field work and data analysis, and wrote the manuscript.*

#### Certification by Co-authors:

If there is more than one co-author then a single co-author can sign on behalf of all

The undersigned certifies that:

- The above statement correctly reflects the nature and extent of the Doctoral candidate's contribution to this co-authored work
- In cases where the candidate was the lead author of the co-authored work he or she wrote the text

Name: *Leanne Morgan* Signature:

Date: 6/5/2021

Deputy Vice-Chancellor's Office  
Postgraduate Research Office

### Co-Authorship Form

This form is to accompany the submission of any thesis that contains research reported in co-authored work that has been published, accepted for publication, or submitted for publication. A copy of this form should be included for each co-authored work that is included in the thesis. Completed forms should be included at the front (after the thesis abstract) of each copy of the thesis submitted for examination and library deposit.

Please indicate the chapter/section/pages of this thesis that are extracted from co-authored work and provide details of the publication or submission from the extract comes:

***Chapter 4: Resolving groundwater sources to a coastal lagoon using major ions, nutrients and stable isotopes.***

***SUBMITTED TO HYDROLOGY AND EARTH SYSTEM SCIENCES***

Please detail the nature and extent (%) of contribution by the candidate:

*My contribution was 90%. In collaboration with co-authors, I designed the experiment, conducted field work and data analysis, and wrote the manuscript.*

#### Certification by Co-authors:

If there is more than one co-author then a single co-author can sign on behalf of all

The undersigned certifies that:

- The above statement correctly reflects the nature and extent of the Doctoral candidate's contribution to this co-authored work
- In cases where the candidate was the lead author of the co-authored work he or she wrote the text

Name: Leanne Morgan Signature:



Date: 6/5/2021

# **1. Groundwater discharge in coastal lagoons: Current literature and key gaps**

This chapter introduces the research presented in this thesis, which examines groundwater discharge to coastal lagoons—an important, but often disregarded component of coastal lagoon water budgets. This chapter explains why understanding groundwater discharge to coastal lagoons is relevant and discusses prior studies examining this phenomenon. The thesis research examines these processes at a coastal lagoon located in Canterbury, New Zealand: Te Waihora (Lake Ellesmere), which is considered a “coastal lake/Waituna-type lagoon”. Following the literature review, the research overview is set out, including the rationale for the study and the research questions this thesis addresses. This chapter concludes with an outline of the thesis chapter organisation.

## **1.1 Groundwater discharge into coastal lagoons**

Coastal lagoons are found on 13% of coastlines throughout the world (Barnes, 1980), and they serve many key ecological, economic, cultural and recreational purposes. They are shallow water bodies that are separated from the ocean by alongshore bars, spits and barrier-island chains (Barnes, 1980). The connectivity with the ocean ranges from “choked” lagoons featuring narrow entrance channels, long water residency times and little tidal fluctuation, to “leaky” lagoons, which have several inlets open to the ocean, strong tidal influence and salinity similar to the ocean (Kjerfve, 1986). They provide important ecosystem services such as contaminant and sediment attenuation, flood protection, aquatic and wetland habitat, food sources, and amenity values (Schallenberg et al., 2013). These lagoons are often located in places that have been significantly influenced by anthropogenic activities, and as a result, worldwide they face many pressures, such as habitat degradation, eutrophication, draining and land development (Beer & Joyce, 2013; Schallenberg et al., 2013). Coastal lagoons are the receiving environments for all up-stream activities in their catchments, so they often have high concentrations of nutrients, heavy metals or other contaminants from land-use practices.

To effectively manage coastal lagoons, it is important to understand their water budgets (i.e., inflows and outflows of water) and how these processes affect the coastal lagoon environment. This thesis explores a poorly understood component of lagoon hydrology—direct groundwater discharge via seepage through the lagoon bed. The influence of groundwater in coastal lagoons has often been overlooked (Menció, Casamitjana, Mas-Pla, Coll, Compte, et al., 2017), but it has been increasingly recognised that groundwater discharge into coastal environments is important to understand because of its potential to be a source of natural and human-derived biogeochemical species (Andrisoa et al., 2019; Santos, Niencheski, et al., 2008). Groundwater has also been found to sustain baseflows to some coastal lagoons during dry seasons (Sadat-Noori et al., 2016).

There are several types of coastal lagoons, and this includes coastal lake-type lagoons (such as the case study site selected for this thesis). Given the overlap in some characteristics of lakes and lagoons, it is relevant to discuss the literature on groundwater inflow to lakes (often referred to as lacustrine groundwater discharge or LGD), because the theories and methods developed in these studies are in many ways applicable to coastal lake-type lagoons. As coastal lagoons occur at the interface between land and the ocean, the field of groundwater research in these environments also intersects with research on submarine groundwater discharge (SGD).

Groundwater discharge into coastal lagoons is an important component of their water and nutrient budgets, however it has long been a “disregarded” component in research (Lewandowski et al., 2015; Rosenberry et al., 2015). This may be partly attributable to research on groundwater-surface water interactions in lakes and coastal lagoons lagging behind studies focused on rivers and streams (Meinikmann et al., 2013). It is typically even more difficult to estimate groundwater seepage in large water bodies, and thus this component is often omitted from water balance calculations (Harvey et al., 2000). Rosenberry et al. (2015) provide several possible explanations for why groundwater is often excluded from water budgets:

- Groundwater discharge is often invisible, except for springs;
- Measured seepage rates are often very small; however as they may occur over large areas, the total input might be significant;
- The distribution of groundwater seepage can change over space and time, which makes it difficult to measure;
- The groundwater-surface water interface can be difficult to access; and
- Although there have been improvements in recent years in techniques for measuring groundwater-surface water interactions, there are still significant challenges. In some systems it is particularly difficult, which in some cases leads to the ‘hope’ that GW is a small component of the water budget.

Traditionally, groundwater and surface water have been managed as separate resources, but in recent decades, the interconnection between the two has been increasingly recognised in research and management (Conant et al., 2019; Winter et al., 1998; Woessner, 2000). The number of studies examining interactions between groundwater and various types of surface water bodies has increased considerably in recent years. Recent reviews include Larned et al. (2015) and Coluccio and Morgan (2019) on rivers; Taniguchi et al. (2019) on SGD; and Lewandowski et al. (2020) on surface water generally. However, as Rosenberry et al. (2015) highlight in their comprehensive review of studies



examining groundwater exchange in lakes, there has been less research on lakes compared to other water bodies.

There appears to be an even greater gap in studies on coastal lakes and lagoons. Of the approximately 100 studies of groundwater seepage in lakes cited by Rosenberry et al. (2015), none appear to have been of coastal lake-type lagoons. Nevertheless, there has been a recent increase in studies examining groundwater processes in coastal lagoons and the effects they have on various aspects of lagoon environments, such as nutrient transport and cycling, water balances, and support of lagoon ecosystems, particularly in the SGD literature. As Lewandowski et al. (2015) note, there has been a considerable increase in the number of SGD studies in the past ~15 years compared to LGD studies. However, the research on groundwater in coastal lagoon environments is still limited, and key gaps remain, such as effective methods for characterising, estimating and sampling groundwater seepage on broad and point scales; studies examining groundwater exchange in large ( $>100 \text{ km}^2$ ) lagoons; and research examining lagoons in a variety of climates and geomorphological settings.

Table 1.1 compiles a list of key studies examining groundwater seepage in coastal lagoons. The majority of these studies were recently published (post-2005), which highlights that this is an emerging area of research. Table 1.1 notes some of the main characteristics of the studies including location, type and size of the lagoon(s) studied, purpose of the study and methods used. The studies in Table 1.1 have been listed in ascending order by lagoon size to highlight that the majority of lagoons studied have been smaller than  $100 \text{ km}^2$ . At many sites, it may be more difficult to measure groundwater exchange in large lagoons because of issues of method scale, so studies demonstrating large-scale applications of techniques are needed. Also, the location of these studies highlights that most studies have been carried out in sub/tropical or Mediterranean climates, with few studies in temperate climates. Climate can significantly influence how lagoons function (e.g., seasonal precipitation patterns and evapotranspiration rates), so it is important that we understand how groundwater exchange affects coastal lagoons in a range of climates (Duque et al., 2018). It is also apparent from Table 1.1 that most of these studies have been conducted in the Northern Hemisphere. Another aspect that may not be clear in Table 1.1, but is important, is that the majority of the lagoons studied are on sandy coastlines and enclosed by sand barriers. Thus, there is an apparent lack of studies of lagoons on mixed sand and gravel coastlines, and these differences in sediment types can correspond with significant differences in lagoon environments, such as lagoon bed and barrier permeability, coastline wave energy, and sediment deposition and erosional processes (Austin et al., 2013; Hart, 2007; Nielsen et al., 2007).

Table 1.1. Studies investigating groundwater discharge in coastal lagoons: Key characteristics and study motivations

Author(s) & Year	Study Category <sup>a</sup>	Study Site(s)	Kjerfve (1986) Classification <sup>b</sup>	Lagoon Size	Focus of Study	Method Keywords
Sadat-Noori et al. (2016)	QUANT	Welsby & Mermaid lagoons, Australia	Choked	0.02-0.09 km <sup>2</sup>	Quantifying groundwater inputs into lagoons	Radon
Ganguli et al. (2012)	QUANT MISC	Malibu Lagoon, California, U.S.	Leaky <sup>b</sup>	0.5 km <sup>2</sup>	Quantifying mercury transport into a coastal lagoon via groundwater	Hydrochemistry Radon
Maher et al. (2019)	QUANT NUT MISC	Avoca Lagoon, Australia	Choked	0.6 km <sup>2</sup>	Examining hydrological and biological drivers of nutrient and CO <sub>2</sub> dynamics in a lagoon	Radon CO <sub>2</sub> Nutrients
Volpi (2014)	QUANT NUT	Pescadero Lagoon, California, U.S.	Choked <sup>b</sup>	1.3 km <sup>2</sup>	Quantifying groundwater discharge and associated nutrient inputs into a lagoon	Electrical resistivity Radon Temperature Hydrochemistry
Chikita et al. (2012)	QUANT	Oikamanai Lagoon, Japan	Choked	1.55 km <sup>2</sup>	Quantifying groundwater outflow from a lagoon	Water budget
Chikita et al. (2015)	QUANT MISC	Oikamanai Lagoon, Japan	Choked	1.55 km <sup>2</sup>	Calculating water and heat budgets in a lagoon	Water & heat budgets
Tait et al. (2013)	SPAT/TEMP QUANT	Muri Lagoon, Cook Islands	Leaky	1.75 km <sup>2</sup>	Quantifying groundwater discharge to a lagoon	Radon Salinity Electrical resistivity
Manzoni et al. (2020)	QUANT	Gialova Lagoon, Greece	Choked	2.25 km <sup>2</sup>	Calculating a water balance for a lagoon	Water & salt budgets
Sánchez-Martos et al. (2014)	MISC	Punta Entinas; Salinas de Cerrillos lagoons, Spain	Unclear	~2-3 km <sup>2</sup>	Examining groundwater-wetland interaction in a lagoon	Hydrochemistry
Rodellas et al. (2018)	QUANT NUT	La Palme Lagoon, France	Choked	5 km <sup>2</sup>	Examining nutrient dynamics in a groundwater-fed lagoon	Nutrients Radon
Rodellas et al. (2020)	MISC	La Palme Lagoon, France	Choked	5 km <sup>2</sup>	Investigating temporal variations in porewater fluxes	Temperature Salinity

Medina-Gómez & Herrera-Silveira (2006)	NUT	Dzilam Lagoon, Mexico	Choked	9.4 km <sup>2</sup>	Examining nutrient dynamics in a groundwater-fed lagoon	Hydrochemistry Nutrients
Bernard et al. (2014)	NUT	Little Lagoon, Alabama, U.S.	Choked	~12.5 km <sup>2</sup>	Examining nutrient fluxes in a groundwater-influenced coastal lagoon	Nutrients
Liefer et al. (2014)	NUT	Little Lagoon, Alabama, U.S.	Choked	~12.5 km <sup>2</sup>	Examining nutrient dynamics in a groundwater-fed lagoon	Radon Hydrochemistry Nutrients
Su et al. (2014)	QUANT NUT MISC	Little Lagoon, Alabama, U.S.	Choked	~12.5 km <sup>2</sup>	Assessing impacts of groundwater discharge on algal blooms	Radon Radium Nutrients Electrical resistivity
Knapp et al. (2020)	NUT	Saipan lagoon system, Mariana Islands	Leaky	13 km <sup>2</sup>	Impact of groundwater discharge on nitrogen transport	Radon Radium Nutrients
Mencio et al. (2017)	QUANT	3 lagoons in La Pletera salt marshes, Spain	Choked	Max surface area between 2.4-17.2 km <sup>2</sup>	Improving understanding of role of groundwater in lagoons	Hydrochemistry Stable water isotopes Numeric modelling
Herrera-Silveira et al. (2002)	NUT	Celestun, Chelem, Dzilam lagoons, Mexico	Choked <sup>b</sup>	10-20 km <sup>2</sup>	Examining nutrient dynamics in a groundwater-fed lagoon	Nutrients
Herrera-Silveira (1996)	NUT	Celestun Lagoon, Mexico	Leaky <sup>b</sup>	~20 km <sup>2</sup>	Examining nutrient dynamics in a groundwater-fed lagoon	Nutrients
Herrera-Silveira (1998)	NUT	Celestun Lagoon, Mexico	Leaky <sup>b</sup>	~20 km <sup>2</sup>	Examining nutrient-phytoplankton relationships in a groundwater-influenced lagoon	Nutrients
Young et al. (2008)	SPAT/TEMP MISC	Celestun Lagoon, Mexico	Leaky <sup>b</sup>	~20 km <sup>2</sup>	Characterising groundwater discharge source	Radium Hydrochemistry
Johannes & Hearn (1985)	NUT MISC	Marmion Lagoon, Perth	Leaky <sup>b</sup>	25 km <sup>2</sup>	Examining effect of groundwater discharge on nutrients and salinity regimes	Nutrients Salinity
Ji et al. (2013)	QUANT NUT	Laoye Lagoon, China	Choked	26 km <sup>2</sup>	Quantifying groundwater discharge and associated nutrient inputs into a lagoon	Radium Nutrients Hydrochemistry
David et al. (2019)	NUT	Or Lagoon, France	Choked or Restricted <sup>b</sup>	29.6 km <sup>2</sup>	Examining nutrient dynamics in a groundwater-fed lagoon	CO <sub>2</sub>

Wang et al. (2016)	QUANT NUT	Laoye Lagoon, Xiaohai Lagoon, China	Choked	Laoye (26 km <sup>2</sup> ); Xiaohai (44 km <sup>2</sup> )	Quantifying groundwater discharge and associated nutrient inputs into a lagoon	Radium Nutrients
Andrisoa et al. (2019)	NUT	La Palme, Salses- Leucate lagoons, France	La Palme (choked) Salses-Leucate (restricted)	La Palme (5 km <sup>2</sup> ); Salses- Leucate (56 km <sup>2</sup> )	Examining primary production supported by groundwater discharge to lagoons	N & C isotopes
Stieglitz et al. (2013)	QUANT	La Palme, Salses- Leucate, Thau lagoons, France	La Palme (choked) Salses-Leucate (restricted) Thau Lagoon (choked <sup>b</sup> )	La Palme (5 km <sup>2</sup> ); Thau (75 km <sup>2</sup> ); Salses- Leucate (56 km <sup>2</sup> )	Quantifying groundwater discharge to these lagoons	Radon Salinity
Bejannin et al. (2017)	QUANT	La Palme, Salses- Leucate, Thau lagoons, France	La Palme (choked) Salses-Leucate (restricted) Thau Lagoon (choked <sup>b</sup> )	La Palme (5 km <sup>2</sup> ); Thau (75 km <sup>2</sup> ); Salses- Leucate (56 km <sup>2</sup> )	Detecting and measuring groundwater discharge to these lagoons	Airborne thermal infrared imaging Radium
Gattacceca et al. (2011)	QUANT	Southern basin of Venice Lagoon, Italy	Restricted	102 km <sup>2</sup> (southern basin)	Quantifying groundwater discharge into a lagoon	Radon Radium
Leote et al. (2008)	QUANT NUT	Ria Formosa Lagoon, Portugal	Leaky	111 km <sup>2</sup>	Examining groundwater as a source of nutrients to a lagoon	Seepage meters Nutrients
Ibáñez et al. (2013)	NUT	Ria Formosa Lagoon, Portugal	Leaky	111 km <sup>2</sup>	Examining nutrient dynamics in a groundwater-fed lagoon	Seepage meters Nutrients
Rocha et al. (2016)	QUANT SPAT/TEMP	Ria Formosa Lagoon, Portugal	Leaky	111 km <sup>2</sup>	Quantifying groundwater discharge, source and dispersal mechanisms	Radon Stable water isotopes
Hugman et al. (2017)	NUT	Ria Formosa Lagoon, Portugal	Leaky	111 km <sup>2</sup>	Examining nutrient dynamics in a groundwater-fed lagoon	Numeric modelling
Stumpp et al. (2014)	SPAT/TEMP	Köycegiz–Dalyan Lagoon, Turkey	Unclear	130 km <sup>2</sup>	Examining water balance sources and their spatial distribution in a lagoon	Stable water isotopes Hydrochemistry

Baudron et al. (2015)	QUANT	Mar Menor, Spain	Restricted	135 km <sup>2</sup>	Quantifying groundwater discharge into a lagoon	Radon Radium Hydrodynamic modelling
Alcolea et al. (2019)	QUANT	Mar Menor, Spain	Restricted	135 km <sup>2</sup>	Hydrogeological modelling for watershed management	Numerical modelling
Cable et al. (2004)	QUANT	Indian River Lagoon, Florida, U.S.	Leaky	250 km (long)	Quantifying groundwater discharge into a lagoon	Seepage meters Radon Radium
Smith et al. (2008)	QUANT SPAT/TEMP	Indian River Lagoon, Florida, U.S.	Leaky	250 km (long)	Characterising groundwater discharge source and seasonal variability	Radon
Johannesson et al. (2011)	MISC	Indian River Lagoon, Florida, U.S.	Leaky	250 km (long)	Examining groundwater discharge source of rare earth elements	Hydrochemistry
Haider et al. (2015)	SPAT/TEMP MISC	Ringkøbing Fjord, Denmark	Choked	300 km <sup>2</sup>	Detecting groundwater inflow; modelling salinity distribution in a lagoon	Airborne Electromagnetics
Duque et al. (2016)	QUANT	Ringkøbing Fjord, Denmark	Choked	300 km <sup>2</sup>	Examining role of thermal conductivity in using temperature to estimate groundwater discharge to a lagoon	Temperature
Duque et al. (2018)	QUANT SPAT/TEMP	Ringkøbing Fjord, Denmark	Choked	300 km <sup>2</sup>	Quantifying and looking at spatial/temporal patterns of groundwater inflow into a lagoon	Seepage meters Conductivity
Duque et al. (2019)	NUT	Ringkøbing Fjord, Denmark	Choked	300 km <sup>2</sup>	Investigating nutrient sources to a lagoon	Stable water isotopes Nutrients Slug tests Hydrochemistry Seepage meters
Tirado-Conde et al. (2019)	QUANT	Ringkøbing Fjord, Denmark	Choked	300 km <sup>2</sup>	Quantifying groundwater discharge to a lagoon	Seepage meters Temperature

Garcia-Solsana et al. (2008)	QUANT	Venice Lagoon, Italy	Restricted	550 km <sup>2</sup>	Quantifying groundwater discharge to a lagoon	Radium
Rapaglia, Di Sipio et al. (2010)	QUANT	Venice Lagoon, Italy	Restricted	550 km <sup>2</sup>	Examining groundwater flow under a barrier beach	Hydrochemistry Electrical resistivity Darcy methods Stable water isotopes Seepage meters
Rapaglia, Ferrarin et al. (2010)	QUANT	Venice Lagoon, Italy	Restricted	550 km <sup>2</sup>	Quantifying groundwater discharge and residence time in a lagoon	Radium
Viezzoli et al. (2010)	SPAT/TEMP	Venice Lagoon, Italy	Restricted	550 km <sup>2</sup>	Measuring surface water-groundwater interactions in a lagoon	Airborne Electromagnetics
Santos, Niencheski et al. (2008)	QUANT	Mangueira Lagoon, Brazil	Choked <sup>b</sup>	900 km <sup>2</sup>	Quantifying groundwater discharge to a lagoon	Radon Radium Stable water isotopes Methane Conductivity
Santos, Machado et al. (2008)	MISC	Mangueira Lagoon, Brazil	Choked <sup>b</sup>	900 km <sup>2</sup>	Examining the influence of groundwater discharge on ion chemistry in a lagoon	Hydrochemistry
Danish et al. (2020)	QUANT	Chilika Lagoon, India	Restricted	~1165 km <sup>2</sup> (during monsoon season)	Quantifying groundwater discharge to a lagoon	Strontium
González-De Zayas et al. (2013)	NUT	Laguna Larga, Cuba	Choked	?	Examining nutrient dynamics in a groundwater-fed lagoon	Hydrochemistry Nutrients

Notes: <sup>a</sup> Study categories: QUANT = studies that quantified groundwater seepage in/out of lagoons; NUT = studies that examined groundwater-related nutrient dynamics; SPAT/TEMP = studies that examined spatiotemporal dynamics of groundwater seepage in lagoons; MISC = other study objectives relating to groundwater. <sup>b</sup> Where lagoon classifications were not provided, I have assigned them based on the lagoon's characteristics, and <sup>b</sup> indicates uncertainty as to the classification.

It is important to discuss groundwater discharge to coastal lagoons within the context of their management as water resources. Often, this management requires a complex balance of many cultural, economic, ecological and recreational values and stakeholders. Many lagoons are in highly developed areas, such as the eastern and southern coasts of the United States and the Mediterranean, where their environments have often been modified to suit urbanisation needs. Coastal lagoons often form expansive wetlands that have been drained or destroyed to make way for development (Beer & Joyce, 2013; Kennish & Paerl, 2010). In several cases, lagoon levels are now carefully managed by way of manmade outlets to the sea (e.g., Venice Lagoon, Italy; Te Waihora, New Zealand) to assist with draining of surrounding low-lying land and flush poor quality water to the ocean. Coastal lagoon catchments are also often under considerable surface and groundwater abstraction pressure from a range of uses including agriculture, industries and town drinking water supplies. Globally, these environments are now significantly degraded in many cases, largely due to the various direct anthropogenic pressures they face, as well as natural (often human-induced) factors such as sea level rise and high nutrient inputs (Kennish & Paerl, 2010).

## **1.2 Coastal lagoon characteristics**

Coastal lagoons are features that hold significant ecological, cultural and socioeconomic values (Beer & Joyce, 2013; FitzGerald et al., 2008; Kennish & Paerl, 2010; Lotze et al., 2006). They are typically nutrient-rich, highly biodiverse environments (Beer & Joyce, 2013). They provide a number of ecosystem services including nutrient attenuation, sediment retention, coastline stabilisation, habitat, food sources such as fisheries and waterfowl, recreational opportunities and amenity values (Beer & Joyce, 2013; Costanza et al., 1997; Gedan et al., 2011; Mitsch & Gosselink, 2000).

Coastal lagoons are typically parallel to the coast, separated to the sea by a barrier, and are usually less than 2 m deep (Kennish & Paerl, 2010) (Figure 1.1). They can range in salinity from freshwater to hypersaline depending on factors like surface water inflows, tidal mixing and amount of time the barrier is open to the sea (Kennish & Paerl, 2010; Kjerfve, 1994). The barriers may open naturally due to wave action or high lagoon levels, and in several locations, they are mechanically opened to the sea. Similarly, the ocean opening may be mechanically closed, or it may naturally close due to wave action or littoral drift (Kjerfve, 1994). Coastal lagoon entrances to the sea are narrow in comparison to the coastwise extent of their barriers (Bird, 1994). Bird (1982) defines coastal lagoons as having inlets that at high tide are only 20% of the width of their enclosing barrier. The size of coastal lagoons can vary widely, from less than 1 km<sup>2</sup> to the 10,200 km<sup>2</sup> Lagoa dos Patos in Brazil (Kjerfve, 1994). Coastal lagoons are usually microtidal, with tidal ranges of less than 2 m, and in their natural states they are usually bordered by extensive wetlands (Kennish & Paerl, 2010). They provide diverse

habitat such as open water, wetlands, submerged vegetation, bare sediment, tidal flats and streams for many terrestrial and aquatic organisms (Kennish & Paerl, 2010).

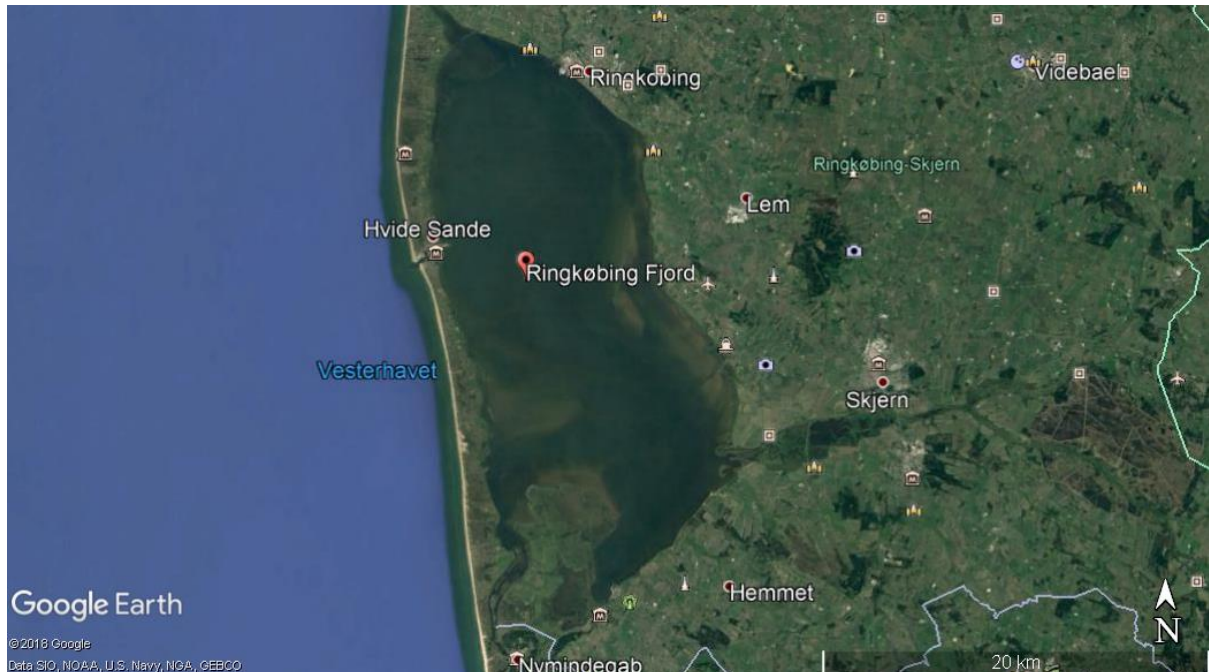


Figure 1.1. Ringkøbing Fjord, a coastal lagoon in Denmark with minimal connection to the ocean.  
Image source: Google Earth.

Coastal lagoons formed during Holocene and Pleistocene sea level rise and as a result of marine processes that have built the barriers that separate these water bodies from the sea (Kjerfve, 1994). The lagoons have usually formed where depressions in the land (e.g., valley floors) have been submerged by rising sea levels during the marine transgression of the Late Quaternary (Bird, 1994). In geological terms, coastal lagoons are relatively short-lived features (Bird, 1994), and because of this, they often require human intervention to maintain desired states (Beer & Joyce, 2013) (such as manmade openings of the barriers to the sea). Their existence is linked to several factors such as sea level rise, tectonic activity and human-induced factors such as river damming, water extraction and land-use practices (Kjerfve, 1994). Coastal lagoon distribution and dynamics are determined by several natural factors: antecedent geomorphology (e.g., they are usually found on low-lying coasts); materials available for formation of a barrier (they are most likely to form in areas with supplies of sand and gravel, rather than large rock outcrops or fine sediment); sediment supply to the lagoon; tectonics (specifically whether the coastline is subsiding or rising); tidal range (small tidal ranges are more likely to form small entrances and complete barriers; and climate (i.e., evaporation and rainfall rates) (Bird, 1994).

Coastal lagoons are located on every continent except Antarctica (Kennish & Paerl, 2010). They are typical features of barrier coasts, comprising 17.6% of the coast in North America, 12.2% in South



America, 5.3% in Europe, 17.9% in Africa, 13.8% in Asia, and 11.4% in Australia (Barnes, 1980). The Atlantic and Gulf coastlines of the U.S. have the most extensive stretch of coastal lagoons, comprising 2800 km of coastline (Nichols & Boon, 1994). Bird (1994) notes there are coastal lagoons on coasts with high-retreating cliffs (such as in southern New Zealand, the rocky coasts of Norway, British Columbia and Chile, and on the northern Canadian coast), but they are poorly formed in these locations.

Coastal lagoons are subject to the influence of several physical factors that affect their dynamics, such as river inputs, groundwater seepage, evaporation, surface heat, exchange with the ocean, tides and wind. This affects physical, chemical, geological and ecological dynamics in lagoons such as eutrophication, salt balances and residence times (Kjerfve, 1994). Understanding these dynamics is key for managing these features (Kjerfve, 1994). Several factors affect the physicochemical makeup of coastal lagoons including the size and configuration of tidal outlets; surface water and groundwater inputs; the size and land use development of their catchments; water depth; and wind conditions (Alongi, 1998). Seasonal rainfall patterns may significantly affect salinity levels in lagoons (Kennish & Paerl, 2010). Due to the often high residence times in the lagoons, nutrient inputs may be recycled several times before they flow out to the ocean, which enables coastal lagoons to be highly productive fisheries, however for this reason they are also prone to eutrophication (Kennish & Paerl, 2010). Various ecological conditions, such as temperature and salinity, are significant in how a coastal lagoon develops because they determine the type and extent of vegetation that develops on the lagoon shorelines, which in turn affects sedimentation rates and patterns, and forms organic matter deposits (Bird, 1994).

Coastal lagoons are very susceptible to anthropogenic impacts and are now considered among some of the most human-affected aquatic ecosystems (Kennish & Paerl, 2010). The nature and degree of human impact on coastal lagoons is a factor of the morphological features of these water bodies (Correia et al., 2012; Félix et al., 2015; Mateus et al., 2016; Menció, Casamitjana, Mas-Pla, Coll, Compte, et al., 2017). While most coastal habitats face these threats, coastal lagoons are often more acutely threatened (Gönenç & Wolflin, 2004). In many places, they are at risk of disturbance from land use change and population growth (FitzGerald et al., 2008; Kennish & Paerl, 2010; Lotze et al., 2006). Human activities such as land development, and changes to water quality and flow rates into coastal lagoons have caused water quality degradation, the introduction or expansion of invasive species, and wetland loss (Crivelli, 1995; La Jeunesse & Elliot, 2004; Lotze et al., 2006; Menció, Casamitjana, Mas-Pla, Coll, Compte, et al., 2017). The limited flushing and long residence times typical of coastal lagoons make them susceptible to nutrient enrichment and pollutant build-up (Kennish & Paerl, 2010). Kennish and Paerl (2010) argue that eutrophication may be the greatest threat to the ecological wellbeing of coastal lagoons. They also face increasing pressure from climate

change due to factors such as sea level rise, increased evaporation rates and changes in precipitation patterns.

Beer and Joyce (2013) call for more research on coastal lagoons, including studies that recognise the complexity, dynamism and diversity of these features. Beer and Joyce (2013) highlight that each physiographic type of coastal lagoon is so unique that it warrants a customised management regime, which is often not reflected in broader policies and legislation such as the current EU Water Framework Directive. Further, Benedetti-Cecchia (2001) argues that coastal lagoons may be so diverse even within each system, that management regimes that address them as homogeneous systems may not be appropriate.

### **1.3 Identifying areas of groundwater inflow to coastal lake/lagoons**

It is difficult to accurately quantify groundwater inputs to coastal lake/lagoons without first understanding how groundwater inputs are distributed spatially. Groundwater discharge is often temporally variable and spatially diffuse (Burnett et al., 2003). A lack of knowledge of the spatial distribution of seepage in a lagoon may lead to estimates of groundwater seepage fluxes being over or underestimated. Also, transport of contaminants, like nutrients, may be heterogeneous in the groundwater discharge across an entire water body (Meinikmann et al., 2013). Thus, insight into seepage patterns is key for addressing questions of groundwater impacts on biogeochemical processes in lagoons.

Groundwater inflow to a given water body is regulated by several factors, including the hydraulic gradient between the water levels in groundwater and an adjacent surface water body, properties of the underlying strata, vegetation in and around surface water, and in the case of coastal water bodies, effects from tides and seawater influence (Duque et al., 2018; McBride & Pfannkuch, 1975; Rosenberry et al., 2015). The classical theory of how groundwater inflow to lakes is distributed is that seepage tends to occur at the margins of the surface water body and decrease with distance from the margin, particularly in the case of lakebeds with low slope (Barwell & Lee, 1981; Genereux & Bandopadhyay, 2001; McBride & Pfannkuch, 1975). This conceptualisation of seepage patterns is based largely on differences in hydraulic pressures between surface water and underlying and adjacent groundwater. The argument here is that for lakes that gain groundwater, there is a positive hydraulic gradient inducing groundwater flow to the lake, and these groundwater flow lines typically converge at or near the lakes' edges (Winter et al., 1998). Particularly in the case of lakes or lagoons with low-slope beds, it is thought that in most cases, there is minimal change in the hydraulic head with increased distance from the margins, such that most groundwater seepage will occur at the edges (McBride & Pfannkuch, 1975). In cases where lakebeds have steep bathymetry or sudden changes in

bed slope, this may result in a sufficient hydraulic gradient to induce seepage away from the lake or lagoon edge (Genereux & Bandopadhyay, 2001).

Some earlier studies investigated hydraulic properties that affect groundwater seepage rates and patterns in lakes: e.g., McBride and Pfannkuch (1975) numerically modelled seepage rates and distribution to a lake; Barwell et al. (1981) developed a method for determining anisotropy ratios in lakes; Cherkauer and Nader (1989) examined the effect of heterogeneity on groundwater discharge to lakes; and Genereux and Bandopadhyay (2001) developed a model to look at factors that affect seepage patterns in lakes such as lake depth, bed slope and bed sediment properties. As this area of research has evolved, it has become clearer that the early conceptual model that located most groundwater seepage at the margins may be too simplistic to describe the complexities of many lakes. Rosenberry et al. (2015) notes that this seepage pattern is likely only dominant in cases where the geology underlying and adjacent to the lake is homogeneous. Also, lakebed sediments are often anisotropic, i.e., horizontal and vertical hydraulic conductivity are not equal. The higher the anisotropy, the less seepage is focused at the margins (Genereux & Bandopadhyay, 2001). Several studies have found groundwater seepage in lakes and coastal lagoons to follow atypical patterns (e.g., Cherkauer & Nader, 1989; Duque et al., 2018; Gibbs et al., 2005). As Rosenberry et al. (2015) highlight, often in these cases, geology was the determining feature over other factors that might influence seepage patterns (e.g., erosion or deposition of sediment; manipulation of near-shore sediment by biological or physical processes; or manmade modifications). There also may be groundwater upwelling offshore due to confined aquifers underlying a lake or lagoon (Vainu et al., 2014). In the case of coastal lagoons, Duque et al. (2018) found the presence of a saline wedge forcing upwards flow; vegetation and organic material deposition on the shoreline; and the recirculation of brackish water due to wave pumping offshore to be drivers of “atypical” patterns of seepage.

In addition to factors controlling seepage varying spatially, groundwater inflow patterns can also change over time (Burnett et al., 2003), responding to both short and long-term processes. In the case of permeability, fine sediments can settle on lake or lagoon beds, forming impermeable barriers to groundwater inflow, or alternatively, fine sediment can be altered thereby causing increased seepage rates (Rosenberry et al., 2010). Adjacent groundwater levels may be affected by weather patterns and abstraction, which may affect the hydraulic gradient between groundwater and surface water (Sebestyen & Schneider, 2001). Similarly, fluctuations in surface water levels from varying tributary inflows; precipitation and evaporation rates; openings to the sea (in the case of coastal lagoons), or wind-induced water level changes will alter hydraulic gradients (Rodellas et al., 2020; Rosenberry et al., 2013). Coastal lakes may be affected by tides, which may change groundwater seepage rates (Rosenberry et al., 2013). Due to seasonal factors such as precipitation, snowmelt and groundwater use for irrigation, several studies have observed seasonal fluctuations in seepage rates (Sadat-Noori et al., 2016; Sebestyen & Schneider, 2001).

It is relevant to highlight here that bed seepage in surface water bodies may be a contribution of regional groundwater inputs as well as recirculation of surface water in bed sediments. Hyporheic or porewater exchange—as it is often referred to—can be driven by a number of factors including wave run-up on margins, surface water level fluctuations, density-driven convection, tidal pumping, sediment compaction, bioturbation and changes to hydraulic gradients on land (Precht et al., 2004; Rodellas et al., 2020; Santos et al., 2012; Wang & Du, 2016). With the techniques commonly used for groundwater seepage investigations, it is often difficult to distinguish between regional groundwater inputs and recirculated water through bed sediments (Sadat-Noori et al., 2016). However, studies examining key questions around porewater exchange in coastal water bodies have been increasing, and these have included quantifying porewater fluxes (Cook et al., 2018; Santos et al., 2014; Stieglitz et al., 2013) and investigating porewater exchange drivers (Rodellas et al., 2020; Santos et al., 2012).

Research investigating the spatial distribution of seepage to coastal lagoons has increased in recent years: e.g., Duque et al. (2018); Tait et al. (2013); Stumpp et al. (2014); Viezzoli et al. (2010); and Haider et al. (2015). These authors acknowledge the difficulty of characterising the spatial variations in seepage to lagoons, particularly in those with heterogeneous geology or large surface areas. While inflows from groundwater-fed tributaries may be relatively easy to constrain when the confluences with lagoons are known, locating diffuse seepage or springs in a lagoon bed can be much more complicated. There is a need to demonstrate the use of effective methods for overcoming the challenges discussed here regarding spatial mapping of groundwater fluxes, particularly distinguishing between regional groundwater inputs and porewater exchange, measuring fluxes across large heterogeneous water bodies, and capturing the temporal variations in seepage patterns.

Methods used for spatial mapping of groundwater seepage to lagoons have ranged from remote sensing (Haider et al., 2015; Viezzoli et al., 2010); salinity and radionuclides (Stumpp et al., 2014; Tait et al., 2013); to direct seepage measurements (Duque et al., 2018). Selecting the appropriate scale methods is one of the key considerations when designing studies of groundwater-surface water interactions (Kalbus et al., 2006). Point-scale methods for directly measuring seepage, such as Lee-type seepage meters (Lee, 1977), are a well-demonstrated method for measuring seepage, and have been used in many lagoons (e.g., Cable et al., 2004; Duque et al., 2018; Ibáñez et al., 2013; Leote et al., 2008), but the data they provide is only reflective of the location where they are installed. It can be quite labour intensive to install a large number of seepage meters, and in places with coarse substrate, it may be impossible. Thus, it is often dubious to extrapolate local-scale seepage meter measurements to characterise seepage across an entire lake or lagoon (Blume et al., 2013). While there have been improvements in recent years in the development of techniques, there is still a lack of effective methods for measuring groundwater inflow to lakes and lagoons at scales greater than point measurements (Blume et al., 2013). The application of qualitative methods has increased in recent years, with researchers measuring radionuclides such as radon and radium, as well as other

physicochemical parameters like salinity and temperature to locate areas of groundwater inflow (Santos, Niencheski, et al., 2008; Stieglitz, 2005; Stumpp et al., 2014; Tait et al., 2013). There have also been some recent examples of applying remote sensing for characterising seepage distributions across lagoons such as airborne electromagnetics (Haider et al., 2015; Viezzoli et al., 2010) and airborne thermal infrared imaging (Bejannin et al., 2017). Remote sensing methods may help address issues of collecting data across entire water bodies, though there are other issues of scale that they present, namely, that sensor data must be at an appropriate scale for observing groundwater seepage signals (Lovett et al., 2015).

#### **1.4 Quantifying groundwater discharge**

Estimations of groundwater inputs into coastal lagoons are important for understanding contaminant loads, water residence times, and the groundwater proportion of lagoon water budgets (Duque et al., 2018; Menció, Casamitjana, Mas-Pla, Coll, Compte, et al., 2017; Rudnick et al., 2015; Stieglitz et al., 2013). Many studies have shown that groundwater inflow to coastal environments is a vector for transport of chemical species such as heavy metals, nutrients, carbon and rare earth minerals (e.g., Ganguli et al., 2012; Ji et al., 2013; Johannesson et al., 2011; Maher et al., 2019; Santos, Machado, et al., 2008). Studies have found groundwater inputs to range from a minimal component of lagoon water budgets (e.g., Stieglitz et al., 2013) to the main contributor to water balances, either year-round or on a seasonal basis (e.g., Menció, Casamitjana, Mas-Pla, Coll, Compte, et al., 2017; Sadat-Noori et al., 2016). Even if in some cases in which groundwater discharge comprises a small proportion of a lagoon's water balance, it could contribute a significant nutrient load, because groundwater often contains high concentrations of dissolved species (Meinikmann et al., 2013; Santos, Niencheski, et al., 2008; Stieglitz et al., 2013). Further, in some cases fresh groundwater inputs to lagoons have been found to play a major role in maintaining salinity levels despite being a small proportion of total inflows (Stieglitz et al., 2013).

Estimating groundwater inputs to coastal lagoons by considering it the residual quantity in volumetric water balances, as has often been the case (e.g., Alcolea et al., 2019; Chikita et al., 2012; Chikita et al., 2015), is only valid if all other variables in the water budget are well constrained. Limited understanding of the groundwater component of lagoon water balances can hinder effective management of water resources in lagoon catchments, such as groundwater abstraction for irrigation or town water supplies. In some systems, groundwater has been shown to play a significant role in residence times and flushing rates (e.g., Rapaglia, Ferrarin, et al., 2010). Coastal lagoons can have a range of water residence times, largely determined by how often, if at all, they are connected to the sea. Choked lagoons for example generally have long water residence times because they have narrow

ocean inlets, which may only be intermittently open to the sea. Residence times in coastal lagoons are often difficult to determine but important, because this time determines whether the components of the water will have sufficient time to biogeochemically affect the lagoon (Rapaglia, Ferrarin, et al., 2010). Thus, understanding groundwater's role in lagoon residence times is important.

Much of what regulates changes in seepage rates to coastal lagoons are the hydraulic gradients between lagoon water levels, underlying and adjacent groundwater, and the sea (Duque et al., 2018; Rosenberry et al., 2015). These pressure gradients change due to various factors. Lagoon levels rise and fall due to variations in surface water inflows, precipitation, evaporation rates and groundwater seepage. Lagoons that are usually closed to the sea may intermittently open, either by naturally breaching their barriers to the sea or by mechanical opening. Sudden opening of a lagoon barrier would generally cause a lowering of the lagoon level, thereby affecting hydraulic gradients with adjacent groundwater and the sea. Groundwater levels also fluctuate as a result of various factors including changes in precipitation, groundwater pumping and land surface recharge. On a longer timescale, sea level rise will also affect the hydraulic gradient with lagoons. Thus, it is important to understand these temporal variations, as a point-in-time "snapshot" might not reflect a reliable range in seepage rates over time. However, there are only a limited number of studies that have examined temporal changes in lagoon seepage. Rocha et al. (2016) used radon measurements and stable isotope chemistry to examine spatiotemporal variations in seepage to the Ria Formosa Lagoon in Portugal and found that groundwater inputs to the lagoon did not occur on a consistent basis. Smith et al. (2008) found that seepage rates seasonally varied by a factor of nine or less in the Indian River Lagoon in Florida. Notably, Duque et al. (2018) found in the case of the Ringkøbing Fjord in Denmark, the seasonal variations in seepage rates were less than the spatial variations of discharge within the lagoon.

Several methods can be used for estimating the groundwater component of lagoon water budgets, and there is some overlap here with methods that can also be used for identifying locations of seepage. Radon and radium mass balances have been the most often-used techniques for estimating groundwater discharge to lagoons (Baudron et al., 2015; Bejannin et al., 2017; Cable et al., 2004; Ganguli et al., 2012; Gattacceca et al., 2011; Ji et al., 2013; Knapp et al., 2020; Maher et al., 2019; Rapaglia, Ferrarin, et al., 2010; Rocha et al., 2016; Rodellas et al., 2018; Sadat-Noori et al., 2016; Santos, Niencheski, et al., 2008; Smith et al., 2008; Stieglitz et al., 2013). Other methods include water and salt budgets (Chikita et al., 2012; Chikita et al., 2015; Manzoni et al., 2020; Stieglitz et al., 2013); temperature profiles (Duque et al., 2016; Rodellas et al., 2020); strontium isotopes (Danish et al., 2020); seepage meters (Cable et al., 2004; Duque et al., 2018; Ibánhez et al., 2013; Rapaglia, Ferrarin, et al., 2010; Tirado-Conde et al., 2019); and numeric modelling (Alcolea et al., 2019; Menció, Casamitjana, Mas-Pla, Coll, Compte, et al., 2017).

It is difficult to quantify groundwater discharge into coastal lagoons, and as is apparent in Table 1.1, most studies have used more than one method to achieve their studies' objectives, which can help overcome some of these challenges (Kalbus et al., 2006). There is however, a lack of studies that have compared both point and broad-scale techniques for quantifying seepage (e.g., Rapaglia, Di Sipio, et al., 2010) and overcome issues of scale. Where there have been comparisons made, there have often been wide discrepancies in groundwater discharge estimates, so there is a need for more consistency between these approaches (Robinson et al., 2018).

When examining previous studies quantifying groundwater discharge to coastal lagoons, there are apparent gaps in some types of lagoon environments where there have been fewer studies. Previous study sites have ranged in size from less than 1 km<sup>2</sup> (e.g., Ganguli et al., 2012; Maher et al., 2019; Sadat-Noori et al., 2016) to over 200 km<sup>2</sup> (Cable et al., 2004; Danish et al., 2020; Duque et al., 2016; Rapaglia, Ferrarin, et al., 2010; Santos, Niencheski, et al., 2008; Smith et al., 2008). Of these studies quantifying groundwater discharge in coastal lagoons larger than 200 km<sup>2</sup>, this list only comprises five sites (Table 1.1). Thus, as highlighted earlier, there appears to be a lack of studies examining groundwater processes in large lagoons. Of these four sites, only one was in a temperate climate (Ringkøbing Fjord (Duque et al., 2018; 2016; Tirado-Conde et al., 2019)) with a mixed sand and gravel coastline, while the other sites were in Mediterranean or tropical climates with sandy coastlines.

## **1.5 Groundwater source characterisation**

Investigating sources of groundwater inputs to lagoons can shed light on a number of important processes, and there has been an increase in studies in this area in recent years. Source analysis can help resolve key questions relating to hydrological and hydrogeological processes in lagoons. For example, it can shed light on the proportions of source water that contribute to groundwater inputs—e.g., groundwater recharge locations, source aquifer depths or influence of rain-recharged shallow groundwater (Rocha et al., 2016; Stumpp et al., 2014; Young et al., 2008). For coastal lagoons, groundwater source delineation can provide information on interactions between the lagoon, seawater and the freshwater systems underlying barrier islands (Rapaglia, Di Sipio, et al., 2010; Röper et al., 2012; Schmidt et al., 2011). These investigations can also help determine the proportions of fresh versus recirculated groundwater fluxes. Some studies have found the majority of the seepage into lagoons to be recirculated lagoon water (Baudron et al., 2015; Gattacceca et al., 2011).

A variety of techniques can reveal groundwater sources and their impacts on biogeochemical processes in lagoons. Stable water isotopes (oxygen-18 or <sup>18</sup>O and deuterium or <sup>2</sup>H) are frequently used in source analysis (Bratton et al., 2009; Duque, Jessen, et al., 2019; Rocha et al., 2016; Röper et

al., 2012; Santos, Niencheski, et al., 2008; Schmidt et al., 2011; Stumpp et al., 2014). They have been found to be reliable naturally occurring tracers in many locations, as they are chemically non-reactive and typically have distinguishable signatures in source waters. Analysing the hydrochemistry in surface and groundwater (e.g., major ions, trace metals), is also commonly done to delineate groundwater sources, as source waters will often present with specific chemical signatures depending on a variety of factors such as geology, groundwater depth and proximity to the ocean (Bratton et al., 2009; Ganguli et al., 2012; González-De Zayas et al., 2013; Liefer et al., 2014; Medina-Gómez & Herrera-Silveira, 2006; Röper et al., 2012; Santos, Machado, et al., 2008; Stumpp et al., 2014; Young et al., 2008). Age dating tracers such as tritium, sulphur hexafluoride (SF<sub>6</sub>), chlorofluorocarbons (CFCs) and carbon-14 are also often used to group water types by age (Bratton et al., 2009; Röper et al., 2012). To determine the contribution of recirculated porewater to groundwater inputs, tracers such as radon, radium and salinity have been commonly used (Rodellas et al., 2020; Santos et al., 2014; Stieglitz et al., 2013). This tracer data has often been used as the basis for end-member mixing models to determine proportions of water sources (Stumpp et al., 2014; Su et al., 2014; Young et al., 2008).

## 1.6 Literature on groundwater discharge to Waituna-type lagoons

Kirk and Lauder (2000) argue that there are two distinct types of coastal lagoons on the east and south coasts of the South Island of New Zealand: river mouth lagoons (*hapua*<sup>1</sup>) and coastal lakes (Waituna-type lagoons), which would both be considered “choked” lagoons by Kjerfve’s (1986) definition. Waituna-type lagoons occur on microtidal coastlines with mixed sand and gravel sediment, have long water residence times and are infrequently opened to the sea via narrow ocean outlets (Hume et al., 2016; Kirk & Lauder, 2000).

Hume et al. (2016) identified sixteen coastal lagoons as Waituna-type in New Zealand, and these lagoons serve numerous important ecological purposes such as sediment retention, nutrient attenuation and habitat for many flora and fauna. Despite the importance of groundwater discharge into coastal lagoons as highlighted in this chapter, it is an underexplored area of research in New Zealand. To my knowledge, there have been no peer-reviewed publications in international journals that have specifically examined groundwater processes in Waituna-type lagoons. However, there does appear to be an increasing recognition in the New Zealand scientific community that groundwater discharge to these lagoons is important to consider, particularly for nutrient dynamics, (Allan et al., 2018; Jenkins, 2016; Larned & Schallenberg, 2006; Rissmann et al., 2012), yet studies on this topic

---

<sup>1</sup> Many Māori also use the term *hapua* to refer to Waituna-type lagoons (pers. communication D. Perenara-O’Connell, 10 June 2019), however this thesis refers to *hapua* and Waituna-type lagoons as distinct features as classified by Kirk and Lauder (2000).



have been limited to a relatively small number of technical reports and theses. For studies that provided an estimate of groundwater discharge lagoons, these figures were largely based on volumetric-based water budgets, rather than direct measurements of seepage (Allan et al., 2018; Berry & Webster-Brown, 2012; Hall, 2003; Horrell, 1992). It appears there have only been attempts to estimate groundwater discharge to Waituna-type lagoons by way of in-situ direct (e.g., seepage meters) or inferred (e.g., hydrochemistry, temperature) measurements at two sites: Waituna Lagoon in Southland (Guérin & Wourms, 2016; Rissmann et al., 2012) and Te Waihora in Canterbury (Ettema & Moore, 1995). These three studies were all regional council technical reports, of which only one (Rissmann et al., 2012) is freely available online.

## **1.7 Research rationale**

This thesis seeks to improve the understanding of groundwater discharge into coastal lagoons, a crucial but under-researched component of water budgets. Groundwater inputs can be a significant source of nutrients and other chemical species into coastal lagoons—environments which are prone to eutrophication. To estimate nutrient loads via groundwater and sources of seepage, groundwater discharge must first be located and quantified. Without an understanding of the proportion that groundwater inflow makes up in a lagoon water balance, it is very difficult to manage catchment water use to attain desired outcomes in lagoons.

### **Key gaps in understanding of groundwater processes in coastal lagoons this study addresses:**

- The groundwater component of lagoon water budgets has often been disregarded because it was either assumed to be small and/or difficult to measure.
- Prior research on groundwater processes in coastal lagoons has focused on lagoons with sand barriers in tropical and Mediterranean climates. Very few studies have examined groundwater discharge to Waituna-type coastal lagoons.
- It is not clear that the prevailing theory that most groundwater seepage into lakes occurs at the margins holds true in all coastal lagoons, particularly in cases where the lagoon is underlain by an artesian groundwater system and/or heterogeneous geology.
- While radon mass balances are now commonly used to estimate groundwater discharge to surface water bodies, the models have rarely accounted for the complexities of coastal lagoons (e.g., sea openings, barrier interactions) when applied in those settings. Further, it has been rare for radon mass balances to include an in-depth examination of analytical and conceptual uncertainties of the models.

- Groundwater seepage sources to lagoons are often difficult to resolve, but this knowledge is critical for catchment water use management and quantifying nutrient loads to lagoons.

## **1.8 Research aim**

To understand groundwater discharge into a coastal lagoon in terms of its spatial distribution, magnitude and sources.

This thesis research will specifically address the following questions:

- (1) How is groundwater discharge to a New Zealand coastal lagoon distributed spatially?
- (2) What is the quantity of groundwater seepage discharging to a coastal lagoon?
- (3) What are the seepage sources to a coastal lagoon in New Zealand?
- (4) How does groundwater discharge to lagoons affect nutrient loads?

This study was carried out at Te Waihora (Lake Ellesmere), a shallow, brackish, coastal lagoon on a mixed sand and gravel coastline in Canterbury, New Zealand. Te Waihora is a choked lagoon (Kjerfve, 1986) and has been classified in New Zealand as a Waituna-type coastal lagoon (Kirk & Lauder, 2000). The lagoon is relatively large (~150 km<sup>2</sup>) with a mean depth of 1.4 m.

## **1.9 Structure of thesis**

The remaining chapters in this thesis are structured as follows:

Chapter 2 addresses Research Question (1)—How is groundwater seepage in coastal lagoons distributed spatially? This chapter reports the results of airborne thermal imaging and spatial surveys using radon and physicochemical parameters to locate seepage locations across Te Waihora.

Chapter 3 addresses Research Question (2)—What is the quantity of groundwater seepage discharging to a coastal lagoon? This chapter reports the results of a radon mass balance model created to estimate groundwater seepage into the lagoon.

Chapter 4 addresses Research Questions (3) and (4)—What are the seepage sources to a coastal lagoon in Canterbury, New Zealand and how does groundwater discharge to lagoons affect nutrient loads?

Chapter 5 synthesises the findings presented in the previous chapters. This chapter addresses the implications of groundwater seepage in coastal lagoon management and discuss priorities for further research.

## **2. Mapping groundwater discharge to a coastal lagoon using combined spatial airborne thermal imaging, radon ( $^{222}\text{Rn}$ ) and multiple physicochemical variables**

### **2.1 Abstract**

Coastal lagoons are significant wetland environments found on coastlines throughout the world. Groundwater seepage may be a key component of lagoon water balances, though only a few studies have investigated large ( $>100\text{ km}^2$ ) coastal lagoons. In this study, we combined airborne thermal infrared imagery with continuous measurements of radon ( $^{222}\text{Rn}$ —a natural groundwater tracer), conductivity, water temperature and dissolved oxygen to map groundwater seepage to a large coastal lagoon in New Zealand. We found evidence of seepage along the margins of the lagoon but not away from the margins. Our findings confirmed previously known seepage zones and identified new potential locations of groundwater inflow. Both point-source and diffuse seepage occurred on the western and north-western margins of the lagoon and parallel to the barrier between the lagoon and sea. These observations imply geologic controls on seepage. The combination of remote sensing and in-situ radon measurements allowed us to effectively map groundwater discharge areas across the entire lagoon. Combined, broad-scale qualitative methods built confidence in our interpretation of groundwater discharge locations in a large, dynamic coastal lagoon.

### **2.2 Introduction**

Coastal lagoons are found on 13% of coastlines throughout the world (Barnes, 1980). They serve many key ecological, economic, cultural and recreational purposes such as contaminant and sediment attenuation, flood protection, aquatic and wetland habitat, food sources and amenity values (Schallenberg et al., 2013). These lagoons are often located in places that have been significantly influenced by anthropogenic activities. As a result, coastal lagoons worldwide face many pressures, such as habitat destruction, eutrophication, draining and land development (Beer & Joyce, 2013; Schallenberg et al., 2013). To effectively manage and protect coastal lagoons, it is vital to understand the inflows and outflows of water, and how hydrological processes affect coastal lagoon water quality and ecology.

The influence of groundwater discharge to coastal lagoon water budgets has been broadly overlooked (Menció, Casamitjana, Mas-Pla, Coll, Comptee, et al., 2017). Groundwater discharge can be a point or diffuse source of natural and human-derived biogeochemical species (Andrisoa et al., 2019; Santos, Niencheski, et al., 2008). Since coastal lagoons are receiving environments for all up-stream activities

in their catchments, they often accumulate high concentrations of nutrients, heavy metals or other contaminants from land-use practices (Fujita et al., 2014; Ganguli et al., 2012; Ji et al., 2013; Johannes & Hearn, 1985; Ünlü & B., 2017). Research into groundwater processes in coastal lagoons has considered water balances (e.g., Chikita et al., 2015); nutrient transport and cycling (e.g., Leote et al., 2008; Maher et al., 2019); and the importance of groundwater in supporting lagoon primary productivity (e.g., Andrisoa et al., 2019; Sánchez-Martos et al., 2014).

Understanding the spatial distribution of groundwater discharge is important. Nutrient concentrations are often heterogeneous in groundwater discharging across an entire water body (Meinikmann et al., 2013). Spatially heterogeneous groundwater fluxes can make the estimate of discharge rates across entire water bodies difficult (Blume et al., 2013). Few studies have examined the spatial distribution of groundwater seepage into coastal lagoons (e.g., Duque et al., 2018; Stumpp et al., 2014; Young et al., 2008). McBride and Pfannkuch (1975), Barwell and Lee (1981), and Genereux and Bandopadhyay (2001) have hypothesised that seepage tends to occur at the margins of lakes and decrease with distance from the margin. It remains unclear whether spatial seepage patterns in coastal lagoons follow traditional models developed for lakes.

There have been few studies that have demonstrated the use of practical and effective methods to obtain broad-scale data on groundwater seepage across large ( $>100\text{ km}^2$ ) coastal lagoons (e.g., Baudron et al., 2015; Santos, Niencheski, et al., 2008). Many studies instead have focused on using small-scale methods (e.g., discrete water samples, vertical temperature profiles, seepage meters) or conducting in-depth studies of subset areas of large lagoons (e.g., Cable et al., 2004; Haider et al., 2015; Stumpp et al., 2014). It may be difficult to extrapolate small-scale studies across entire lagoons where groundwater discharge is often temporally variable and spatially diffuse (Burnett et al., 2003). Small-scale methods for directly measuring seepage, such as Lee-type seepage meters (Lee, 1977), are a well-demonstrated method for measuring seepage (e.g., Cable et al., 2004; Duque et al., 2018; Leote et al., 2008; Rapaglia, Di Sipio, et al., 2010). In a previous study of the present study site, Te Waihora (Lake Ellesmere), seepage meters were installed mainly on the western and north-western margins on the lagoon, and a smaller number on the eastern side and along the barrier, to spatially map and quantify groundwater discharge to the lagoon (Ettema & Moore, 1995). There have also been examples of broad-scale methods for characterising seepage distribution across lagoons in recent years such as continuous radon measurements (Baudron et al., 2015; Santos, Niencheski, et al., 2008), airborne electromagnetics (Haider et al., 2015; Viezzoli et al., 2010) and airborne thermal infrared imaging (Bejannin et al., 2017).

There are a number of physical properties and chemical species in water that serve as effective indicators of water sourced from either groundwater or surface water (Cook & Herczeg, 2000). This requires a sufficient difference in tracer concentration between groundwater and surface water at the

location of interest (Kalbus et al., 2006). The tracers should also be conservative on the scale of the investigation, i.e., some parameters, such as dissolved oxygen, may be affected by biogeochemical processes, which may render them ineffective as tracers. Hydrochemical tracers such as radioactive and stable isotopes, salinity, alkalinity, dissolved oxygen and nutrients have been used in a variety of environments for investigating groundwater-surface water exchange, including in coastal lagoons (e.g., Menció, Casamitjana, Mas-Pla, Coll, Comptee, et al., 2017; Mudge et al., 2008; Rapaglia, Ferrarin, et al., 2010; Sadat-Noori et al., 2016). Groundwater discharge into lakes and lagoons might be patchy or diffuse, which makes geochemical tracers useful because they mix with surface water and smooth out the heterogeneities in seepage distribution (Santos, Niencheski, et al., 2008).

Thermal infrared (TIR) imaging has been used in several previous studies for identifying areas of groundwater-surface water interaction (e.g., Lewandowski et al., 2013; Mundy et al., 2017; Rautio et al., 2018), including in coastal lagoons (e.g., Ahmed et al., 2009; Bejannin et al., 2017; Ferri et al., 2000). TIR cameras are used to measure the temperature on the surface (top 0.1 mm) of a water body to highlight areas of relative temperature difference, which may indicate groundwater-surface water mixing (Bejannin et al., 2017). In most places, groundwater temperatures remain relatively stable throughout the year. Therefore, when surface water temperatures are at their minimum and maximum annual temperatures, groundwater inflow to a surface water body will either present as a cool or warm patch relative to the surface water temperature. Here, and in prior studies, TIR imaging was combined with in-situ measurement of geochemical tracers like  $^{222}\text{Rn}$  or stable isotopes (e.g., Bejannin et al., 2017; Johnson et al., 2008; Lee et al., 2016; Tamborski et al., 2015).

In this study, we tested the hypothesis that groundwater seepage predominantly occurs on the margins of coastal lagoons, as has been shown previously for inland lakes. We combined multiple broad-scale sampling methods—spatial airborne thermal infrared imaging and physicochemical surveys ( $^{222}\text{Rn}$ , water temperature, conductivity and dissolved oxygen), to detect areas of groundwater inflow to a large coastal lagoon in New Zealand during two seasons. We demonstrate the practical and effective use of broad-scale methods to understand seepage into a large, dynamic lagoon ( $\sim 150 \text{ km}^2$ ) with many surface water tributaries and complex geomorphology and hydrogeology.

## **2.3 Materials and methods**

### **2.3.1 Site description**

Te Waihora (Lake Ellesmere) is a shallow (mean depth 1.4 m), brackish, hypertrophic, turbid and highly wind-affected coastal lagoon in the South Island of New Zealand (Figure 2.1). It is the fifth largest lake in New Zealand covering  $\sim 150 \text{ km}^2$ . Te Waihora holds important ecological, cultural,

economic, social and recreational value for many stakeholders. The lagoon is a *taonga* (treasure) to the local indigenous Māori tribe, Ngāi Tahu, particularly for food gathering. It is an internationally recognised habitat for birds, and it is a popular recreational spot for fishing, hunting, cycling and walking. The Te Waihora catchment is also intensively farmed, which has contributed to declining water quality in the lagoon. Given the multitude of stakeholders, integrated management of the lagoon remains a challenge. The 256,000-hectare Te Waihora catchment is largely situated within the Central Plains, and the tributaries in this catchment flow from the foothills of the Southern Alps. The climate is temperate with rainfall well distributed throughout the year and mean annual rainfall of ~475 mm at Taumutu, based on the previous 12 years of data (Environment Canterbury, 2020b).

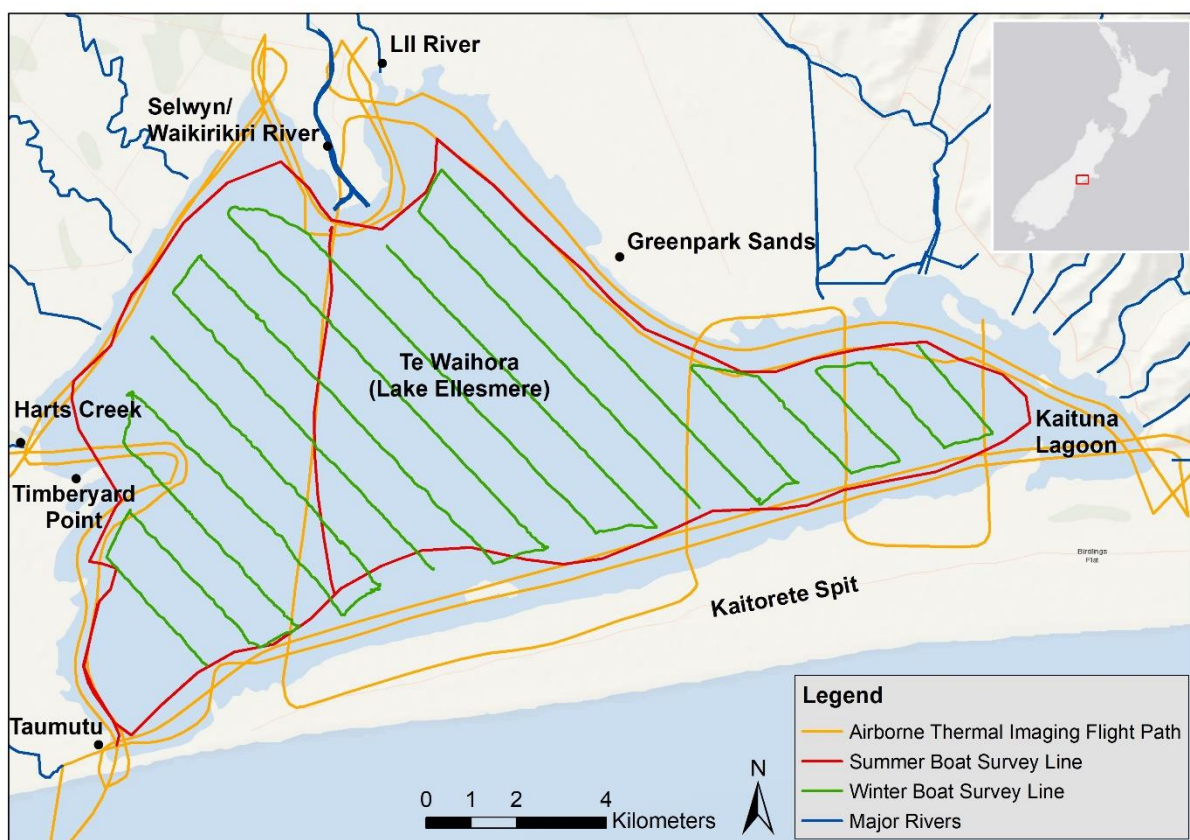


Figure 2.1. Map of Te Waihora (Lake Ellesmere) showing the location of sites referred to throughout the paper and survey lines from field data collection. Note that this figure does not include the survey lines from the survey on 27 August, which overlapped lines on 28 August. Map base layer credits: Esri, Garmin, GEBCO, NOAA NGDC, and other contributors. Map includes GIS data from Land Information New Zealand (Land Information New Zealand, 2019, 2020).

Te Waihora has been classified as a coastal lake/Waituna-type coastal lagoon (Kirk & Lauder, 2000), and in terms of Kjerfve's (1986) classification of lagoon types, Te Waihora would be considered a highly "choked" lagoon. It has formed in the depression created by the intersecting alluvial fans of

gravel-bed braided rivers to the north and south. The lagoon is separated from the Pacific Ocean by Kaitorete Spit (Figure 2.1), a barrier comprised of mixed sand and gravel. The Kaitorete barrier is nearly 30 km long and its highest point is 11 masl (metres above mean sea level). It is widest (3.2 km) at its north-eastern end, and it narrows to 0.2 km wide at its south-western tip near Taumutu (see Figure 2.1). The lagoon is usually closed to the sea, but it is mechanically opened at the Taumutu end of the barrier once the lagoon level exceeds set trigger levels to aid drainage of the surrounding land, flush poor-quality water and to enable fish passage. The lagoon is only influenced by tides when the barrier outlet is open. The lagoon water is brackish due to evaporation, mixing with ocean water when the outlet is open, and from salt spray and rough seas overtopping the barrier (Spigel, 2009). The lagoon bed is mostly comprised of fine-grained muds and silts with areas of gravels on the western margins and along the barrier (Kitto, 2010).

Most of the surface water flowing into Te Waihora is thought to have originated from groundwater sources (Hughey & Taylor, 2009). In the upper catchment, groundwater has a strong negative vertical hydraulic gradient, therefore most of the rivers in the upper catchment lose their flow to groundwater (Larned et al., 2008), with some rivers flowing only during times of flooding (Vincent, 2005). Other sources of recharge to groundwater in the catchment include land surface recharge (comprised of infiltration of rainfall and irrigation water), seepage from stockwater races and manmade drains, and seepage from the large braided rivers to the north and south. Groundwater in the Te Waihora catchment generally flows from higher elevations in the northwest towards the coast in the southeast of the catchment (Brown, 2001). Closer to the coast, the sequence of marine sediments deposited from interglacial sea level rise form confining units that alternate with artesian gravel layers (Brown & Weeber, 1992). This coastal aquifer system extends beneath the lagoon and out to sea for several kilometres (Brown & Weeber, 1992). Towards the coast, where groundwater becomes confined, it is forced to the surface by a positive hydraulic gradient, emerging at the surface as springs (Smith, 2003). Te Waihora has around 40 surface inflows, mostly comprised of spring-fed streams, with a lesser proportion of flow into the lagoon from manmade drains.

### **2.3.2 Sampling and analysis**

This study used broad-scale methods to identify potential areas of groundwater discharge to the lagoon, making use of several naturally occurring groundwater tracers:  $^{222}\text{Rn}$ , temperature, conductivity and dissolved oxygen. We collected data via an airborne thermal imaging survey and by multi-day boat surveys during summer and winter.



### 2.3.2.1 *Airborne thermal infrared imaging*

The thermal infrared imaging survey was carried out at Te Waihora during summer on 21 January 2019 from 7:30 am to 8:45 am on a day with moderate wind speeds and relatively clear sky conditions. Two laps of the perimeter of the lagoon were flown (with an offset of ~300 m between the two flight lines) (Figure 2.1). Following that, four transects were flown across the lagoon in a north-south direction. An Optris PI 450 TIR (Thermal InfraRed) camera with an 80° (wide angle) lens was used, which has an optical resolution of 382 x 288 pixels and thermal accuracy of  $\pm 2^{\circ}\text{C}$ . The Optris PI 450 measures target brightness temperatures corresponding to long-wave radiation across a broadband wavelength between 7.5 to 14  $\mu\text{m}$ . The camera was mounted on a gimbal (motion stabiliser) in the camera hatch of a Cessna aircraft. The survey was flown at an altitude of approximately 300 m above the lagoon surface with an approximate flight speed of 80 knots, which resulted in an image footprint size of 490 m (horizontal) by 320 m (vertical) and an individual pixel size (internal field of view) of 974 mm. The camera video sampling frame rate was 27 Hz, and each frame was tagged with GPS coordinates. As the objective of the survey was to observe spatial differences in temperature patterns on the surface of the lagoon, knowing the absolute temperature of the water was not necessary. For that purpose, the camera's high thermal sensitivity of 40 mK was suitable. However, to further understand the relationship between surface brightness temperatures and actual water column temperatures, we compared the TIR imaging results with in-situ temperature loggers.

The TIR dataset required multi-stage image processing. The raw video files from the Optris camera were converted to a Radiometric Video File (or RAVI file), which was then converted to factory-calibrated brightness temperature files (in CSV format) used in the analysis, with one file for each image. We sub-sampled the full dataset to three frames per second after verifying this frame rate would produce sufficient image overlap for the mosaics of the images. We wrote Python-based scripts to handle most of the image processing, which we have made available on GitHub (Coluccio & Coluccio, 2020). These scripts include the NumPy (Oliphant, 2006) and Pillow (Clark, 2015) modules. To correct for lens distortion, we used the OpenCV module (Bradski, 2000) in Python to adjust the CSV files using calibration images taken with the same Optris camera. RGB (Red Green Blue) values were assigned to the temperature values and converted to TIF (Tagged Image File Format) images. We used Agisoft Metashape Pro to create orthomosaics; however, this was unsuccessful for most of the final images due to an insufficient number of tie points between the images. In these cases, individual images were manually overlaid on satellite imagery in ArcMap 10.7.

### 2.3.2.2 Spatial $^{222}\text{Rn}$ and physicochemical surveys

During the two multi-day boat surveys on Te Waihora in January 2019 (summer) and August-September 2019 (winter), we measured  $^{222}\text{Rn}$ , conductivity, dissolved oxygen, water temperature and wind speed (survey details in Figure 2.2 and Table 2.1) to locate groundwater inflow areas. As with the TIR survey, we carried out the physicochemical surveys to detect relative spatial changes of parameter concentrations, rather than their absolute values. We also recorded GPS coordinates during the surveys so that all data points could be georeferenced.

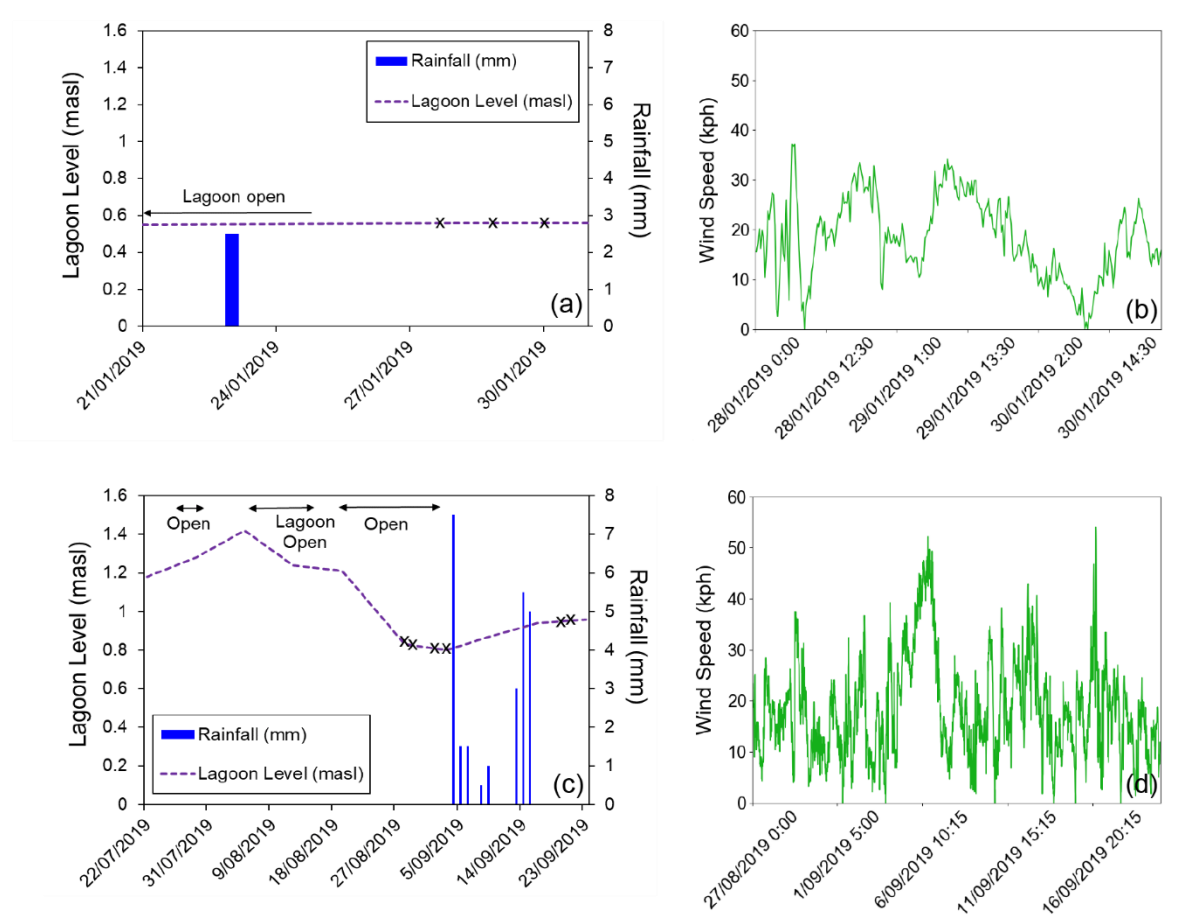


Figure 2.2. Time series of lagoon level, rainfall and wind speed prior to and during the summer (a and b) and winter surveys (c and d). To be concise, wind plots (b and d) only include data from the start to end of the survey period, not prior. Survey days are indicated by x symbols in the plots on the left-hand side. Lagoon levels are based on average readings from two permanent Environment Canterbury-operated gauges in the lagoon.

Table 2.1 Parameters measured during the continuous boat surveys

Parameter (Units)	Method	Sampling Rate	Accuracy
$^{222}\text{Radon}$ ( $\text{Bq/m}^3$ )	RAD7	10 minutes	$\sim \pm 5\%$ <sup>a</sup>
Conductivity ( $\mu\text{S/cm}$ )	Solinst LTC	2 seconds	$\pm 2\%$

Water temperature (°C)	Solinst LTC	2 seconds	±0.05°C
Depth of measurement (m)	Solinst LTC	2 seconds	±0.05%
Dissolved oxygen (summer) (% sat)	Orion Star A329	~10 minutes	±0.5% of reading ±1 digit for conductivity >3 µS
Dissolved oxygen (winter) (% sat)	HOBO U26-001	1 minute	±0.2 mg/L <8 mg/L; ±0.5 mg/L 8-20 mg/L
Barometric pressure (summer) (hPa)	Lufft WS501-UMB	15 minutes	±0.5 hPa
Barometric pressure (winter) (kPa)	Solinst Barologger	5 minutes	±0.05 kPa
Wind speed/direction (kph/degrees)	Kestrel 5500	1 minute	3%
Wind speed/direction (kph/degrees)	Lufft WS501-UMB	Averaged over 15 minutes	±1.08 kph (wind speed)
GPS	Garmin eTrex Touch 25	Continuous	5 m (horizontal)

<sup>a</sup> This refers to the manufacturer-rated accuracy of the RAD7.

We expected the highest rates of seepage to be close to the shoreline (McBride & Pfannkuch, 1975), so in the first survey (in summer) we followed the perimeter of the shoreline (Figure 2.1), and most measurements were in water approximately 0.5 m deep. We expected this shallow depth to be advantageous for detecting signs of groundwater seepage, as there would be less mixing, and observations would have been made closer to the point of entry of groundwater into the lagoon. We also surveyed one transect across the centre of the lagoon to look for indications of seepage. For the winter survey, one of the main objectives was to detect signs of discharge away from the margins in deeper waters, so we surveyed in 1-km spaced transects across the entire lagoon (Figure 2.1).

During the spatial survey, we measured <sup>222</sup>Rn using a radon detector (RAD7, Durrige, Inc., Billerica, MA). <sup>222</sup>Rn is a radioactive isotope of the noble gas radon, and it is part of the Uranium-238 radioactive decay series. Uranium is present in nearly all rocks, so as groundwater passes by rocks, it becomes enriched in <sup>222</sup>Rn. Once <sup>222</sup>Rn is exposed to air, it rapidly evades to the atmosphere, so concentrations of <sup>222</sup>Rn in surface waters are typically 2-3 orders of magnitude lower than in groundwater (Stieglitz, 2005). We continuously pumped lagoon water with a bilge pump (Rule 360GPH) through a filter into an air-water showerhead exchanger (RAD AQUA, Durrige, Inc., Billerica, MA), which brings the radon concentration in water into equilibrium with the radon concentration in the headspace of the exchanger (Burnett et al., 2001). Air from the headspace of the exchanger was pumped into the RAD7. The RAD7 provides real-time data by detecting alpha particles emitted from <sup>222</sup>Rn radioactive decay daughters (<sup>214</sup>Po and/or <sup>218</sup>Po). The boat speed during the survey was approximately 5 km/h, and measurements on the RAD7 were integrated over a ten-minute period, representing a spatial survey resolution of ~800 m. During the winter survey, we used two RAD7s connected in parallel (similar to Dulaiova et al., 2005), both set at the same 10-minute counting interval, to reduce the counting uncertainty.

The  $^{222}\text{Rn}$ -in-air readings were converted to  $^{222}\text{Rn}$  in water using DurrIDGE's CAPTURE software as a function of water temperature and salinity (Schubert, Paschke, Lieberman, et al., 2012). We incorporated into our data analysis 15-minute averaged wind speeds from a long-term weather station installed in the centre of the lagoon. To georeference the  $^{222}\text{Rn}$  data, the RAD7 readings were offset by 30 minutes to account for lag time due to the time required for the radon in water to reach equilibrium with the radon in the air (15-20 min.), as well as the time it takes for  $^{218}\text{Po}$  to decay ( $T_{1/2} = 3.10$  min) (Schubert, Paschke, Bednorz, et al., 2012). For the winter survey when two RAD7s were used in parallel, the  $^{222}\text{Rn}$  concentrations in water were averaged and the uncertainty values calculated to account for both machines being used.

Conductivity, temperature and depth in the water column were measured with a Solinst LTC Levelogger Edge (Solinst Canada Ltd, Georgetown, ON) at a 2-second measurement interval. As the water in Te Waihora is brackish, we suspected that fresh groundwater inflow could be inferred by decreases in conductivity levels. Similarly, we expected water temperature to be a useful indicator of groundwater inflow, as during both the summer and winter surveys, there were several degrees of temperature difference between groundwater and the lagoon water. Raw conductivity was converted to specific conductivity (i.e., conductivity at 25°C) and water level was compensated for barometric pressure, which was measured with a Solinst Barologger. During the summer survey, the data logger was mounted on a fixed point at the back of the boat. For the winter survey, a second logger was added to record any potential vertical differences in parameters. The winter data loggers were mounted on a height-adjustable pole at the side of the boat to ensure that the lower logger was only just above the lagoon bed.

Dissolved oxygen is often lower in groundwater than in surface water, so we suspected decreases in dissolved oxygen to indicate possible locations of groundwater inflow. During the summer survey, we manually measured dissolved oxygen on an approximately ten-minute basis with an Orion Star A329 multi-parameter meter (Thermo Fisher Scientific, Inc., Waltham, MA). During the winter survey, we recorded dissolved oxygen readings at 1-minute intervals using a HOBO Dissolved Oxygen Logger (U26-001) (Onset Computer Corporation, Bourne, MA). Dissolved oxygen readings were compensated for temperature and specific conductivity, and measurements were converted from mg/L to percent saturation.

Wind speed and direction were measured on the boat using a Kestrel 5500 Weather Meter (Kestrel Meters, Boothwyn, PA), and wind data from a permanent Environment Canterbury weather station in the centre of the lagoon was also used during data analysis (Environment Canterbury, 2020b).

The survey lines for the August 27<sup>th</sup> and 28<sup>th</sup> surveys largely overlapped, so for clarity and due to the high number of data points, for in-situ water temperature, conductivity and dissolved oxygen, only

data from August 28<sup>th</sup> is included in this paper. Radon results from August 27<sup>th</sup> have been included here.

#### *2.3.2.3 Integrated analysis of the full dataset*

All the georeferenced data points were plotted on maps to identify spatial trends in the results. We examined the data for indicators of possible groundwater inflow by highlighting areas of relative highs and lows (i.e., high <sup>222</sup>Rn and winter water temperature; low conductivity, dissolved oxygen and summer water temperature). To produce robust interpretations of the results, we examined all the datasets together, as each parameter has its limitations.

## **2.4 Results**

### **2.4.1 Thermal infrared imaging**

The TIR survey revealed spatial temperature differences on the lagoon surface (Figure 2.3). The imagery identified both localised (Figure 2.3a, b, g) and diffuse areas of colder water (Figure 2.3c, d, e, f). We detected colder temperatures near the margins of the lagoon but not in the centre of the lagoon. At the time of the survey, the temperatures measured by TIR imagery (i.e., the equivalent surface temperature) in the centre of the lagoon were approximately between 19 and 21°C, while most surface tributaries were between 17 and 18°C. The coldest lagoon surface temperatures measured in the survey were between 15 and 16°C.

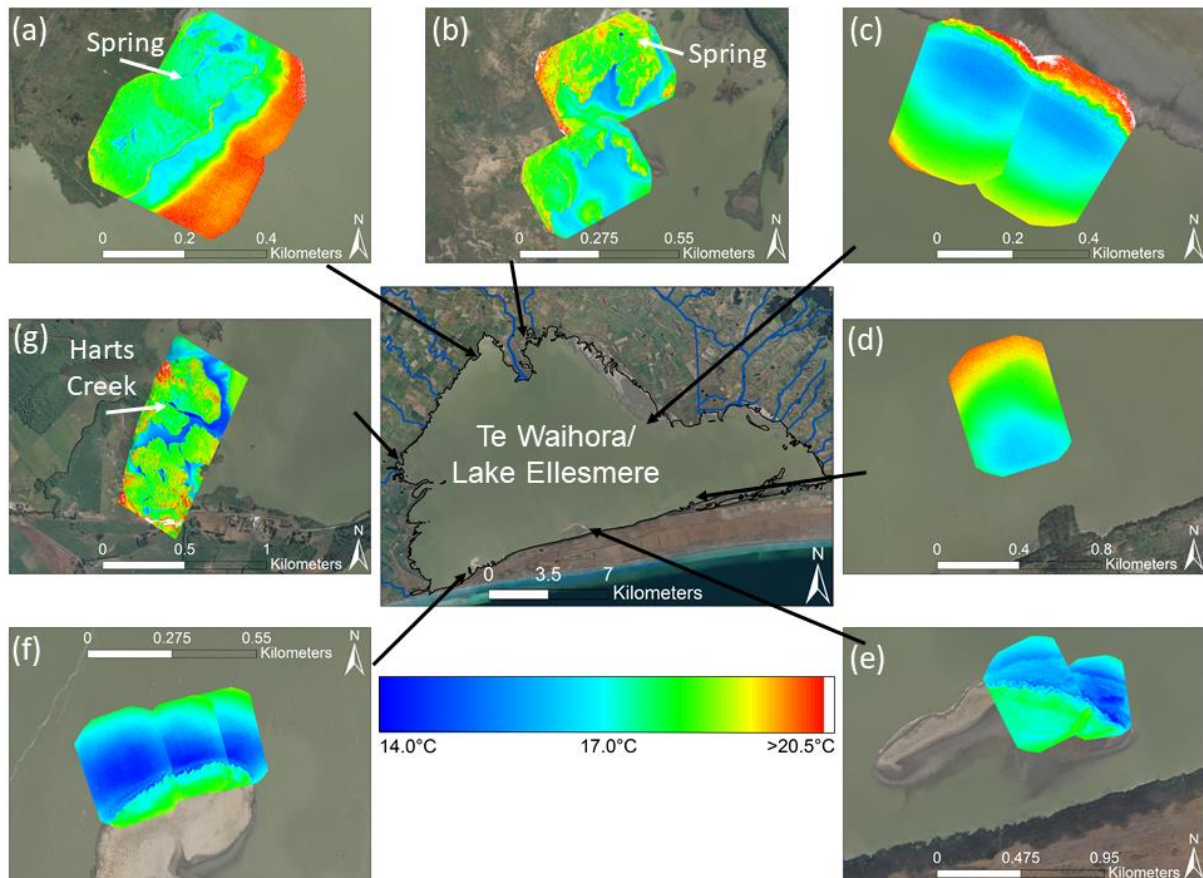


Figure 2.3. Results from the January 2019 airborne thermal imaging survey from selected areas of Te Waihora. In sub-figures (a) and (b), springs that were detected by the TIR imaging are marked with arrows. In sub-figure (g), Harts Creek, a tributary of Te Waihora, is labelled. Map base layer credits: Esri, DigitalGlobe, GeoEye, Earthstar Geographics, CNES/Airbus DS, USDA, USGS, AeroGRID, IGN, and the GIS User Community. Map includes GIS data from Land Information New Zealand (Land Information New Zealand, 2019, 2020).

The TIR imaging revealed several locations of cooler water that could not be linked to tributary inflows (Figure 2.3c, d, e, f). We also detected cold plumes entering the lagoon from tributaries, particularly from streams that are groundwater fed, such as Harts Creek (Figure 2.3g). In addition, the TIR imaging showed areas of the lagoon where surface springs emerge on the shore or in shallow mudflat areas that flow into the lagoon (Figure 2.3a-b).

The TIR imaging was carried out during the summer, as this season has the largest thermal contrast between groundwater ( $\sim 12\text{--}13^{\circ}\text{C}$  on average) and the lagoon ( $\sim 20\text{--}25^{\circ}\text{C}$  on average). As TIR imaging measures brightness temperatures related to the in-situ surface temperatures of the lagoon, to be effective, it would be necessary for the temperature signal (i.e., the cold plume) from the groundwater discharge to reach the surface of the lagoon. During the time of the survey, the lagoon was on average only 0.5 masl with an average depth of approximately 1 m, which are very shallow conditions for Te Waihora. We suspected this would be to our advantage for detecting groundwater seepage, as in these

conditions, there would be only a shallow water column for the cold groundwater plume to travel upwards through to the top. In addition, where we surveyed on the perimeter of the lagoon, the water depths would have generally been less than 0.5 m. Given the brackish water in the lagoon (14,000-25,000  $\mu\text{S}/\text{cm}$  at time of survey), we expected the density difference between fresh groundwater and brackish lagoon water would facilitate the movement of less dense groundwater to the top of the water column and make it more likely the TIR imaging would detect freshwater plumes. In contrast, we considered that the water column could have thermal stratification at the time of the survey, with cold groundwater remaining at the bottom of the water column, which may have made the imaging ineffective. However, temperature data from in-situ loggers in the lagoon revealed no temperature stratification in the lagoon during the flight.

#### **2.4.2 In-situ water temperature**

In the summer, lagoon water temperatures ranged from 20.8 to 29.3°C (Figure 2.4a), and in the winter, temperatures ranged from 8.6 to 14.9°C (Figure 2.4b). The summer survey did not reveal temperature decreases that might signal groundwater inflow, except for offshore of the island midway on the Kaitorete barrier where temperatures suddenly dropped from 29°C to as low as 24.6°C (see marker 1 in Figure 2.4a). The winter survey detected several high, anomalous temperature readings. For example, near Timbaryard Point on the west side of the lagoon, the temperatures sharply increased from 9.3°C to 10.7°C and then dropped to ~9.5°C (see marker 1 in Figure 2.4b). In addition to Timbaryard Point, anomalously high temperature readings were also detected during the winter survey in the centre of the lagoon, mostly near the Selwyn/Waikirikiriri River peninsula (Figure 2.4b, marker 2), near the southern tip of Greenpark Sands (Figure 2.4b, marker 3), in Kaituna Lagoon (Figure 2.4b, marker 4), and along the Kaitorete barrier, at its east (Figure 2.4b, marker 5) and southwest ends (Figure 2.4b, marker 6).



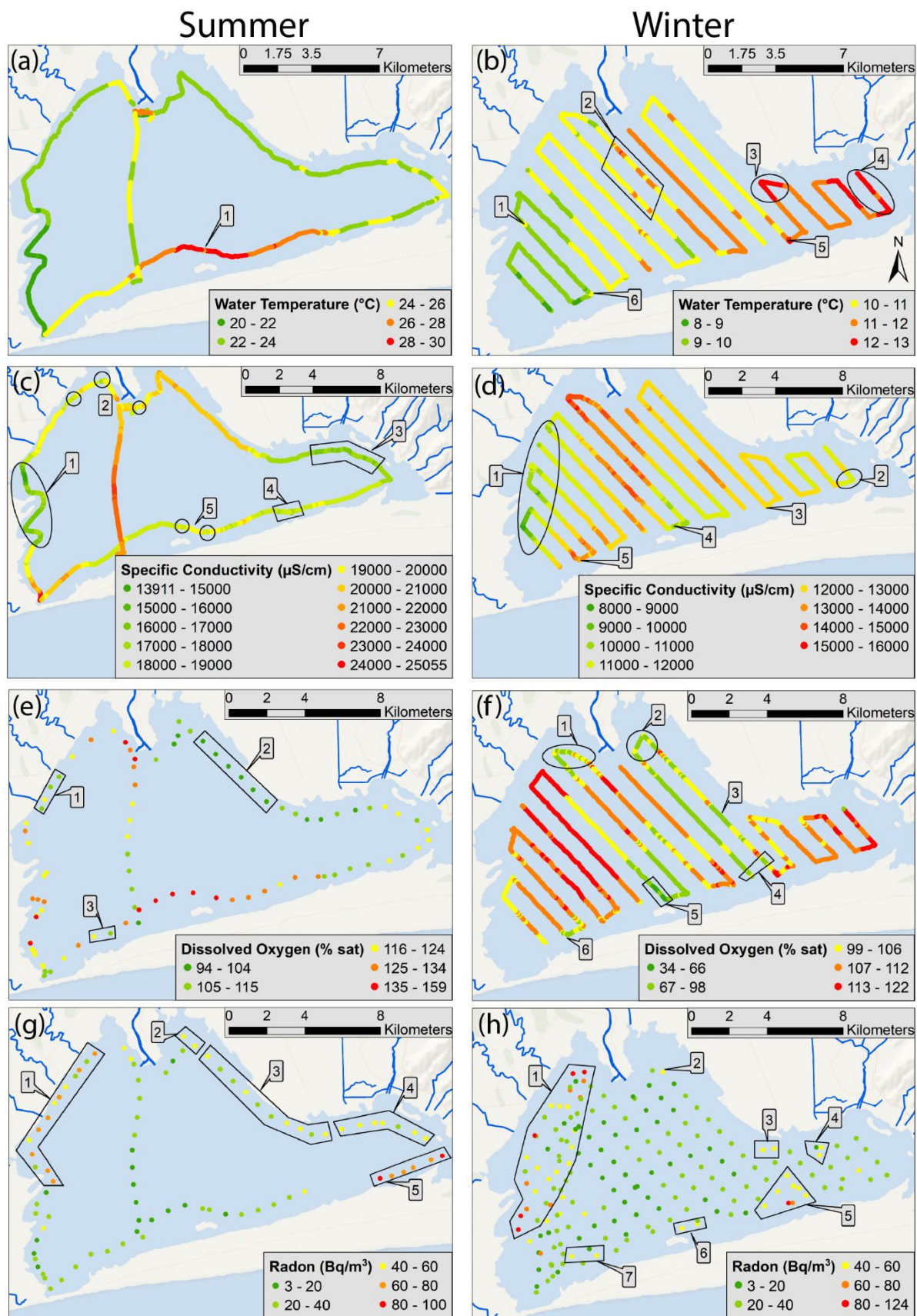


Figure 2.4. Results from the continuous boat surveys in January 2019 (summer) and August-September 2019 (winter): (a) summer in-situ water temperature, (b) winter in-situ water temperature, (c) summer conductivity, (d) winter conductivity, (e) summer dissolved oxygen, (f) winter dissolved



oxygen, (g) summer  $^{222}\text{Rn}$ , (h) winter  $^{222}\text{Rn}$ . Numbered markers on figures refer to areas discussed in the text. Map base layer credits: Esri, Garmin, GEBCO, NOAA NGDC, and other contributors. Map includes GIS data from Land Information New Zealand (Land Information New Zealand, 2019, 2020).

### **2.4.3 Conductivity**

In the summer and winter surveys, we observed considerable spatial variability in specific conductivity across the lagoon (Figure 2.4c-d). Shallow groundwater sampled on the lagoon shore had conductivity values between 2800-8300  $\mu\text{S}/\text{cm}$ . We expected the conductivity difference to provide a sufficiently strong freshwater signal to detect in the lagoon. We measured lagoon specific conductivity in the range of 13900-25000  $\mu\text{S}/\text{cm}$  in summer with two main areas of low readings: on the western side of the lagoon around Timbervard Point (as low as 14300  $\mu\text{S}/\text{cm}$ ) and on the eastern side in Kaituna Lagoon (Figure 2.4c, markers 1 & 3, respectively). There were also localised areas of low readings around the Selwyn/Waikirikiriri peninsula and along the Kaitorete barrier (Figure 2.4c, markers 2, 4 & 5, respectively). In winter, we measured specific conductivity ranging from 8600-15500  $\mu\text{S}/\text{cm}$  with similar areas of low conductivity as in summer: near Timbervard Point (though in this case low conductivity along the entire western edge) (Figure 2.4d, marker 1), in Kaituna Lagoon (Figure 2.4d, marker 2), and along the Kaitorete barrier (Figure 2.4d, markers 3, 4 & 5).

We measured relatively high conductivity ( $>20000$   $\mu\text{S}/\text{cm}$  in summer and  $>13000$   $\mu\text{S}/\text{cm}$  in winter) in the centre of the lagoon during both surveys. In the winter survey, this area of high conductivity extended even further north than in the summer survey to the western side of the Selwyn/Waikirikiriri River peninsula (Figure 2.4). These results were surprising, as the Selwyn/Waikirikiriri River and the LII River (directly to the east of the outlet of the Selwyn) are the two largest tributaries, so we suspected lower conductivity in this area due to inflows of surface freshwater. This is also far from the lagoon's outlet to the sea. Previous studies have shown the lagoon to be most saline near the ocean outlet (Lineham, 1983; Spigel, 2009).

### **2.4.4 Dissolved Oxygen**

Dissolved oxygen ranged from 94 to 159% saturation (Figure 2.4e) and from 34 to 122% saturation (Figure 2.4f) in the summer and winter surveys, respectively. In the summer survey, the area of the lagoon with the lowest dissolved oxygen was along Greenpark Sands where the saturation dropped to its lowest level (94%) across the 3-day survey (Figure 2.4e, marker 2). We also recorded areas of low dissolved oxygen on the western side of the lagoon north of Timbervard Point and at the southwest end of the Kaitorete barrier (Figure 2.4e, markers 1 & 3, respectively). The winter survey, which had

significantly more data points, with automated readings every minute compared to manual readings approximately every 10 minutes, revealed more noteworthy data points than the summer survey. There were several readings of interest to the east and west of the Selwyn/Waikirikiriri River peninsula (Figure 2.4f, markers 1 & 2, respectively), one location of low readings at the southern end of Greenpark Sands (Figure 2.4f, marker 3 & 4) and areas of low readings along the Kaitorete barrier (Figure 2.4f, markers 5, 6 & 7).

#### 2.4.5 Radon

During the summer and winter surveys, we measured a range of  $^{222}\text{Rn}$  concentrations in the lagoon (3-87 Bq/m<sup>3</sup> and 3-124 Bq/m<sup>3</sup>, respectively) (Figure 2.4g-h). The overall 1-sigma counting uncertainty was 19 Bq/m<sup>3</sup> for both surveys, when integrating observations over 10 minutes. Because the  $^{222}\text{Rn}$  readings were measured while moving in the boat, we can only draw qualitative conclusions about a given location in the lagoon from the data.

In general, the measured  $^{222}\text{Rn}$  concentrations were higher at the lagoon margins. The area with the highest readings was the west side of the lagoon, with several readings between 60-80 Bq/m<sup>3</sup> during summer and five measurements above 80 Bq/m<sup>3</sup> in winter (see marker 1 in Figure 2.4g-h). We found localised areas of high readings on the north side of the lagoon on the east side of the Selwyn/Waikirikiriri River peninsula (Figure 2.4g-h, marker 2). We measured higher radon concentrations along Greenpark Sands in summer and on the margins of a smaller portion of Greenpark Sands at its southern tip during winter (Figure 2.4g-h, marker 3). There were higher radon measurements on the eastern side in Kaituna Lagoon as well (Figure 2.4g-h, marker 4). Along the Kaitorete barrier, there was a more pronounced radon signal in the winter survey (Figure 2.4h, markers 5, 6 & 7). Whereas in the summer survey, there was only evidence of high radon at the eastern end of the barrier with five readings between  $64 \pm 24$  and  $87 \pm 27$  Bq/m<sup>3</sup> (Figure 2.4g, marker 5), which was at the higher end of the measured radon concentrations. In regard to markers 2, 3, 4, 6 and 7 in Figure 2.4h, while the radon concentrations are only slightly elevated compared to the background radon concentrations in the lagoon, we deemed these areas noteworthy to highlight. Markers 2, 3, 4 and 6 in Figure 2.4h had lower uncertainty (~8-9%) compared to the radon data collected in the summer survey (on average 87% uncertainty). In regard to marker 7 in Figure 2.4h, the two higher radon concentrations highlighted have higher uncertainty (80-100%) than the data points discussed above. However, these two data points were high readings ( $59 \pm 48$  Bq/m<sup>3</sup> and  $43 \pm 43$  Bq/m<sup>3</sup>) compared to nearby radon concentrations, which were between 18-29 Bq/m<sup>3</sup>. We interpreted the  $^{222}\text{Rn}$  results in tandem with wind speeds. To minimise atmospheric evasion that would

complicate the interpretation of the groundwater signal, we collected data at times of relatively low wind speeds to the greatest extent possible.

## 2.5 Discussion

### 2.5.1 Integrating multiple lines of evidence to detect groundwater seepage

We chose a multi-method design to ensure that our findings are robust in light of the limitations of interpretations based on a single parameter alone (Kalbus et al., 2006). Aligning multiple parameters indicates potential groundwater inflow in six main areas of the lagoon (see Figure 2.5). We have qualitatively ranked our confidence levels in each parameter measured at these locations in terms of whether they suggest groundwater seepage (Table 2.2).

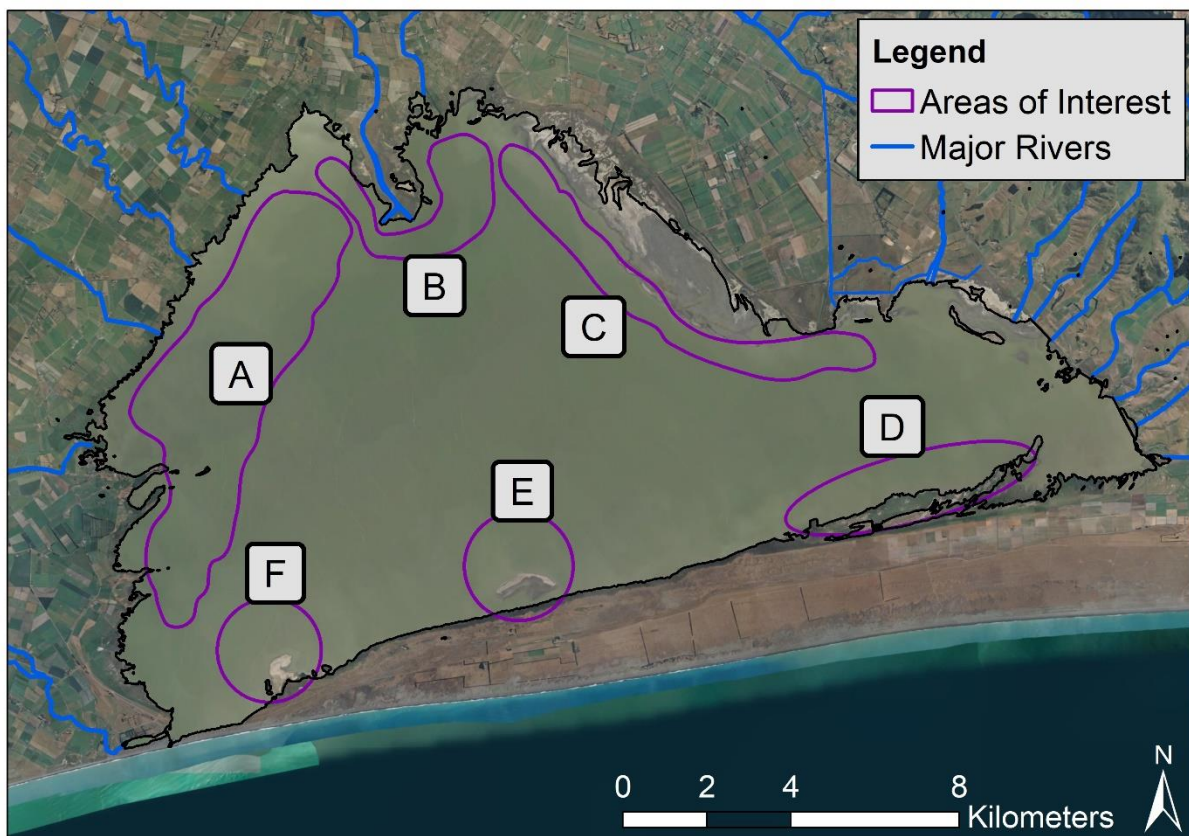


Figure 2.5. Six main areas where results from the broad-scale spatial surveys indicate potential groundwater inflow. A = West Side, B = Selwyn Peninsula, C = Greenpark Sands, D = Kaitorete Barrier East, E = Kaitorete Barrier Mid, F = Kaitorete Barrier Southwest. There were indications of seepage through the lagoon bed on all sides of the lagoon but only close to the margins. Map base layer credits: Esri, DigitalGlobe, GeoEye, Earthstar Geographics, CNES/Airbus DS, USDA, USGS, AeroGRID, IGN, and the GIS User Community. Map includes GIS data from Land Information New Zealand (Land Information New Zealand, 2019, 2020).

Table 2.2. A qualitative ranking of all parameters measured in terms of confidence level on whether they indicate groundwater seepage at the six main areas of interest in Te Waihora shown in Figure 2.5. Parameters with high confidence are in bold.

Area Name	Parameters Measured								
	Summer					Winter			
	Water Temperature (in-situ)	Conductivity	Dissolved Oxygen	<sup>222</sup> Rn	Airborne Thermal Imaging	Water Temperature (in-situ)	Conductivity	Dissolved Oxygen	<sup>222</sup> Rn
West Side	Low	<b>High</b>	Medium	<b>High</b>	<b>High</b>	Medium/High	<b>High</b>	Low	<b>High</b>
Selwyn Peninsula	Low	Medium/High	Low	Medium	<b>High</b>	Low	Low	Medium	Medium
Greenpark Sands	Low	Low	Medium	Medium	<b>High</b>	Medium	Low	Medium	Medium
Kaitorete Barrier East	Low	Medium	Low	Medium	Medium	<b>High</b>	Medium	Low	<b>High</b>
Kaitorete Barrier Mid	<b>High</b>	<b>High</b>	Low	Low	<b>High</b>	Low	<b>High</b>	<b>High</b>	Medium
Kaitorete Barrier Southwest	Low	Low	Medium	Low	<b>High</b>	<b>High</b>	<b>High</b>	<b>High</b>	Medium

We only found signs of potential seepage on the lagoon margins, despite covering areas away from the margins in the winter survey. This is in line with findings of previous seepage meter measurements that showed maximum seepage rates generally occurring within 20 m of the shore (Ettema & Moore, 1995).

We identified areas of potential groundwater seepage on the western and north-western sides of the lagoon (see area A in Figure 2.5) and around the Selwyn/Waikirikiri peninsula (see area B in Figure 2.5), which is consistent with Ettema and Moore (1995). Piezometric contour maps suggest that the majority of groundwater inflow to Te Waihora originates from the alluvial plains to the north and west and enters the lagoon at the western and north-western margins (Williams, 2010). This correlates well with our evidence of groundwater inflow along these margins. It is also important to note that there are many large surface water tributaries and several smaller streams and drains that enter the lagoon in this area. Many are largely recharged by groundwater, therefore this can make it more difficult to distinguish between freshwater sourced from bed seepage and surface water inflows.

We also identified areas of potential groundwater discharge along the Kaitorete barrier (see areas D-F in Figure 2.5). We have two hypotheses for the source of seepage along the barrier: that seepage is sourced from (1) the confined aquifer system underlying the lagoon and/or (2) shallow groundwater flow from the unconfined aquifer on the barrier. Ettema and Moore (1995) suggest that seepage occurs along the barrier as a result of upwards hydraulic gradients within the confined aquifer system. Ettema and Moore (1995) concluded that upwelling groundwater moved through a thick layer of fine sediments up to 30 m thick. However, we argue that as the lagoon bed becomes coarser towards the mixed sand and gravel barrier, this may form a preferential pathway for groundwater flow. We also hypothesise that the source of groundwater may be from the water table on the barrier intersecting with the lagoon bed, which would be a previously unidentified source of seepage to the lagoon (Bokuniewicz & Pavlik, 1990; Rapaglia, Di Sipio, et al., 2010).

We also found indications of groundwater seepage at Greenpark Sands on the north-eastern side of the lagoon (see area C in Figure 2.5), which had not been found in previous studies. The surface of Greenpark Sands is overlain by a confining layer of fine sediments. Where we found evidence of seepage at the margin of Greenpark Sands, this may be upwelling groundwater from beneath this confining layer. At neither the Kaitorete barrier nor Greenpark Sands are there surface tributaries that could confound the interpretation. However, given we did not detect any areas of low conductivity at Greenpark Sands suggesting freshwater inputs, what we observed may have been evidence of porewater exchange across the sediment-water interface of the lagoon. This cm-scale circulation process, which has been observed in other coastal lagoons, would not result in a net freshwater flux (Martin et al., 2006; Rodellas et al., 2020; Rodellas et al., 2018). Previous studies have shown that bed

porewater exchange can influence the overlying oxygen (Precht et al., 2004) and radon concentrations (Cook et al., 2018).

We initially expected groundwater discharge hotspots away from the edges because there is an artesian groundwater system underneath the lagoon. However, we found little or no evidence of this. Our findings are in line with previous spatial studies of lakes and lagoons revealing seepage rates to be highest at the margins, particularly in shallow and low bed-slope waterbodies (Barwell & Lee, 1981; Genereux & Bandopadhyay, 2001; McBride & Pfannkuch, 1975).

This pattern of concentrated seepage at the margins is unlikely to fit all lake or coastal lagoon settings. Rosenberry et al. (2015) note that this is likely only the case where the geology underlying and adjacent to the lake is homogeneous. While the geology underlying and surrounding the current study site is not homogeneous, our evidence suggests seepage is concentrated at the margins. However, previous seepage meter measurements found an “irregular” seepage pattern in some parts of the lagoon due to non-homogenous bed sediments (Ettema & Moore, 1995). It is important to note though that seepage meter measurements might not adequately capture the spatial heterogeneity of seepage rates, and this may largely depend on the number of seepage meters installed and their locations (Duque et al., 2020; Rosenberry et al., 2020). Lake and lagoon bed sediments are often anisotropic, i.e., horizontal and vertical hydraulic conductivity are not equal. The higher the anisotropy, the less seepage is focused at the margins (Genereux & Bandopadhyay, 2001). Several studies have found groundwater seepage in lakes and coastal lagoons to follow atypical patterns (e.g., Cherkauer & Nader, 1989; Duque et al., 2018; Gibbs et al., 2005). As Rosenberry et al. (2015) highlight, often in these cases, geology is the determining feature over other factors that might influence seepage patterns (e.g., erosion or deposition of sediment; manipulation of near-shore sediment by biological or physical processes; or manmade alterations). However, some studies have contradicted this. For example, in a coastal lagoon in Denmark, a saline wedge forcing upwards flow; vegetation and organic material deposition on the shoreline; and the recirculation of brackish water due to wave pumping offshore drive “atypical” patterns of seepage (Duque et al., 2018).

Analysing the TIR dataset can be challenging due to confounding factors. Groundwater discharge, which was relatively colder than the surface water, might have remained at the bottom of the water column and been missed by our TIR survey. Despite efforts to target a survey time to minimise the impact of lagoon waves on temperature readings, we had moderate winds during the survey (average 19 km/h, ranging between 6-29 km/h). There were higher wind speeds in the three hours prior to the survey (34-41 km/h). Given these wind speeds, we expect the water column was vertically well mixed at the time of the survey. We compared the TIR results with multi-level temperature readings from permanently installed loggers in the centre of the lagoon and at Taumutu. At the time of the survey

(7:30-8:45 am), these loggers did not show any temperature stratification that would have interfered with the TIR results.

It is also possible that colder temperatures at the lagoon shore resulted from cooler water emerging from the sediment due to wave re-circulation. However, we expect this to be unlikely at the time of the survey. Waves would not explain cold temperatures detected on the east and south sides of the lagoon. Several hours prior to and during the survey, the wind direction was easterly, so the surface water would have been pushed westward in the lagoon, making wave re-circulation of water on the eastern and southern shores unlikely. Also, the cooling of lagoon water via wave re-circulation would require cooler ambient temperatures compared to the lagoon water, but at the time of the survey, the air temperature was only marginally cooler than the lagoon (17-19°C compared to 19°C, respectively).

Lagoon bathymetry may have also had an effect on surface temperature distributions (i.e., water temperatures in shallower areas may react more quickly to atmospheric conditions than deeper locations) (Tamborski et al., 2015). If this were the case, we would have expected to in general observe warmer surface temperatures near the lagoon margins as result of the shallow water warming more quickly than deeper waters. However, what we observed was the opposite: the TIR imaging generally showed cooler temperatures at the margins. Future studies should therefore consider measuring temperature gradients along transects perpendicular to the shore to evaluate possible bathymetry effects.

It is also possible that in some locations, colder temperatures detected with the TIR imagery were due to tributary inflows. We analysed the TIR imagery in tandem with satellite imagery to assess the likelihood of surface inflows being the source of colder temperatures.

### **2.5.2 Method advantages and disadvantages**

Each broad-scale approach used to map groundwater discharge has certain advantages and limitations (Table 2.3). The airborne TIR survey was particularly time effective. We covered ~170 km around the perimeter of the lagoon and several transects across the centre in just over one hour. All of the measurement techniques provided real-time data (with a 30-min time lag for the  $^{222}\text{Rn}$  data), which was conducive to making field observations and adapting the sampling strategy along the way, or for making repeated readings at a location of interest. While the findings in this study are qualitative, they provide a general picture of a large, dynamic and geologically heterogeneous system, where a limited number of point measurements cannot (LaBaugh & Rosenberry, 2008). This broad-scale approach allows for key areas of interest to be identified where further investigations can focus, as well as the identification of important areas for management.

Table 2.3. Advantages and disadvantages of the methods used in this study for characterising the spatial distribution of groundwater seepage in coastal lagoons

Method	Advantages	Disadvantages
<sup>222</sup> Rn	<ul style="list-style-type: none"> <li>• Conservative, not affected by biological parameters</li> <li>• Real-time data in the field</li> <li>• Ability to collect additional data to quantify groundwater discharge</li> </ul>	<ul style="list-style-type: none"> <li>• Radon signal is highly wind affected; Surveys should avoid high wind speeds</li> <li>• May be difficult to detect sufficient surface water/groundwater contrast in areas with naturally low radon</li> <li>• Low-frequency acquisition of data</li> <li>• Cost of instrumentation and expertise</li> <li>• Groundwater-fed tributaries may confound radon data</li> <li>• Does not distinguish between net groundwater discharge and bed recirculation</li> </ul>
Water temperature (in-situ)	<ul style="list-style-type: none"> <li>• Simple to measure and analyse</li> <li>• Can provide real-time, high-frequency, automated data in the field</li> <li>• Can easily measure at varying depths in water column</li> </ul>	<ul style="list-style-type: none"> <li>• Diurnal temperature cycles confound interpretation</li> <li>• Water column temperature may be stratified</li> <li>• Tributaries may confound temperature data</li> </ul>
Conductivity	<ul style="list-style-type: none"> <li>• Simple to measure and analyse</li> <li>• Can provide real-time, high-frequency, automated data in the field</li> <li>• Can easily measure at varying depths in water column</li> </ul>	<ul style="list-style-type: none"> <li>• Vertical stratification of salinity</li> <li>• Lagoon salinity often controlled by factors other than groundwater (e.g., wind re-distribution of salts, seawater inputs)</li> <li>• Tributaries may confound conductivity data</li> </ul>
Dissolved oxygen	<ul style="list-style-type: none"> <li>• Simple to measure and analyse</li> </ul>	<ul style="list-style-type: none"> <li>• Diurnal photosynthesis/respiration cycles dominate oxygen distribution</li> </ul>



	<ul style="list-style-type: none"> <li>• Can provide real-time, high-frequency, automated data in the field</li> <li>• Can easily measure at varying depths in water column</li> </ul>	<ul style="list-style-type: none"> <li>• Sufficient gradient between groundwater and surface water must exist</li> </ul>
Airborne thermal infrared imaging (via fixed-wing aircraft)	<ul style="list-style-type: none"> <li>• Can quickly cover a large area</li> <li>• Using fixed-wing aircraft can be very cost effective</li> <li>• Several advantages over surveys done with Unmanned Aerial Vehicles (e.g., no issues with batteries, sight line requirements, launching access/permissions)</li> </ul>	<ul style="list-style-type: none"> <li>• Minimal wind and cloud cover required</li> <li>• Temperature signal from groundwater must reach surface of lagoon</li> <li>• Most effective when there is considerable temperature contrast in images</li> <li>• Surface inflows and diel heating cycles may confound the interpretation</li> <li>• Expensive camera equipment usually required</li> <li>• Close proximity to airport lowers costs</li> <li>• Need to balance flight height/speed/lens size with desired image outputs (may be trade-offs)</li> <li>• Image processing may be difficult and/or time consuming, particularly for large datasets with minimal feature definition</li> </ul>

There are some limitations with this study design, including the time required to obtain high-resolution  $^{222}\text{Rn}$  measurements with the continuous boat surveys. With the parameters measured here, it is not always possible to distinguish between groundwater discharge, spring-fed surface inflows or porewater exchange (Sadat-Noori et al., 2016). Previous studies (e.g., Rodellas et al., 2020; Stieglitz et al., 2013) have found porewater exchange in coastal sediments to be a significant source of recirculated biogeochemical species, including  $^{222}\text{Rn}$ . Porewater exchange has not been measured at this site, so it is not known whether this is a source of  $^{222}\text{Rn}$  to the lagoon.

Natural variability in lagoon conditions such as wind, diurnal temperature change, biological activity, antecedent precipitation and seasonal changes may complicate the collection and interpretation of the data. As a gas,  $^{222}\text{Rn}$  in surface water evades to the atmosphere depending primarily on wind velocity (MacIntyre et al., 1995). Wind speeds are thus important to consider (Crusius & Wanninkhof, 2003) and are particularly relevant at this highly wind-affected site. Wind may also redistribute and mix fresh and brackish water around lagoons (Kennish & Paerl, 2010). Using dissolved oxygen as a groundwater tracer is difficult because oxygen levels fluctuate based on biological activity. In some eutrophic lagoons, such as the current study site, there may be a high concentration of phytoplankton (Gerbeaux & Ward, 1991; Kennish & Paerl, 2010) producing oxygen during the day. Oxygen concentrations may also be influenced by respiration of organic material present in the lagoon bed (Ortega-Arbulú et al., 2019). It is possible that density differences result in vertical stratification in the water column; however, both the present study and Spiegel (2009) found the water to be vertically well mixed in Te Waihora.

Finally, processing airborne thermal imaging data can be a significant undertaking requiring scripting or photogrammetry skills, particularly when working with large data sets. Using photogrammetry software to create orthomosaics of the imagery, as was done here, is best suited for images with distinguishable features. Thus, it is very difficult to use photogrammetry to stitch together images taken over open water or shorelines with minimal distinct features. If it is feasible to simultaneously take visible light images with the TIR images, this may make mosaic stitching easier (e.g., Lee et al., 2016).

While the TIR imagery was processed to remove distortion from the wide-angle lens, there is still some minor geometric lens distortion in the imagery presented in Figure 2.3. The edges of the images also have a radial distortion as a result of differential warming and cooling of the microbolometer sensor array in the camera. This radial distortion resulted in some of the images showing high temperatures at the edges, which are not reflective of actual conditions on the lagoon surface.

## 2.6 Conclusion

This study provides an example of effective techniques for surveying large coastal lagoons to obtain a broad-scale view of groundwater discharge and identify areas of interest. We conducted broad-scale seasonal surveys to determine the spatial distribution of groundwater seepage to a large coastal lagoon in New Zealand. The study site features complex geomorphology and hydrogeology, including a mixed sand and gravel barrier and an underlying multi-layered artesian coastal aquifer system. In addition to these features, the numerous, largely groundwater-fed surface tributaries and dynamic lagoon conditions, have previously made investigations of seepage across the entire site difficult.

We addressed these challenges by combining airborne TIR imagery with continuous boat-based spatial surveys of  $^{222}\text{Rn}$ , conductivity, in-situ water temperature and dissolved oxygen. Multiple lines of evidence allowed us to map groundwater seepage locations with greater confidence. We found seepage along the margins of the lagoon but no strong indications of discharge away from the margins. The main areas of potential groundwater seepage that we highlighted in our surveys were on the western margins of the lagoon and along the barrier between the lagoon and the sea. These observations imply geologic controls on seepage to the lagoon. The combination of methods allowed us to map areas of discharge across the entire lagoon in a cost and time-effective way. This type of broad-based method can be used to identify key areas of interest to be further investigated or incorporated into management processes. This study demonstrates the benefits of these broad-scale qualitative methods for gaining a better understanding of large, dynamic and geologically heterogeneous coastal lagoons.

### **3. Groundwater discharge rates and uncertainties in a coastal lagoon using a radon mass balance**

#### **3.1 Abstract**

Coastal lagoons face anthropogenic pressures worldwide, and understanding groundwater discharge to these sensitive environments can enable better management of water budgets and nutrient inputs. The main objective of the study was to quantify groundwater seepage into a large and shallow coastal lagoon using a detailed radon ( $^{222}\text{Rn}$ , a natural groundwater tracer) mass balance. To assess and reduce uncertainty, three wind-speed scenarios were modelled in two seasons using two  $^{222}\text{Rn}$ -in-groundwater endmembers. Groundwater discharge to the lagoon ranged between  $5.2 \pm 5.8 \text{ m}^3/\text{s}$  to  $19 \pm 20 \text{ m}^3/\text{s}$  during summer and  $0.9 \pm 2.2 \text{ m}^3/\text{s}$  to  $8.1 \pm 10 \text{ m}^3/\text{s}$  during winter. Wind-driven radon evasion was the most influential component of the radon mass balance. Higher summer wind speeds resulted in groundwater discharge estimates 3.5 times greater than those during winter. We carried out an in-depth uncertainty analysis of the radon mass balance results, which confirmed the importance of accounting for individual uncertainties, particularly the most sensitive parameters of the model. Overall, results from the radon mass balance revealed groundwater discharge to the lagoon was 1-2 orders of magnitude greater than previous localised seepage meter estimates. This is likely because radon tracer approaches quantify both one-directional discharge and bi-directional porewater exchange at a larger spatial scale than traditional seepage meter methods. In spite of large uncertainties, the possible range of reasonable estimates revealed groundwater seepage as an important component of the water budget at this site. This study highlights the benefits of broad-scale tracer-based mass balances for quantifying groundwater discharge to coastal lagoons and the value of in-depth uncertainty analysis to increase confidence in seepage flux estimates.

#### **3.2 Introduction**

Coastal lagoons are sensitive, yet threatened, coastal water bodies found throughout the world. Their connectivity with the ocean ranges from “choked” lagoons featuring narrow entrance channels, long water residency times and little tidal fluctuation, to “leaky” lagoons, which have several inlets open to the ocean, strong tidal influence and salinity similar to the ocean. Coastal lagoons are important for ecological, cultural, economic and recreational reasons, however, they face significant anthropogenic pressures such as physical modifications to natural features and habitat degradation (Beer & Joyce, 2013; Schallenberg et al., 2013). Situated at the end of catchments, these water bodies are the receiving environments from all upstream land uses, so they often suffer from eutrophication.

Since it is difficult to quantify groundwater discharge into coastal lagoons, groundwater is often neglected as a component of water and nutrient budgets (Sadat-Noori et al., 2016; Santos, Niencheski, et al., 2008). However, estimates of groundwater inputs into lakes and coastal lagoons can be important for understanding contaminant loads and water budgets (Duque et al., 2018; Menció, Casamitjana, Mas-Pla, Coll, Compte, et al., 2017; Rudnick et al., 2015; Stieglitz et al., 2013). Many studies have shown that groundwater inflow to coastal environments is a vector for transport of chemical species such as acid (Jeffrey et al., 2016), heavy metals (Ganguli et al., 2012), nutrients (Ji et al., 2013; Knapp et al., 2020; Santos, Machado, et al., 2008), carbon (Maher et al., 2019) and rare earth minerals (Johannesson et al., 2011). Even where groundwater discharge comprises a small proportion of a lagoon's water balance, it can contribute a significant nutrient load, because groundwater often contains high concentrations of dissolved species (Meinikmann et al., 2013; Santos, Niencheski, et al., 2008; Stieglitz et al., 2013).

Research quantifying groundwater discharge into coastal lagoons has increased in the past decade. Most of these studies have tended to focus on smaller study sites, coastlines with sand barriers, lagoons featuring minimal surface inflows (seasonally or year-round), and/or on sites in Mediterranean or subtropical/tropical climates (e.g., Ji et al., 2013; Menció, Casamitjana, Mas-Pla, Coll, Compte, et al., 2017; Stieglitz et al., 2013). There have been fewer studies that have attempted to quantify groundwater discharge to large ( $>100 \text{ km}^2$ ) lagoons located in temperate climates, with mixed sand and gravel coastlines, and complex hydrology (e.g., many surface inflows, managed opening regimes to the sea). This may be due to the difficulty in measuring groundwater exchange in larger lagoons because of issues relating to method scale; therefore, more studies demonstrating large-scale applications of techniques are required (Kalbus et al., 2006). Furthermore, climate can significantly influence how lagoons function (e.g., seasonal precipitation patterns and evapotranspiration rates), thus it is important that we understand how groundwater exchange affects coastal lagoons in a range of climates (Manzoni et al., 2020). In regard to lagoons on mixed sand and gravel coastlines, these differences in sediment types can correspond with notable differences in lagoon environments, such as lagoon bed and barrier permeability, coastline wave energy, and sediment deposition and erosional processes (Hart, 2007).

Previous studies have used a variety of indirect and direct measurements to quantify groundwater seepage to lagoons. Some have found seepage to comprise a minimal component of lagoon water budgets (e.g., Stieglitz et al., 2013), while others have found direct groundwater discharge to be the main contributor to water balances, either year-round or during dry months where surface inflows are minimal (e.g., Menció, Casamitjana, Mas-Pla, Coll, Compte, et al., 2017; Sadat-Noori et al., 2016). Various approaches have been used to estimate groundwater inputs to coastal lagoons including point-scale methods such as seepage meters (e.g., Duque et al., 2018; Leote et al., 2008) and broad-scale techniques such as geochemical tracers like salinity (e.g., Stieglitz et al., 2013), radon (e.g., Maher et

al., 2019; Rodellas et al., 2018), radium (e.g., Bejannin et al., 2017; Ji et al., 2013) and strontium (Danish et al., 2020); water budgets; and numeric modelling (e.g., Alcolea et al., 2019). Estimating groundwater inputs to coastal lagoons using volumetric water balances (e.g., Alcolea et al., 2019; Chikita et al., 2012; Chikita et al., 2015) is challenging because all other variables in the water budget also need to be well constrained. Radon mass balances have become an increasingly common technique for quantifying groundwater discharge to coastal areas (Atkins et al., 2013; Burnett & Dulaiova, 2003; Lopez et al., 2020; Sadat-Noori et al., 2015).

Radon ( $^{222}\text{Rn}$ ) is a useful groundwater tracer because it has a relatively short half-life ( $\lambda = 3.82$  days), is chemically non-reactive and its typical concentration in groundwater is 1-2 orders of magnitude higher than in surface water. The availability of real-time, portable radon detectors such as the RAD7 (DurrIDGE Inc., Billerica, MA) and the AlphaGuard (Bertin, Montigny Le Bretonneux, France) (Schubert et al., 2019) has made radon analysis more accessible and precise, especially at remote field sites. The broad-scale nature of radon mass balances enables the quantification of groundwater discharge in large or geologically heterogeneous sites, where point-scale methods would be impractical.

Radon mass balances have become an increasingly popular tool, but the uncertainties surrounding their estimations of groundwater discharge remain poorly understood (Rodellas et al., 2021; Sadat-Noori et al., 2015). While most groundwater discharge rates from radon mass balances are reported with estimated uncertainty, few studies have carried out in-depth uncertainty analysis on all the mass balance variables (e.g., Kluge et al., 2012; Petermann, Knöller, et al., 2018; Sadat-Noori et al., 2015), while some have not reported uncertainty alongside discharge estimates. As radon mass balances are used more frequently for hydrological investigations, and the data these models produce are incorporated in water resource management more often, there is a need to increase the confidence in mass balance estimates.

In this study, we build a detailed radon mass balance for a coastal lagoon with characteristics underrepresented in earlier studies—a large ( $\sim 150 \text{ km}^2$ ) temperate climate lagoon with a managed opening regime to the sea. Our objectives are twofold: (1) quantify groundwater inputs using a broad-scale radon mass balance approach, and (2) perform an in-depth uncertainty analysis to increase confidence in estimates of groundwater inflow. We compare these radon-based discharge estimates to previously reported data estimated using seepage meters (Ettema & Moore, 1995) and hypothesise that the previous seepage rates are underestimated.

### 3.3 Material and methods

#### 3.3.1 Site description

Te Waihora (Lake Ellesmere) is a shallow (mean depth 1.4 m), turbid and wind-affected coastal lagoon on the South Island of New Zealand (43°46'40.3" S 172°28'27.2" E) (Figure 3.1). The ~150 km<sup>2</sup> lagoon is a “choked” lagoon based on Kjerfve’s (1986) classification. It has one narrow entrance to the sea, very limited tidal influence and is located on a high-energy coastline with significant longshore sediment transport. It is mechanically opened to the sea between 2-6 times per year at the narrowest part of the mixed sand and gravel barrier (locally known as Kaitorete Spit) when the lagoon height reaches seasonal trigger levels (Figure 3.2). Te Waihora is located in the depression between the alluvial fans of two large gravel-bed braided rivers. The lagoon is situated above a marine transgression/regression sequence alternating between alluvial sands and gravels and marine sediments deposited during interglacial sea level rise. Groundwater has a strong negative vertical hydraulic gradient in the upper catchment, such that most of the rivers in the upper catchment lose flow to groundwater (Vincent, 2005). This groundwater becomes confined underneath fine-grained marine deposits near the coast and is forced to the surface as springs by a positive hydraulic gradient (Brown & Weeber, 1992). These springs feed many of Te Waihora’s ~40 surface inflows (Smith, 2003). Groundwater also discharges directly into the lagoon or out to sea under the lagoon (Williams, 2010).

The Te Waihora catchment has seen a significant rise in intensive agriculture in recent decades, which has contributed to degradation of the lagoon water quality. Te Waihora is also a central feature of local indigenous Māori (specifically Ngāi Tahu) culture. Effective management of the lagoon has proved challenging in recent years, as it is at the intersection of many stakeholder interests relating to its ecological, cultural, economic and recreational and social values. Earlier work quantified groundwater discharge using seepage meters (Ettema & Moore, 1995) and mapped potential points of entry using airborne thermal infrared imaging and spatial physicochemical surveys (Coluccio et al., 2020). Here, we build on this previous work by quantifying groundwater seepage using a lagoon-scale radon mass balance.

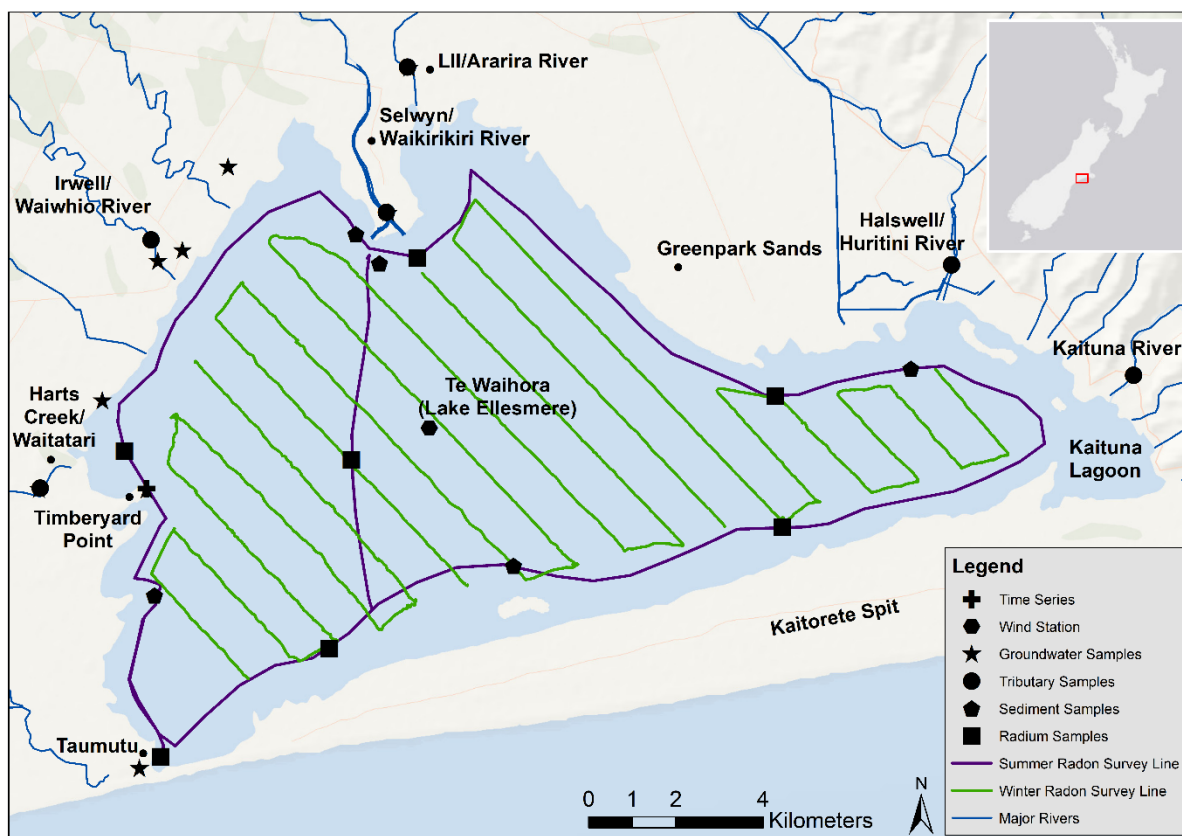


Figure 3.1. Site map of Te Waihora (Lake Ellesmere) with sampling locations highlighted. Basemap credit: Land Information New Zealand, Eagle Technology. Map includes GIS data from Land Information New Zealand (Land Information New Zealand, 2019, 2020).



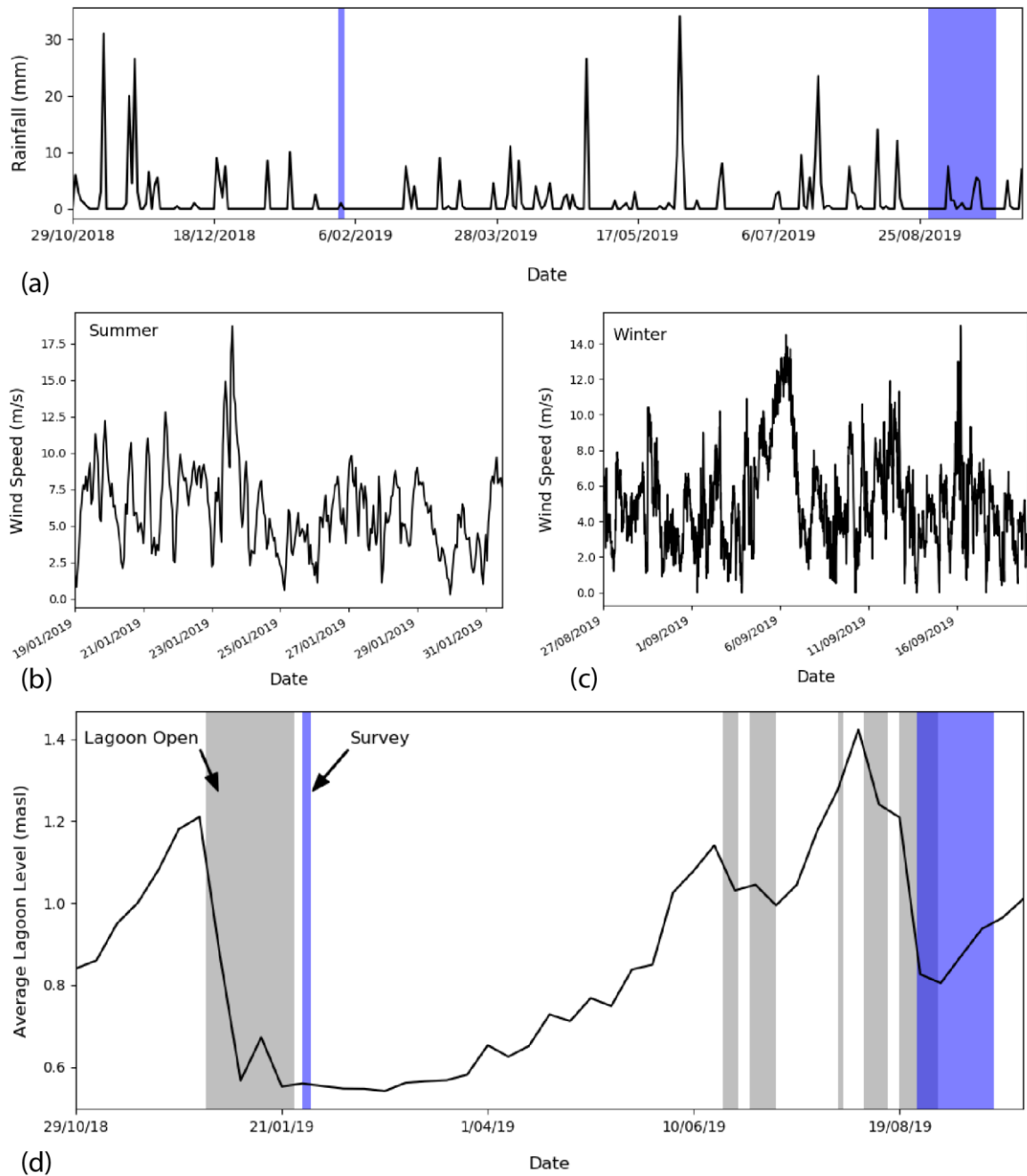


Figure 3.2. (a) Rainfall records from October 2018-September 2019 at Taumutu. Data collection periods are shaded in blue. (b) Wind speeds during summer survey. (c) Wind speeds during winter survey. (d) Time series of lagoon height above mean sea level from October 2018-September 2019. Periods when the lagoon was opened to the sea are shaded in grey. Data courtesy of Environment Canterbury (2020a).

### 3.3.2 Sampling and analysis

To quantify groundwater discharge to the study site, we calculated radon mass balances in the summer and winter. All sources and sinks of radon were accounted for in the models, and the missing component was assumed to be radon input via groundwater discharge to the lagoon. We adapted a

mass balance model for lakes and lagoons assuming steady-state conditions over the time scale of sampling (Perkins et al., 2015; Sadat-Noori et al., 2016) as follows and solved for  $Q_{gw}$ :

$$(Q_{sw} \cdot {}^{222}Rn_{sw}) + (Q_{gw} \cdot {}^{222}Rn_{gw}) + (J_{dif} \cdot A) + (C_{Ra} \cdot \lambda_{Rn} \cdot V) = (J_{atm} \cdot A) + (Q_{outflow} \cdot {}^{222}Rn_{lagoon}) + (Q_{barseepage} \cdot {}^{222}Rn_{lagoon}) + ({}^{222}Rn_{lagoon} \cdot \lambda_{Rn} \cdot V) \quad (1)$$

The radon mass balance variables in Equation 1 and key assumptions are listed in Table 3.1.

Table 3.1. Summary of the radon mass balance variables, estimated uncertainties and key assumptions

Symbol	Description	Unit	Source of data	Estimated uncertainties <sup>a</sup> and key assumptions
$V$	Lagoon volume	$\text{m}^3$	Interpolation based on bathymetry using Leapfrog Geo software	Assumed 5% uncertainty. Based on lagoon level at time of survey, which is an average of two in-situ height gauges.
$A$	Lagoon area	$\text{km}^2$	Interpolation based on bathymetry using Leapfrog Geo software	Assumed 5% uncertainty. Based on lagoon level at time of survey, which is an average of two in-situ height gauges.
$^{222}\text{Rn}_{\text{gw}}$	$^{222}\text{Rn}$ concentration in groundwater	$\text{Bq m}^{-3}$	10 shallow groundwater samples near lagoon	52%. Assumes $^{222}\text{Rn}$ concentrations in samples are representative of $^{222}\text{Rn}$ input from groundwater to lagoon. Assumes no seasonal variations in $^{222}\text{Rn}$ concentrations.
$\lambda_{\text{Rn}}$	$^{222}\text{Rn}$ decay constant	$\text{d}^{-1}$	$0.18 \text{ d}^{-1}$	Zero
$^{222}\text{Rn}_{\text{lagoon}}$	$^{222}\text{Rn}$ in lagoon	$\text{Bq m}^{-3}$	Natural neighbor interpolation of spatial survey results using ArcMap 10.7	63% summer; 43% winter. Assumes $^{222}\text{Rn}$ samples are representative of average lagoon $^{222}\text{Rn}$ concentration. Assumes no vertical stratification of $^{222}\text{Rn}$ in water column.
$^{222}\text{Rn}_{\text{sw}}$	$^{222}\text{Rn}$ in tributaries	$\text{Bq m}^{-3}$	6 largest tributaries sampled for $^{222}\text{Rn}$	18% summer; 15% winter. Assumes samples from rivers are representative of $^{222}\text{Rn}$ concentrations at river mouths. Assumes $^{222}\text{Rn}$ concentrations for remaining tributaries have the same mean $^{222}\text{Rn}$ concentration as tributaries sampled.
$Q_{\text{sw}}$	Tributary discharge	$\text{m}^3 \text{ s}^{-1}$	Flow data from nearby upstream permanent stream recorders or synthetic flow levels	7% assumed (summer); 8% assumed (winter). Assumed that at time of survey these tributaries comprised ~73% of total surface inflows. For remaining surface inflows, estimated flow rates based on remaining total flow percentage; used average $^{222}\text{Rn}$ concentration from 6 measured tributaries.
$J_{\text{dif}}$	$^{222}\text{Rn}$ from bed sediment diffusion	$\text{Bq d}^{-1}$	5 samples spatially distributed around lake perimeter, incl. 1 sample from middle of lake. Grab samples of top 30 cm of bed. $J_{\text{dif}}$ calculated using equation from Martens et al. (1980)	19% summer; 21% winter. Assumes highest possible $^{222}\text{Rn}$ in porewater concentration. Assumes no hyporheic exchange and excludes one outlier.

$C_{Ra}$	$^{226}\text{Ra}$ concentration in lagoon	$\text{Bq m}^{-3}$	7 50-L samples spatially distributed around lake perimeter, incl. 1 sample from middle of lake	10%. Assumed no temporal differences between $^{226}\text{Ra}$ concentrations between summer & winter and excludes one outlier.
$Q_{gw}$	Groundwater seepage rate	$\text{m}^3 \text{s}^{-1}$	Difference of all other terms	Propagates all other assumptions and uncertainties.
$Q_{outflow}$	Lagoon discharge through mechanical barrier opening to sea	$\text{m}^3 \text{s}^{-1}$	Summer: N/A (Outlet closed); Winter: N/A (Outlet opened for only 7 days of sampling period)	Zero. Assumes $Q_{outflow}$ approaches zero during winter survey.
$Q_{barseepage}$	Seepage from lagoon through permeable barrier	$\text{m}^3 \text{s}^{-1}$	Seepage rate from Valentine (1988) and Inpasihardjo (1988) as cited in Horrell (1992)	53%. Assumes that estimated seepage rates are representative across entire barrier length. Assumes no seepage in summer scenario when lagoon is 0.56 masl.
$J_{atm}$	$^{222}\text{Rn}$ evasion to atmosphere	$\text{Bq d}^{-1}$	Equation in MacIntyre et al. (1995)	63-81% uncertainty depending on evasion scenario. Assumes that evasion is wind driven.
$^{222}\text{Rn}_{air}$	$^{222}\text{Rn}$ concentration in air above lagoon <sup>b</sup>	$\text{Bq m}^{-3}$	Observed	135%. Assumes same concentration for mass balance modelling periods and homogeneous $^{222}\text{Rn}$ concentration in air.
$\alpha$	Ostwald solubility coefficient <sup>b</sup>	-	Equation in Burnett and Dulaiova (2003)	8% (summer); 9% (winter). Assumes an average water temperature for summer and winter surveys.
	Lagoon water temperature <sup>b</sup>	$^{\circ}\text{C}$	Average water temperature measured during spatial surveys	8% (summer); 9% (winter). Assumes an average water temperature for summer and winter surveys.
$k$	Wind-driven piston velocity <sup>b</sup>	$\text{m hr}^{-1}$	Average of $k$ equations for lakes from MacIntyre et al. (1995), Cole et al. (2010), Crusius & Wanninkhof (2003), and Cole & Caraco (1998)	30-53% uncertainty depending on wind speed.
$u$	Wind speed <sup>b</sup>	$\text{m s}^{-1}$	Observed	29-53% uncertainty depending on wind speed scenarios for summer and winter surveys. Assumes that average wind speeds used for the various evasion scenarios are valid. Assumes that wind speeds are the same spatially across lagoon.
$Sc$	Schmidt number <sup>b</sup>	-	Equation in MacIntyre et al. (1995)	8% (summer); 9% (winter)

$Dm$	Molecular diffusion coefficient of $^{222}\text{Rn}^b$	$\text{cm}^2 \text{s}^{-1}$	Equation in Peng et al. (1974)	8% (summer); 9% (winter). Assumes an average water temperature for summer and winter surveys.
------	--	-----------------------------	--------------------------------	---

<sup>a</sup> Detailed discussion of the uncertainty calculations is included in section 4.2.

<sup>b</sup> Variable used in atmospheric evasion calculations.

To estimate average radon activity concentrations across the lagoon in summer (January 2019) and winter (August-September 2019), we used the results of high-resolution spatial surveys that measured  $^{222}\text{Rn}$  by boat using radon-in-air detectors (RAD7, DurrIDGE, Inc., Billerica, MA) reported in Coluccio et al. (2020) for a qualitative interpretation. As the study site is a brackish lagoon, salinity was taken into account when converting the radon-in-air concentrations to radon in water (Schubert, Paschke, Lieberman, et al., 2012). We used natural neighbor interpolation (Sibson, 1981) in ArcMap 10.7.1 to calculate the average winter radon concentration in the lagoon. While the winter spatial survey covered the majority of the lagoon, the summer survey focused on the perimeter, with one sampling transect across the centre (Figure 3.1). Given the sparsity of data points in the centre of the lagoon, the summer survey results were not well suited to interpolation, as the relatively higher radon concentrations on the perimeter skew the mean. Therefore, to obtain a more accurate summer average, we infilled the dataset by replicating the data points from the centre of the lagoon transect ( $n = 7$ ) six times, which increased the total sample number from 84 to 120. We used the weighted mean of this infilled dataset as the average radon concentration for the summer period.

We measured surface water  $^{222}\text{Rn}$  concentrations in six of the largest tributaries to Te Waihora (Figure 3.1), accounting for approximately 70% of surface inflows to the lagoon. Summer and winter samples were taken in January-February 2019 and August-September 2020, respectively, using the sampling method of Lee and Kim (2006). Briefly, 5-L water samples were collected in 6-L gas-tight bottles directly from the streams using a peristaltic pump. Samples were analysed within ~six hours of collection using a RAD7 by measuring the concentration of  $^{222}\text{Rn}$  in the headspace above the water in the sample bottles. The sample bottles are connected to the RAD7 with tubing in a closed loop, with a bubbler connected to the tube that returns air to the sample bottle to enhance equilibrium with the water sample headspace. We achieved an average overall counting uncertainty of 5% for the summer samples and 3% for the winter samples. To obtain tributary flow rates, a combination of permanent river discharge recorder data and synthetic flow rate calculations were used (data sourced from Environment Canterbury (2020a)). For the minor tributaries (that comprise the remaining ~30% of surface inflows), their total flow rates were estimated based on a Te Waihora water budget by Horrell (1992), and we used the average  $^{222}\text{Rn}$  concentration from the sampled tributaries to calculate their  $^{222}\text{Rn}$  load.

Ten shallow groundwater samples were taken within 10 m to 2.8 km of the lagoon margin between August 2019 and September 2020 to measure  $^{222}\text{Rn}$  concentrations (Figure 3.1). Groundwater was sampled using a 1.8 m-long steel drive-point mini-piezometer and pumped with a peristaltic pump (similar to Charette and Allen (2006)). Water quality parameters (specific conductivity, pH, dissolved oxygen, water temperature) were measured during pumping with either an Orion Star A329 multi-parameter meter (Thermo Fisher Scientific, Inc., Waltham, MA) or a Hach HQ40D Portable Multi Meter (Hach, Loveland, CO, USA). Once the parameters stabilised, 5-L samples were collected and

analysed using the same method as the tributary samples as above, with an average overall counting uncertainty of <1%. The median radon concentration from the groundwater samples was used as the groundwater radon endmember. Given it is often difficult to accurately estimate a representative groundwater radon endmember (Dulaiova et al., 2006), we also estimated groundwater discharge rates using the radon concentrations obtained from sediment diffusion experiments. The latter is the theoretical maximum  $^{222}\text{Rn}$  concentration in groundwater entering the lagoon assuming similar aquifer substrate in the lagoon bed and no hyporheic bed flow.

Five sediment samples were collected from lagoon sediments (top 30 cm) (Figure 3.1) during January 2019 using a Van Veen grab sampler. The samples were comprised mainly of sands and silts, which reflects the majority of grain sizes on the lagoon bed. The sediment was incubated for 30 days in radium-free water and then the  $^{222}\text{Rn}$  concentrations were analysed with a RAD7 (Corbett et al., 1998). One outlier sample (NZ-2) was excluded from the mass balance analysis as it was less than 10% of the mean of the dataset. The diffusive flux of  $^{222}\text{Rn}$  was calculated using the following equation from Martens et al. (1980):

$$J_{dif} = (\lambda D_s)^{1/2} (C_{eq} - C_w) \quad (2)$$

Where  $\lambda$  is the  $^{222}\text{Rn}$  decay constant (0.181/d);  $D_s$  is the effective wet bulk sediment diffusion coefficient in sediments ( $\text{m}^2/\text{d}$ );  $C_{eq}$  is the  $^{222}\text{Rn}$  equilibrium concentration in sediments; and  $C_w$  is the  $^{222}\text{Rn}$  concentration in the overlying surface water ( $\text{Bq}/\text{m}^3$ ).  $C_{eq}$  is calculated by dividing the  $^{222}\text{Rn}$  released by  $^{226}\text{Ra}$  during the sediment equilibration by the sediment porosity to obtain the  $^{222}\text{Rn}$  concentration in the sediment porewater ( $\text{Bq}/\text{m}^3$ ).

Seven surface water samples were collected from the lagoon in January 2019 for dissolved radium ( $^{226}\text{Ra}$ ) analysis (radioactive parent of  $^{222}\text{Rn}$ , half-life = 1600 years) (Figure 3.1). Briefly, lagoon water was pumped into a 50-L container. The sample water was then filtered through manganese fibre adsorbers, which were later analysed with a radium delayed coincidence counter (RaDeCC) (Peterson et al., 2009). One  $^{226}\text{Ra}$  outlier sample (NZ-1) was excluded from the mass balance due to analysis error. The mean of the radium concentrations was assumed to represent the entire lagoon. Using the  $^{226}\text{Ra}$  concentrations in surface water, we calculated the supported  $^{222}\text{Rn}$  from dissolved  $^{226}\text{Ra}$ . This assumes that the dissolved  $^{226}\text{Ra}$  is in steady state and that the supported  $^{222}\text{Rn}$  is in secular equilibrium with the dissolved  $^{226}\text{Ra}$  (Bateman, 1910).

As Te Waihora features highly variable and strong wind speeds, we expected atmospheric evasion to be an important component of the mass balance. We adopted a scenario-based approach where groundwater discharge was estimated based on several wind speeds in the evasion calculation (e.g., Sadat-Noori et al., 2016). We modelled three wind speed scenarios. For both seasons, we calculated evasion based on the mean wind speed during the spatial survey sampling with the assumption that evasion of  $^{222}\text{Rn}$  was relatively instantaneous—i.e., the  $^{222}\text{Rn}$  loss occurred during sampling (Scenario

1). We also included summer and winter scenarios that used the mean wind speed in the 24 hours preceding sampling—i.e., assuming that wind evasion is not instantaneous (Scenario 2). Finally, we considered an extended wind speed scenario for both seasons—i.e., assuming that radon evasion is occurring on a longer time scale (Scenario 3). For this, we calculated evasion based on the mean wind speed in summer across the three sampling days and the seven days prior to sampling. For winter, we used the mean wind speed across the 25-day sampling period (Petermann, Knöller, et al., 2018).

We used 15-minute to 1-hour averaged wind speed data from a permanent weather station located in the centre of the lagoon (Environment Canterbury, 2020b) (Figure 3.1). For the evasion calculations we also analysed the  $^{222}\text{Rn}$ -in-air concentration in one location at the lagoon on 31 July 2020. We sampled ambient air on the lagoon margin with a RAD7 for 7.5 hours.

Atmospheric evasion,  $J_{atm}$ , was then calculated using MacIntyre (1995):

$$J_{atm} = (^{222}\text{Rn}_{lagoon} - (^{222}\text{Rn}_{air} * \alpha)) * k \quad (3)$$

To calculate the wind speed-based parameterisation of  $k$ , we used an average of four different  $k$  equations (Macklin et al., 2018) for each wind speed scenario: MacIntyre et al. (1995), Cole et al. (2010), Crusius and Wanninkhof (2003), and Cole and Caraco (1998). Wind heights were converted to the equivalent wind height at 10 m above the lagoon surface.

Radon loss via lagoon seepage through the mixed sand and gravel barrier (Kaitorete Spit) was estimated using calculations from Valentine (1988) and Inpasihardjo (1988) as cited in Horrell (1992). Barrier seepage rates are assumed to be a function of lagoon height. To estimate the radon loss from the lagoon via the outlet to the sea, we considered the number of days the outlet was opened and the hydraulic gradient between the lagoon and sea (i.e., the lagoon height above sea level) during the summer and winter surveys.

To calculate volume and surface area for the lagoon, we used the average lagoon water height above mean sea level calculated from two permanent gauges at the site (Environment Canterbury, 2020b). For the three-day summer sampling period, we assumed a static lagoon level of 0.56 masl (metres above mean sea level). There was no precipitation during this period and the lagoon was not opened to the sea. For the winter sampling period, we used the average (0.88 masl) lagoon height. We used these lagoon heights and bathymetric contours (Irwin & Main, 1989) to calculate the surface area and volume of the lagoon using Leapfrog Geo software (Seequent Ltd, Christchurch, New Zealand).

We also carried out a 24-hour  $^{222}\text{Rn}$ /wind time series measurement at Te Waihora on 13-14 August 2019 using the same methods for the spatial radon surveys, though in one location only (Timberyard Point—see Figure 3.1). This time series was done to examine the relationship between nearshore radon concentrations in the surface water of the lagoon and wind speeds.



The spatial data used to calculate the average radon concentrations in the lagoon were originally published in Coluccio et al. (2020). All other data and the mass balance presented here are original.

The precision of each mass balance term was calculated by Gaussian error propagation (Enke, 2000), as used in previous radon mass balance studies (e.g., Kluge et al., 2012; Sadat-Noori et al., 2015; Santos et al., 2014). For  $^{222}\text{Rn}_{\text{lagoon}}$  and  $^{222}\text{Rn}_{\text{gw}}$ , the standard deviations of the respective datasets were considered the uncertainty for these variables, as done previously in radon mass balance models (e.g., Schmidt et al., 2010). For  $^{222}\text{Rn}$  diffusion from sediment and  $^{222}\text{Rn}$  production from  $^{226}\text{Ra}$  decay, the standard deviations of the datasets were used, as well as the variance of the lagoon surface area and volume calculations, respectively. The uncertainty of the surface water contribution of  $^{222}\text{Rn}$  was calculated from the RAD7 counting error for the tributary measurements and the variance of the stream discharge measurements. The uncertainty of the atmospheric evasion term involved propagating the errors of the variables included in the calculation, which included the standard deviations of  $^{222}\text{Rn}_{\text{lagoon}}$ ,  $^{222}\text{Rn}_{\text{air}}$ , lagoon water temperature and wind speed, as well as the variance of the lagoon surface area calculation. For  $Q_{\text{barseepage}}$  the standard deviation of  $^{222}\text{Rn}_{\text{lagoon}}$  and the variance of the barrier seepage rate were used to calculate uncertainty.  $Q_{\text{outflow}}$  uncertainty was assumed to be zero. The uncertainties of the final groundwater discharge estimates were calculated by propagating all the other errors in the mass balance. The specific considerations that were involved in calculating the uncertainty for each mass balance term are discussed in detail in section 4.2.

### 3.4 Results

#### 3.4.1 Environmental conditions

Environmental conditions for Te Waihora during the mass balance periods are summarised in Table 3.2. The summer survey period (28-30 January 2019) was dry (Table 3.2) and the lagoon was low, at 0.56 masl, and it was open to the sea for 44 days before closing on 25 January 2019. The winter survey period (27 August-20 September 2019) was characterised by cooler temperatures and wetter weather (Figure 3.2 and Table 3.2). The lagoon was open to the sea for the first seven days of the winter survey period having opened a week prior to the survey.

Table 3.2. Environmental conditions at Te Waihora during summer and winter survey periods

Variable	Summer	Winter	Unit
	(28-30 Jan 2019)	(27 Aug-20 Sept 2019)	
Lagoon average water level height <sup>a</sup>	0.56	0.88	m above MSL
Lagoon surface area	134	150	km <sup>2</sup>
Lagoon volume	100	146	GL
Ambient air temperature range <sup>a</sup>	16.9-25.8	3.9-18.2	°C
Precipitation in 7 days before survey <sup>a</sup>	2.5	0	mm
Precipitation during survey <sup>a</sup>	0	25.5	mm

Days lagoon open to sea <sup>a</sup>	0	7	days
Wind speed (scenario 1) <sup>b</sup>	6.5	3.7	m s <sup>-1</sup>
Wind speed (scenario 2)	5.4	4.3	m s <sup>-1</sup>
Wind speed (scenario 3)	6.4	5.5	m s <sup>-1</sup>

<sup>a</sup> Data source Environment Canterbury (2020a)

<sup>b</sup> Scenario 1 is the mean wind speed during sampling. Scenario 2 is the mean wind speed across sampling days. Scenario 3 (summer) is the mean wind speed during sampling + 7 days prior. Scenario 3 (winter) is the mean wind speed across the survey period.

### 3.4.2 Spatial <sup>222</sup>Rn surveys

<sup>222</sup>Rn concentrations ranged from 3-87 Bq/m<sup>3</sup> in the summer ( $n = 84$ ,  $1-\sigma$  SD = 19 Bq/m<sup>3</sup>) (Figure 3.3). The average <sup>222</sup>Rn concentration from the summer dataset using the infilled data was 32 Bq/m<sup>3</sup> ( $n = 120$ ,  $1-\sigma$  SD = 20 Bq/m<sup>3</sup>, uncertainty = 63%). <sup>222</sup>Rn concentrations during the winter survey were 3-124 Bq/m<sup>3</sup> ( $n = 189$ ,  $1-\sigma$  SD = 19 Bq/m<sup>3</sup>). The general spatial trend in <sup>222</sup>Rn concentrations was similar in winter and summer with higher concentrations closer to the lagoon margins (Coluccio et al., 2020). The average <sup>222</sup>Rn concentration from the interpolated winter dataset was 30 Bq/m<sup>3</sup> ( $1-\sigma$  SD = 13 Bq/m<sup>3</sup>, uncertainty = 43%). When the spatial survey <sup>222</sup>Rn concentrations are converted to <sup>222</sup>Rn inventories (i.e., accounting for water depth at the sampling location), the general trends of higher <sup>222</sup>Rn values at the margins of the lagoon, particularly on the western side are the same (Figure 3.3). The <sup>222</sup>Rn inventories ranged in summer from 3-153 Bq/m<sup>2</sup> and in winter from 2-84 Bq/m<sup>2</sup>.

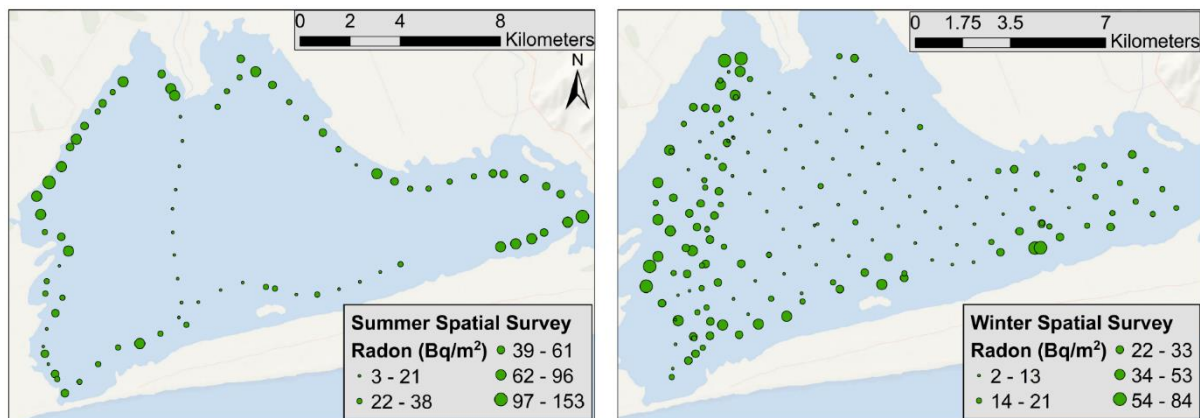


Figure 3.3. Radon inventory results from the summer and winter spatial <sup>222</sup>Rn surveys. Inventories calculated from data originally reported in Coluccio et al. (2020). Basemap credit: Land Information New Zealand, Eagle Technology.

### 3.4.3 Shallow groundwater sampling

Radon concentrations in the groundwater samples ( $n = 10$ ) ranged from 667 to 6880 Bq/m<sup>3</sup> with a median concentration of 3580 ( $1-\sigma$  SD = 1878 Bq/m<sup>3</sup>, uncertainty = 52%).

### 3.4.4 Sediment diffusion

$^{222}\text{Rn}$  in water equilibrated with sediment ranged from 7950-9530 Bq/m<sup>3</sup> with a mean of  $8760 \pm 724$  Bq/m<sup>3</sup>. Diffusive fluxes had a mean of  $8.9 \pm 1.7$  Bq/m<sup>2</sup>/d in summer and  $7.4 \pm 1.5$  Bq/m<sup>2</sup>/d in winter. Extrapolated across the surface area of the lagoon, the diffusive flux was  $1.2 \times 10^9$  Bq/d (uncertainty 20%) in the summer and  $1.1 \times 10^9$  Bq/d (uncertainty 21%) in the winter.

### 3.4.5 Radium decay

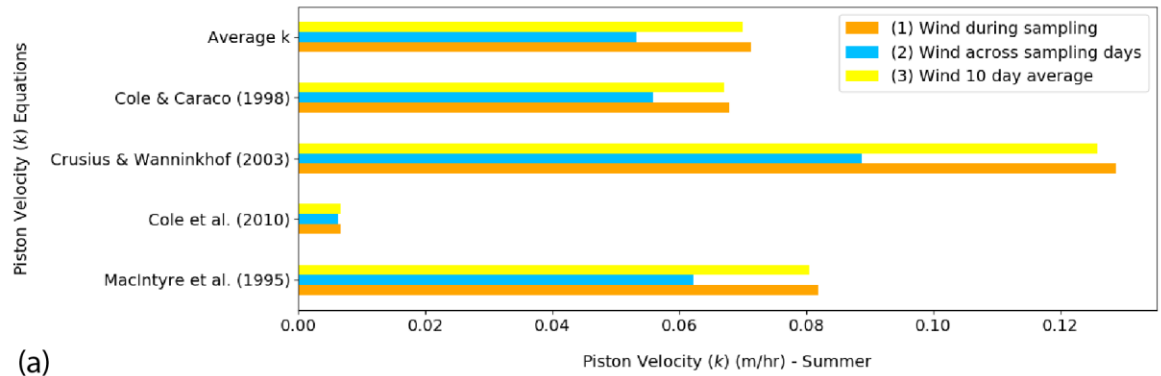
$^{226}\text{Ra}$  concentrations ranged from 15-20 Bq/m<sup>3</sup> with an average counting uncertainty of 4%. During the summer survey, the  $^{222}\text{Rn}$  input from  $^{226}\text{Ra}$  decay was  $3.1 \times 10^8$  Bq/d (uncertainty 11%), while during the winter survey, the  $^{222}\text{Rn}$  flux was  $4.5 \times 10^8$  Bq/d (uncertainty 11%).

### 3.4.6 Surface water sampling

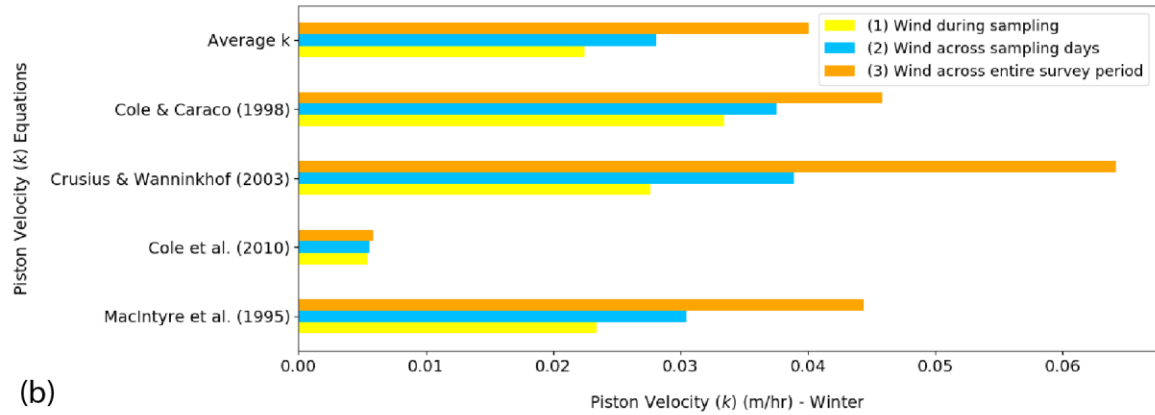
Tributary sampling revealed  $^{222}\text{Rn}$  concentrations ranging from 49-2400 Bq/m<sup>3</sup> in summer and 128-1710 Bq/m<sup>3</sup> in winter. Sampling in summer was in dry conditions representing baseflow conditions. There was a small amount of rainfall preceding the winter sampling (6.5 mm four days before the 28 August 2020 sampling and 9 mm three days before the 4 September 2020 sampling (Environment Canterbury, 2020a)). Average river discharge rates for the tributaries ranged from 0.1-1.7 m<sup>3</sup>/s during summer sampling on 31 January-1 February 2019 and 0.8-3.2 m<sup>3</sup>/s during the winter mass balance period (27 August-20 September 2019) (Environment Canterbury, 2020a). Uncertainties for  $^{222}\text{Rn}$  input from tributaries in summer and winter were 27% and 26%, respectively.

### 3.4.7 Atmospheric evasion

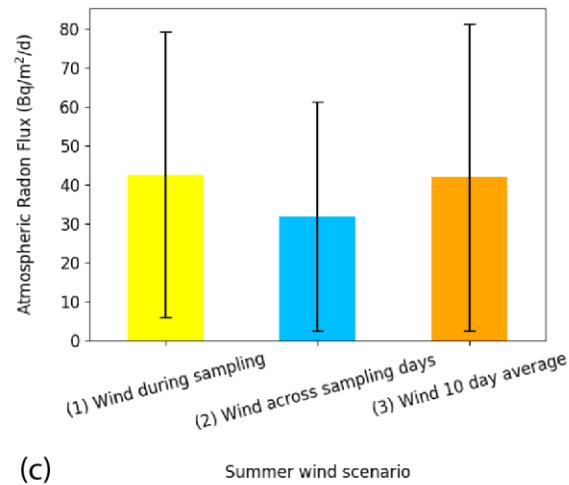
Here, we report atmospheric evasion of  $^{222}\text{Rn}$  under several scenarios (Figure 3.4). In summer, the atmospheric  $^{222}\text{Rn}$  evasion ranged from 32-43 Bq/m<sup>2</sup>/d. Scenario 1 (mean wind speeds during sampling) had the highest mean wind speed (6.5 m/s) of the three scenarios but the lowest uncertainty (86%) in the  $^{222}\text{Rn}$  flux. In winter, the atmospheric  $^{222}\text{Rn}$  flux ranged from 16-28 Bq/m<sup>2</sup>/d. Uncertainties ranged from 63-70% for the winter scenarios, with Scenario 2 (mean wind speed across survey days) producing the lowest uncertainty in the  $^{222}\text{Rn}$  flux rate. The average uncertainty across the three evasion scenarios was 77% in summer and 67% in winter. We also report  $k$  under the three wind speed scenarios for both the summer and winter mass balances using four piston velocity ( $k$ ) equations from the literature (Figure 3.4). Lastly, the measurement of  $^{222}\text{Rn}$  in the air above the lagoon was  $2.8 \pm 3.8$  Bq/m<sup>3</sup>.



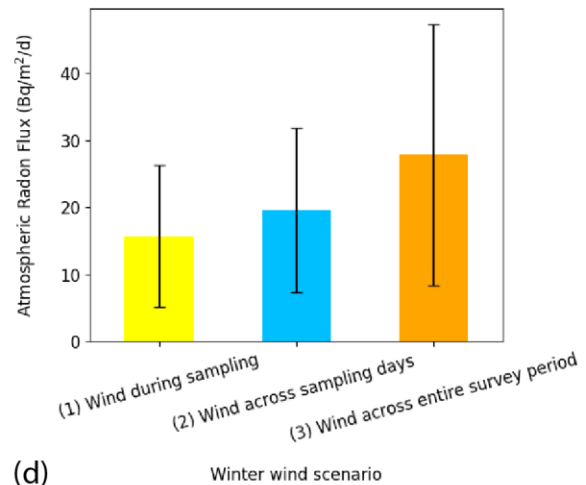
(a)



(b)



(c)



(d)

Figure 3.4. Plots showing piston velocity ( $k$ ) calculations using four  $k$  equations and the average  $k$  for the summer (a) and winter (b) mass balances. Subplots (c) and (d) show the atmospheric radon flux in summer and winter, respectively.

### 3.4.8 Lagoon exchange with the sea

During the summer, the lagoon outlet was closed, so we assumed a zero  $^{222}\text{Rn}$  surface water flux from the lagoon to the sea. During the winter survey, the lagoon was open for the first seven days of the sampling period. By the first day of the winter survey on 27 August, the lagoon level had already dropped to its lowest extent during the sampling period (from 1.21 masl to 0.83 masl) (Figure 3.2).

Hence, we assumed the majority of the lagoon water that flowed out to sea during this opening event did so in the seven days prior to sampling. From 27 August until the lagoon closed on 2 September, the lagoon height was relatively stable, so we assumed minimal exchange between the lagoon and the sea so that the net flux of  $^{222}\text{Rn}$  via the lagoon outlet approached zero.

In regard to seepage of lagoon surface water through the permeable mixed sand and gravel barrier, during the summer survey, the lagoon was at 0.56 masl. This would result in an insufficient hydraulic gradient between the lagoon and sea to drive flow through the barrier based on transmissivity estimates from three sets of wells on Kaitorete Spit (Valentine (1988) and Inpasihardjo (1988) as cited in Horrell (1992)). In the winter period, the lagoon was on average 0.88 masl, which according to Horrell (1992), would result in seepage from the lagoon through the barrier at  $1.0 \pm 0.3 \text{ m}^3/\text{s}$  with a resulting radon outflow of  $2.7 \times 10^6 \text{ Bq/d}$  (53% uncertainty).

#### **3.4.9 Radon/wind speed time series**

Results from the 24-hour  $^{222}\text{Rn}$ /wind time series showed a general trend of lower  $^{222}\text{Rn}$  concentrations in the lagoon surface water during and following periods of higher wind speeds (Figure 3.5).

Relatively higher wind speeds ( $>2.5 \text{ m/s}$ ) had a greater influence on  $^{222}\text{Rn}$  concentrations.

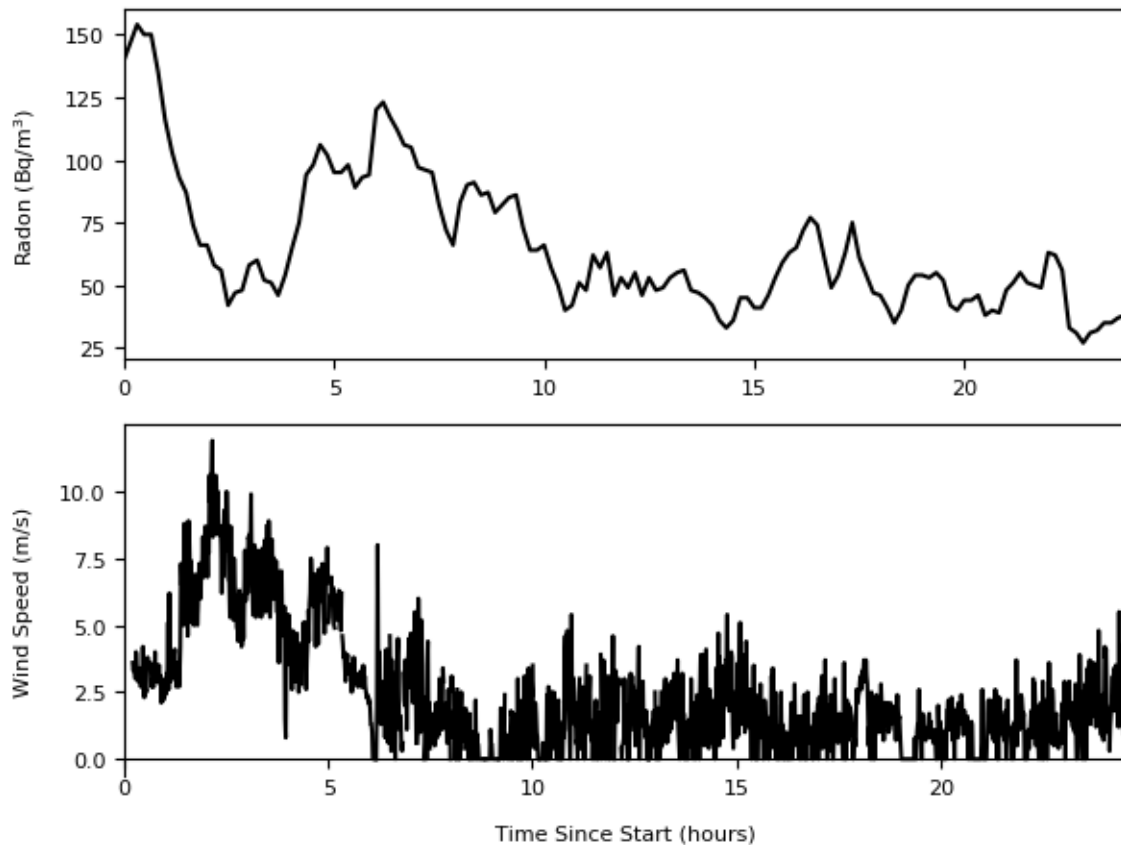


Figure 3.5. Radon surface water concentrations and wind speed data from a 24-hour time series measurement located at Timbervard Point at Te Waihora.

#### 3.4.10 Radon mass balance

Groundwater discharge estimates ranged from  $5.2 \pm 5.8$  to  $18.7 \pm 19.6$  m<sup>3</sup>/s in summer to  $0.9 \pm 2.2$  to  $8.1 \pm 10.5$  m<sup>3</sup>/s in winter incorporating the two radon endmembers and the three wind speed scenarios for each season. (Table 3.3).

Table 3.3. Estimations of groundwater discharge and cumulative uncertainties to Te Waihora during summer and winter using radon mass balances calculated with a variety of wind speed and radon endmember scenarios

Scenario	Groundwater discharge – <sup>222</sup> Rn in groundwater endmember (m <sup>3</sup> /s)	Groundwater advective rates – <sup>222</sup> Rn in groundwater endmember (cm/d)	Uncertainty %	Groundwater discharge – <sup>222</sup> Rn from sediment diffusion (m <sup>3</sup> /s)	Groundwater advective rates – <sup>222</sup> Rn from sediment diffusion (cm/d)	Uncertainty %
<b>Summer</b>						
(1) Mean wind speed during sampling	$18.7 \pm 19.6$	1.16	105%	$7.6 \pm 7$	0.47	92%

(2) Mean wind speed across sampling days	12.6 ± 15.6	0.78	123%	5.2 ± 5.8	0.32	112%
(3) Mean wind speed during survey + 7 days prior	18.2 ± 21.3	1.13	117%	7.4 ± 7.8	0.46	104%
<b>Winter</b>						
(1) Mean wind speed during sampling	2.2 ± 5.5	0.12	253%	0.9 ± 2.2	0.05	247%
(2) Mean wind speed across sampling days	4.1 ± 6.6	0.23	161%	1.7 ± 2.5	0.10	153%
(3) Mean wind during survey period	8.1 ± 10.5	0.47	129%	3.3 ± 3.9	0.19	119%

### 3.5 Discussion

#### 3.5.1 Quantifying groundwater discharge in coastal lagoons

Due to the windy nature and high variability in wind speeds at the site, we expected  $^{222}\text{Rn}$  evasion to be important, yet difficult to estimate (Crusius & Wanninkhof, 2003; Lopez et al., 2020). Indeed, radon loss due to wind evasion was the most influential variable in the mass balance. The evasion scenarios with the highest wind speeds resulted in the highest  $^{222}\text{Rn}$  evasion (Figure 3.4) and the highest groundwater discharge estimates, demonstrating the influence of the evasion term to the radon mass balances for this site. Atmospheric evasion has been shown to be significant in other shallow coastal sites (Borges et al., 2004; Jeffrey et al., 2018; Lopez et al., 2020; Zappa et al., 2003). In addition to wind speeds, atmospheric evasion can also be affected by currents that enhance turbulence at water-air interfaces (Atkins et al., 2013; Borges et al., 2004). However, due to the absence of tidal influence at this site and small surface area of the lagoon entrance (when open), we suspect current-driven evasion to be minimal and therefore did not account for this in the mass balance. Also, given the large surface area of the lagoon and the margins largely consisting of low-lying vegetation, we expect wind attenuation to have little effect on atmospheric radon evasion.

In general, the summer mass balance results were dominated by only a few of the variables, whereas in the winter scenarios, there was a more even contribution from several variables (Figure 3.6). In summer, the dominant radon loss was atmospheric evasion (average 92% of all outputs) with the remainder of the output from radon decay and none from barrier seepage or the outlet to the sea. In

other studies, atmospheric evasion losses were also the most dominant term in the radon budget, corresponding with similar results from Sadat-Noori et al. (2016) and Schmidt et al. (2010) for coastal lagoons and lakes, respectively. The summer radon sources were somewhat more evenly distributed, with 4%, 9% and 17% contributions from radium decay, tributaries and sediment diffusion, respectively. The remainder of the input was groundwater seepage (70%). The winter models revealed a wider distribution of contributing variables with a decreased contribution from atmospheric evasion (79%), followed by radon decay (21%) and negligible barrier seepage (0.07%). Winter radon sources were also more evenly distributed amongst the variables with 35% comprising of groundwater seepage and 29%, 24% and 12% accounted for by diffusion, tributaries and radium decay, respectively. This lower proportion of groundwater seepage as a source of radon to the lagoon contrasts with results from Sadat-Noori et al. (2016), who found over 90% of radon inputs sourced from groundwater seepage across four seasons in three coastal lagoons in Australia.



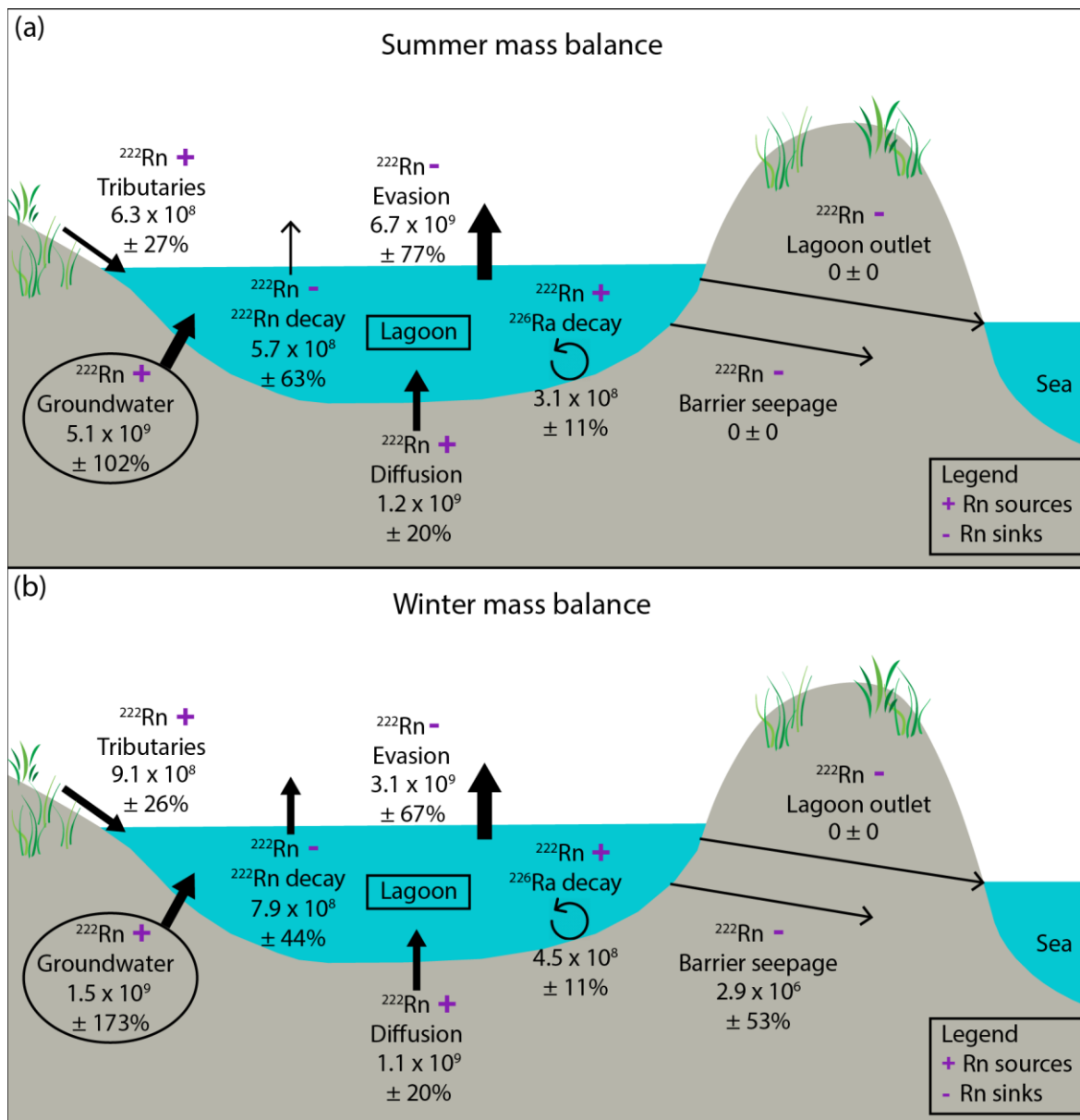


Figure 3.6. Conceptual diagram showing the radon sources and sinks from the summer (a) and winter (b) mass balances in  $\text{Bq/m}^3$  and uncertainty as  $\pm$  percentage. The thicker the arrow, the higher proportion the given variable is in the mass balance. Note that radon concentrations for evasion and groundwater are averages of the three wind speed scenarios. Diagram concept adapted from Sadat-Noori et al. (2016).

The summer mass balance estimates for groundwater discharge were five and two-fold greater than the winter discharge estimates for the low and high ends of the discharge ranges, respectively. The average across the six discharge estimates (Table 3.3) in summer was  $11.6 \text{ m}^3/\text{s}$  and in winter was  $3.4 \text{ m}^3/\text{s}$ . Perkins et al. (2015) and Sadat-Noori et al. (2016) also found seasonal variability in groundwater seepage estimates from radon mass balances. In two tropical Australian lagoons, Sadat-Noori et al. (2016) found seasonal changes in groundwater seepage sources to be largely driven by precipitation—i.e., in the wet season with higher precipitation, radon contributions from surface

waters were greater. This contrasts with the current study, where despite the winter survey occurring during a relatively wetter period (i.e., higher surface inflows, higher lagoon level), this does not appear to have been a major contributor to the lower discharge estimates in winter. In a study of a coastal Australian lake, Perkins et al. (2015) found wind speed fluctuations during seasonal surveys to be a major driver of differences in groundwater discharge estimates from radon mass balances. This finding corresponds with the current study, where lower wind speeds (ranging from 3.7-5.5 m/s for the three scenarios) during the winter appear to be the main driver of lower groundwater discharge estimates compared to the summer. It is also important to note that the current study only estimated groundwater discharge in two seasons within one 12-month period. Groundwater discharge to Te Waihora during other seasons or years is likely to vary to some extent from the estimates reported here due to short-term seasonal influences and long-term factors such as climate change.

### 3.5.2 Uncertainty analysis

Reported uncertainties in discharge estimates from radon mass balances in previous studies of lakes and lagoons have ranged widely from 11% to 253% (Table 3.4). Results from the current study are at the higher end of this range: between 92-253% (Table 3.3). We note that a higher proportion of radon from seepage to the total inputs will always result in a lower uncertainty of the final discharge estimates (Rodellas et al., 2021). For example, in summer Scenario 1, radon from seepage made up 73% of total radon inputs, with 92-105% uncertainty for the two radon endmembers in the final discharge estimate. This compares to winter Scenario 1 in which radon from seepage comprised only 21% of radon inputs with much higher (247-253%) overall uncertainty (Table 3.3).

Table 3.4. Groundwater discharge estimates and reported uncertainties in published studies on lakes and coastal lagoons

Location	Type of waterbody	Surface area (km <sup>2</sup> )	Groundwater discharge estimate <sup>a</sup> (m <sup>3</sup> /d)	Uncertainty <sup>a</sup>	Authors
Lake Willersinnweiher, Germany	Lake	0.145	$4.40 \times 10^2$	32%	Kluge et al. (2012)
Lake Ainsworth, Australia	Lake	0.125	$8.40 \times 10^2$	91%	Perkins et al. (2015)
Welsby ICOLL, Australia	Coastal lagoon	0.088	$3.00 \times 10^3$	62%	Sadat-Noori et al. (2016)
South Welsby Lagoon, Australia	Coastal lagoon	0.003	$2.29 \times 10^2$	122%	Sadat-Noori et al. (2016)
Mermaid ICOLL, Australia	Coastal lagoon	0.037	$9.73 \times 10^2$	42%	Sadat-Noori et al. (2016)
La Palme Lagoon, France	Coastal lagoon	5	$1.25 \times 10^4$	206%	Rodellas et al. (2018)
Cudgen Lake	Coastal lagoon	1.6	$7.71 \times 10^2 - 2.62 \times 10^4$	22-33%	Jeffrey et al. (2016)

Lake Ammelshainer See, Germany	Lake	0.54	$1.12 \times 10^3$	11%	Petermann et al. (2018)
Ximen Co Lake	Lake	3.6	$3.71 \times 10^4$	80%	Luo et al. (2018)
Green Lake & Black Lake, Italy	Lakes	~0.023	$4.66 \times 10^4$	30%	Tuccimei et al. (2005)
Unnamed boreal lake, Canada	Lake	0.112	6.90	83%	Schmidt et al. (2010)
Unnamed boreal lake, Canada	Lake	1.912	$9.44 \times 10^2$	63%	Schmidt et al. (2010)
Newnans Lake	Lake	29.8	$1.50 \times 10^5$	54%	Dimova et al. (2013)
Butler Lake	Lake	6.38	$1.90 \times 10^4$	63%	Dimova et al. (2013)
Clear Lake	Lake	1.45	$4.40 \times 10^3$	25%	Dimova et al. (2013)
Haines Lake	Lake	2.91	$2.90 \times 10^4$	22%	Dimova et al. (2013)
Shipp Lake	Lake	1.12	$1.60 \times 10^3$	9%	Dimova et al. (2013)
Josephine Lake	Lake	5.8	$9.40 \times 10^4$	35%	Dimova et al. (2013)
Te Waihora (Lake Ellesmere), New Zealand (summer)	Coastal lagoon	~150	$4.5 \times 10^5 - 1.6 \times 10^6$	92-123%	This study
Te Waihora (Lake Ellesmere), New Zealand (winter)	Coastal lagoon	~150	$8.7 \times 10^4 - 7.2 \times 10^5$	119-253%	This study

<sup>a</sup> Note: In some cases the discharge rates are averages where discharge estimates were calculated for different time periods in the studies.

Obtaining a representative  $^{222}\text{Rn}$  endmember in groundwater is often one of the most difficult parameters to estimate in radon mass balances (Dulaiova et al., 2006). Natural heterogeneities in geology over small spatial scales, and in the case of shallow unconfined samples, groundwater mixing with land-surface recharge can result in groundwater with varying  $^{222}\text{Rn}$  concentrations (Mullinger et al., 2009; Tommasone et al., 2011). It is also possible that shallow groundwater samples collected near the edges of surface water bodies may be influenced by surface water mixing and thus have a lower  $^{222}\text{Rn}$  concentration. Kluge et al. (2012) noted that the radon-in-groundwater endmember accounted for 50-90% of the total uncertainty in their radon mass balance for a lake. We took a straightforward approach to calculating the uncertainty for the average radon concentration in groundwater, using the standard deviation ( $1878 \text{ Bq/m}^3$ ) of the sample dataset, as used in other radon mass balance investigations (e.g., Schmidt et al., 2010). However, the uncertainty was relatively high (52%) given the radon concentrations measured in the shallow groundwater samples ranged by an order of magnitude ( $667\text{-}6880 \text{ Bq/m}^3$ ). We adopted a dual assumption mass balance approach (Santos et al., 2014) by calculating mass balances using the average  $^{222}\text{Rn}$  concentration from groundwater sampling, as well as the mean  $^{222}\text{Rn}$  concentration obtained from the sediment equilibration experiments ( $8760 \pm 725 \text{ Bq/m}^3$ ). The latter is the theoretical maximum  $^{222}\text{Rn}$  concentration in

groundwater entering the lagoon. Thus, these two  $^{222}\text{Rn}$  concentrations serve as high and low estimates for groundwater discharge to the lagoon, respectively. If we compare the standard error from the current study to the median (17%), this is lower than the standard error in Sadat-Noori et al. (2015) of 20%, which was based on 27 samples. Given the difficulty in assigning a radon in groundwater endmember, Sadat-Noori et al. (2015) tested the number of groundwater samples required to stabilise the standard error and found the standard error to change little beyond a sample size of 12 (current study  $n = 10$ ). Ultimately however, the variability of the geology and the length of the coastline will likely be the greatest determinants of how many groundwater samples are required to stabilise the standard error (Duque, Knee, et al., 2019). Other radon mass balances models relied on similar sample sizes and obtained comparable uncertainties. For example, Atkins et al. (2013) took 10 groundwater samples near a coastal creek in Australia and obtained a standard error of 25%. Corbett et al. (1997) sampled 12 groundwater wells around a reservoir in South Carolina and obtained an overall standard error of 37%.

Estimating the average radon concentration in the lagoon is critical because it is required for all of the output terms ( $^{222}\text{Rn}$  decay;  $^{222}\text{Rn}$  wind evasion; ocean and barrier outflow) (Rodellas et al., 2021). The models were highly sensitive to fluctuations in this term—a 10% increase in the radon-in-lagoon concentration resulted in a 14-16% increase in the final seepage flux across the modelled scenarios. We chose not to use a direct average for the radon-in-lagoon concentration, as this was unlikely to be representative of the radon concentration throughout the lagoon due to limited spatial sampling coverage (in summer) and a bias of high radon concentrations from shallow areas near the lagoon edges (Rodellas et al., 2021). Interpolating spatial tracer data using methods like kriging, inverse distance weighting or natural neighbor may reduce uncertainty compared to using direct averages (Rodellas et al., 2021). Indeed, despite having a wider range of winter radon concentrations in the lagoon (3-124 Bq/m<sup>3</sup>) compared to the summer dataset (3-87 Bq/m<sup>3</sup>), interpolating the winter dataset produced a lower uncertainty—43% compared to 63%.

Atmospheric evasion of radon can also be a difficult component of the radon mass balance to estimate (Dulaiova & Burnett, 2006). Calculation of the atmospheric radon evasion is based on several interconnected terms, and we considered their various degrees of uncertainty. For example, the uncertainty of the radon-in-air measurement was high (135%), mainly due to the low radon concentration and relatively short (~8 hour) measurement period. The uncertainty of the water temperature for both mass balance periods was ~8%. We used the standard deviation of the wind speed measurements for the evasion scenarios, and these uncertainties ranged from 29% to 53% depending on wind speed variability. While other studies have used nearby land-based wind speed measurements (e.g., Stieglitz et al., 2013), our data was from a weather station installed at the centre of the lagoon, so this ensures that the wind speed measurements are representative of actual lagoon conditions (Rodellas et al., 2021). We also propagated the errors from the terms above to calculate

uncertainties for the Ostwald solubility coefficient (8-9%), piston velocity (30-53%), Schmidt number (8%) and molecular diffusion coefficient for  $^{222}\text{Rn}$  (8%). Overall, this resulted in high evasion uncertainties, as reported in Figure 3.6. For piston velocity ( $k$ ), we based the assigned uncertainty on the wind speed and Schmidt number, but given our  $k$  values represent averages of four different empirical  $k$  models, our uncertainty for this term may be over-reported. Piston velocity uncertainty is important to consider, especially for systems with long residence times (e.g., coastal lagoons) and where  $^{222}\text{Rn}$  loss from wind-driven evasion is dominant (Kluge et al., 2012; Rodellas et al., 2021). Previous studies have been able to assess the potential  $k$  uncertainties by calculating  $k$  using several models (Macklin et al., 2018; Rodellas et al., 2021), as was done here. We also note that at the beginning of a 24-hour time series measurement at Te Waihora (Figure 3.5), a sharp increase in wind speeds corresponded with a steep drop in radon surface water concentrations, indicating that radon in the lagoon responds quickly to wind speed changes. This suggests that modelling evasion using wind speeds during sampling (Scenarios 1 and 2) may be an appropriate time scale for this system (Rodellas et al., 2021).

Uncertainty analysis for the radon contribution from surface inflows remains challenging. For the six large tributaries that were sampled, we included the measurement uncertainty of the RAD7 analysis and the river discharge rates. The RAD7 measurements had on average 4% uncertainty, while the river discharge was gathered from various sources with varying degrees of accuracy. We assumed that the six largest tributaries accounted for 73% of long-term mean tributary inflows (Horrell, 1992), and we proportioned the flow accordingly for the major and minor tributaries for the two modelling periods. For the minor tributaries, we assumed a 20% uncertainty on the river discharge, and based on the standard deviation of the radon concentrations in the major tributaries, we assigned an uncertainty of 130% in summer and 108% in winter for the average radon concentrations.

Several terms in the mass balance (sediment diffusion, evasion, radium decay, radon decay) required volume and surface area calculations to estimate radon inflows and outflows across the entire lagoon. Hence, accurate estimates of these terms are important, particularly for shallow systems where lagoon shapes and bathymetry may be complex (Trigg et al., 2014). The volume and area of the lagoon were estimated for the summer and winter mass balance periods by interpolating the lagoon bathymetry (Irwin & Main, 1989) using Leapfrog Geo software assuming a 5% uncertainty. For both the diffusion and radium decay terms, we used the standard deviation of the sample datasets as the uncertainty for the  $^{222}\text{Rn}$  and  $^{226}\text{Ra}$  analyses. The overall uncertainty for diffusion was 19/21% (summer/winter) and 10% for radium decay (summer only). It is possible that our diffusive  $^{222}\text{Rn}$  fluxes are overestimated because we only sampled relatively fine bed sediment, and the lagoon bed has some gravel (although a minor component), which would have produced lower diffusive fluxes (Rodellas et al., 2021). However, we also note that the diffusive  $^{222}\text{Rn}$  flux is the minimal flux from a benthic source (i.e., there may also be  $^{222}\text{Rn}$  flux from porewater exchange) (Cook et al., 2018). Although seasonal

differences in  $^{226}\text{Ra}$  decay are possible, we expect  $^{226}\text{Ra}$  concentrations to vary less than  $^{222}\text{Rn}$  (Moore, 2007).  $^{226}\text{Ra}$  decay only contributed 11% of all radon sources in the current study, and therefore is a less sensitive term of the mass balance. It is also important to highlight that the advective rates presented in Table 3.3 were calculated across the entire large surface area ( $\sim 150 \text{ km}^2$ ) of the lagoon. Thus, the rates in Table 3.3 do not reflect possible localised areas of higher groundwater flow rates (e.g., from springs).

While there are outstanding questions as to the connectivity between the lagoon and the sea at this site, we carried out a straightforward uncertainty analysis for these terms. As we assumed zero inflow or outflow of radon from the outlet to the sea, we did not include this term in the final uncertainty calculations. As for uncertainty of the barrier seepage term, we assumed a 30% uncertainty for the barrier seepage rate (based on the variance given in Horrell (1992)) and the radon-in-lagoon uncertainty used in the winter mass balance mentioned above. Overall, this resulted in 53% uncertainty for the barrier seepage term in winter. The lagoon outlet to the sea, which is controlled by a managed opening regime, introduces another layer of complexity to the radon mass balance. However, it is important to note that this type of “horizontal” loss can be one of the more difficult aspects of the mass balance to estimate (Santos, Niencheski, et al., 2008).

The key environmental conditions that varied during the two mass balance periods were lagoon level, tributary discharge and wind speeds. The lagoon level above the sea was higher in winter than in summer, and this greater depth resulted in higher surface area and volume. When these higher values were tested in the summer mass balance, the discharge estimates changed little, so the model is less sensitive to fluctuations in lagoon levels. The higher tributary discharge in winter resulted in increased radon inputs from rivers in winter; however, this resulted in minimal impact to the groundwater discharge estimates. The most sensitive parameter in the model is atmospheric evasion, which is driven in the mass balance to a large degree by wind speeds, and to a lesser extent by water temperature, both of which were higher during the summer period. This dominance of the atmospheric evasion term agrees with radon mass balance results from other lakes and coastal lagoons (Perkins et al., 2015; Sadat-Noori et al., 2016; Schmidt et al., 2010).

Using Gaussian error propagation to evaluate uncertainty requires that the variables must not be correlated (Tellinghuisen, 2001), however this is not the case here where some terms are included more than once in the overall mass balance (e.g., the radon in lagoon concentration). While Gaussian error propagation may be valid for most of the individual mass balance terms (with the exception perhaps of evasion), it may not be appropriate for quantifying uncertainty for the final groundwater discharge estimate. Given this limitation of the method used here, it may be wiser not to consider the variances of the final seepage flux estimates as absolute values given the uncertainty can vary considerably depending on the method used to calculate it (Rodellas et al., 2021).

### 3.5.3 Mass balance results in context of lagoon water balance

Previous studies of other coastal lagoons have found groundwater discharge to range from being a minimal proportion of their water budgets (e.g., Menció, Casamitjana, Mas-Pla, Coll, Comptee, et al., 2017; Stieglitz et al., 2013) to the main source of fresh inflows (e.g., Menció, Casamitjana, Mas-Pla, Coll, Comptee, et al., 2017; Sadat-Noori et al., 2016). Here, an earlier study using seepage meters estimated groundwater discharge into the lagoon to be  $0.44 \text{ m}^3/\text{s}$  or  $\sim 2.3\%$  of the total mean inflow of  $18.81 \pm 2.15 \text{ m}^3/\text{s}$  (Ettema & Moore, 1995; Horrell, 1992). This estimate was based on measurements from seepage meters installed at 14 locations on the northwest and western sides of the lagoon and did not include measurements of any springs (Ettema & Moore, 1995). Therefore, this may have missed groundwater inputs along the barrier revealed by radon surveys (Coluccio et al., 2020) or underestimated seepage rates along the northern and north-western margins given the exclusion of spring measurements. Our groundwater discharge estimates range from 1-2 orders of magnitude higher than these seepage meter-based estimates. Put into the context of the overall water budget, our estimates range from  $\sim 10\text{-}100\%$  of the total mean water inflows to the lagoon (Horrell, 1992). Given the difference in spatial scale of the seepage meter and radon mass balance methods, it can be difficult to compare results (Burnett et al., 2006). Future studies introducing alternative methods for quantifying groundwater seepage such as water isotopes (e.g., Petermann, Schubert, et al., 2018) or modelling (e.g., Menció, Casamitjana, Mas-Pla, Coll, Comptee, et al., 2017) would add additional insight.

Given even our lowest groundwater discharge estimates are twice as high as the previously estimated groundwater inflow to the lagoon, we are forced to reconsider estimates of input and output proportions of the current Te Waihora water balance (Horrell, 1992) to examine whether our results are plausible. First, the water balance is based on a multi-year period ( $\sim 20$  years) (Horrell, 1992), whereas our radon mass balances consider a much shorter time scale. Hence, it is difficult to reconcile the results of the radon mass balances with the water budget. Besides groundwater inflow, the remaining inflows are relatively well constrained (i.e., rainfall, tributaries, waves overtopping the barrier and inflows during the artificial barrier opening). In terms of outflows, discharge from the artificial barrier opening is relatively well quantified. However, estimates of evaporation rates used in Horrell (1992) were based on evaporation rates measured  $\sim 20 \text{ km}$  from Te Waihora. Because evaporation comprised  $34\%$  of outflows in the Horrell (1992) water budget, an accurate estimate of evaporation is important.

Outflows from seepage through the barrier are poorly understood and based on studies by Valentine (1988) and Inpasihardjo (1988), as cited in Horrell (1992), which relied on seepage estimates from only one cross-section of wells installed in the barrier. Given the permeable nature and heterogeneity of the mixed sand and gravel barrier, we hypothesise that seepage rates were likely underestimated.

Permeable coastal lagoon barriers have varying levels of groundwater connectivity with the sea driven by hydraulic gradients, tides and wave run up (e.g., Austin et al., 2013; Evans & Wilson, 2017). Tamborski et al. (2019) highlighted that subterranean flow between coastal lagoons and the ocean is an understudied area, especially in highly permeable gravel barriers (Austin et al., 2013). Better understanding of the interactions between coastal lagoons, their barriers and the sea is not only important for water budget purposes but also for understanding solute transport (Evans & Wilson, 2017).

### 3.6 Conclusion

Studies examining groundwater inputs to coastal lagoons have increased in the past decade and several studies have shown the importance of groundwater discharge in the water and nutrient budgets of receiving waters. A radon mass balance revealed groundwater discharge to a large coastal lagoon in New Zealand to be between  $5.2 \pm 5.8$  and  $18.7 \pm 19.6$  m<sup>3</sup>/s in summer and  $0.9 \pm 2.2$  and  $8.1 \pm 10.5$  m<sup>3</sup>/s in winter. Atmospheric evasion of radon was the most influential component of the radon mass balance. We carried out a detailed uncertainty analysis on the radon mass balance estimations. Results from the radon mass balance revealed significantly more groundwater discharge to the lagoon compared to previous estimates based on seepage meters, which highlights the usefulness of applying techniques capturing flow on different spatial and temporal scales. However, this study did not distinguish between fresh groundwater input and sediment porewater exchange, thus, it is possible that some proportion of the total groundwater discharge estimate is comprised of porewater recirculation. Where it was previously thought that direct groundwater seepage into the lagoon was a small proportion of the water balance, it appears now that it may be an important component of the water budget at scales comparable to regional river inputs.

### 3.7 Appendix: Supplementary data

Table 3.5. Radon diffusion results from Te Waihora sediment equilibrium experiments

Sample <sup>a</sup>	Date Collected	Lat	Long	<sup>222</sup> Rn in sediment porewater (Bq/m <sup>3</sup> )	Diffusive Flux Summer (Bq/m <sup>2</sup> /d)	Diffusive Flux Winter (Bq/m <sup>2</sup> /d)
NZ-1	28 Jan 2019	-43.74447	172.43488	8378	8.3	6.9
NZ-3	29 Jan 2019	-43.77293	172.59297	9533	11.2	9.5
NZ-4	30 Jan 2019	-43.81313	172.47924	9176	9.2	7.3
NZ-5	30 Jan 2019	-43.81876	172.37667	7947	7.1	5.8



<b>Mean</b>				<b>8758</b>	<b>8.9</b>	<b>7.4</b>
<b>Standard Deviation</b>				<b>725</b>	<b>1.7</b>	<b>1.5</b>

<sup>a</sup> Sample NZ-2 excluded as an outlier.

Table 3.6. <sup>226</sup>Ra concentrations in Te Waihora water samples

<b>Sample<sup>a</sup></b>	<b>Date Collected</b>	<b>Lat</b>	<b>Long</b>	<b><sup>226</sup>Ra (Bq/m<sup>3</sup>)</b>
NZ-2	28 Jan 2019	-43.78897	172.36842	18.7
NZ-3	29 Jan 2019	-43.74943	172.45230	15.9
NZ-4	29 Jan 2019	-43.77851	172.55420	19.9
NZ-5	30 Jan 2019	-43.80549	172.55598	17.0
NZ-6	30 Jan 2019	-43.82998	172.42653	16.3
NZ-7	30 Jan 2019	-43.79103	172.43316	15.3
<b>Average</b>				<b>17.2</b>
<b>Standard Deviation</b>				<b>1.8</b>

<sup>a</sup> Sample NZ-1 excluded as an outlier.

Table 3.7. Shallow groundwater samples collected near Te Waihora to estimate the average  $^{222}\text{Rn}$  concentration in groundwater

Sample	Date Collected	Lat	Long	Water Level Below Ground (m)	$^{222}\text{Rn}$ (Bq/m <sup>3</sup> )	Counting Uncertainty (Bq/m <sup>3</sup> )	Water Temperature (°C)	Specific Conductivity (µS/cm)	pH	Dissolved Oxygen (% sat)
Selwyn Huts	10 Sept 2019	-43.74002	172.44415	0.400	3056	31	9.9	8352	6.52	9.1
Timberyard Point	14 Aug 2019	-43.79686	172.37461	0.338	2172	33	8.6	2835	6.35	21.9
Fishermans Point	6 Jul 2020	-43.85437	172.37202	0.884	2291	18	10.5	1106	6.56	46.4
Lake Road South	6 Jul 2020	-43.74748	172.38541	0.828	4104	25	10.7	310	6.93	9.3
Coes Ford	14 Jul 2020	-43.69590	172.41375	0.852	4153	23	12.0	327	6.48	12.9
LII River	14 Jul 2020	-43.71019	172.45034	0.770	2187	16	9.7	614	5.86	10.8
Dickies Road	31 Aug 2020	-43.73031	172.39860	0.710	6880	48	10.3	418	6.54	14.6
Drain Road	31 Aug 2020	-43.77838	172.36222	0.895	5693	43	11.3	219	7.11	9.6
Harts Creek	31 Aug 2020	-43.79657	172.34392	0.526	4786	30	10.5	221	7.04	5.9
Irwell Reserve	31 Aug 2020	-43.74967	172.37837	0.683	667	11	10.8	427	6.94	9.4
<b>Median</b>					<b>3580</b>					
<b>Standard Deviation</b>					<b>1878</b>					

Table 3.8. Results of Te Waihora tributary sampling for  $^{222}\text{Rn}$

Sample	Date Collected	Lat	Long	$^{222}\text{Rn}$ (Bq/m <sup>3</sup> )	Water Temperature (°C)	Specific Conductivity (µS/cm)	pH	Dissolved Oxygen (% sat)	Wind Speed (kph) <sup>a</sup>	River Discharge Rate <sup>b</sup> (m <sup>3</sup> /s)
<i>Summer</i>										
Selwyn River	31 Jan 2019	-43.74000	172.44362	336	23.5	2108	8.03	143.6	2.8	0.904
LII River	31 Jan 2019	-43.71004	172.44992	2399	22.3	226	7.01	95.2	5.4	1.726 <sup>c</sup>
Halswell River	31 Jan 2019	-43.75150	172.60469	49	27.3	4471	7.99	114.9	11.5	1.106 <sup>c</sup>
Kaituna River	31 Jan 2019	-43.77447	172.65646	163	28.5	402	7.26	93.4	5.4	0.136
Irwell River	1 Feb 2019	-43.74531	172.37648	128	20.1	186	7.57	68.9	5.0	0.384 <sup>c</sup>
Harts Creek	1 Feb 2019	-43.79643	172.34433	1249	15.4	296	7.77	84.9	3.6	1.071
<i>Winter</i>										
Selwyn River	28 Aug 2020	-43.74000	172.44362	348	10.7	1070	7.74	104.4	2.8	3.254
LII River	28 Aug 2020	-43.71004	172.44992	1713	13.5	221	7.25	85.7	3.0	2.439
Halswell River	4 Sept 2020	-43.75150	172.60469	141	9.6	5780	7.65	87.2	10.0	1.017
Kaituna River	4 Sept 2020	-43.77447	172.65646	205	8.6	823	7.25	94.5	3.0	0.850
Irwell River	28 Aug 2020	-43.74531	172.37648	128	8.0	331	7.14	88.4	3.5	1.350 <sup>c</sup>
Harts Creek	28 Aug 2020	-43.79643	172.34433	1349	11.8	265	7.35	91.3	0	1.662

<sup>a</sup> Summer wind speed measurements were taken at water surface. Winter wind speed measurements were taken 1.5 m above water surface.

<sup>b</sup> Summer discharge rates are the average flow rate on the date of sampling. Winter discharge rates are the average flow rate across the winter mass balance period (27 August-20 September 2019).

<sup>c</sup> Discharge rates derived from synthetic flow rate calculations or spot flow gaugings correlated with upstream flow recorder sites

Table 3.9. Atmospheric evasion of  $^{222}\text{Rn}$  under several scenarios during the summer and winter mass balance periods

Scenario	Wind speed at 10 m (m/s)	Average $k$ (m/hr)	Atmospheric $^{222}\text{Rn}$ Flux (Bq/m <sup>2</sup> /d)	Atmospheric $^{222}\text{Rn}$ Flux Uncertainty
<i>Summer (28-30 Jan 2019)</i>				
(1) Mean wind during sampling	6.5	0.07	42.6	86%
(2) Mean wind across survey days	5.4	0.05	31.8	92%
(3) Mean wind during survey days + 7 days prior	6.4	0.07	41.9	94%
<i>Winter (27 Aug-20 Sept 2019)</i>				
(1) Mean wind during sampling	3.7	0.02	15.6	68%
(2) Mean wind across survey days	4.3	0.03	19.6	63%
(3) Mean wind during 25-day sampling period	5.5	0.04	27.9	70%

Table 3.10. Key variables in the summer and winter radon mass balances

Variable	Unit	Best estimate - Summer	Best estimate - Winter	Proportion of variable in mass balance (Summer/Winter) <sup>a</sup>
<b>General</b>				
Lagoon volume	m <sup>3</sup>	$1.00 \times 10^8 \pm 5.01 \times 10^6$	$1.46 \times 10^8 \pm 7.32 \times 10^6$	
Lagoon surface area	km <sup>2</sup>	$138.96 \pm 6.95$	$149.60 \pm 7.48$	
Mean lagoon level	m above MSL	0.56	0.88	
$^{222}\text{Rn}$ concentration in groundwater	Bq m <sup>-3</sup>	$3580 \pm 1878$	$3580 \pm 1878$	
$^{222}\text{Rn}$ concentration from sediment diffusion	Bq m <sup>-3</sup>	$8758 \pm 725$	$8758 \pm 725$	
$^{222}\text{Rn}$ concentration in lagoon	Bq m <sup>-3</sup>	$32 \pm 20$	$30 \pm 13$	
<b>Radon sources</b>				
$^{222}\text{Rn}$ from surface water inflows	Bq d <sup>-1</sup>	$6.32 \times 10^8 \pm 1.69 \times 10^8$	$9.10 \times 10^8 \pm 2.39 \times 10^8$	9% / 24%
$^{222}\text{Rn}$ diffusion from lake sediment	Bq d <sup>-1</sup>	$1.24 \times 10^9 \pm 2.46 \times 10^8$	$1.10 \times 10^9 \pm 2.34 \times 10^8$	17% / 29%
$^{222}\text{Rn}$ inflow from $^{226}\text{Ra}$ decay	Bq d <sup>-1</sup>	$3.09 \times 10^8 \pm 3.56 \times 10^8$	$4.51 \times 10^8 \pm 5.21 \times 10^7$	4% / 12%
$^{222}\text{Rn}$ from groundwater seepage (Scenario 1 <sup>b</sup> )	Bq d <sup>-1</sup>	$5.77 \times 10^9 \pm 5.27 \times 10^9$	$6.69 \times 10^8 \pm 1.65 \times 10^9$	73% / 21%
$^{222}\text{Rn}$ from groundwater seepage (Scenario 2)	Bq d <sup>-1</sup>	$3.90 \times 10^9 \pm 4.36 \times 10^9$	$1.26 \times 10^9 \pm 1.92 \times 10^9$	64% / 34%

<sup>222</sup> Rn from groundwater seepage (Scenario 3)	Bq d <sup>-1</sup>	$5.64 \times 10^9 \pm 5.87 \times 10^9$	$2.50 \times 10^9 \pm 2.96 \times 10^9$	72% / 50%
Total Input (excl. groundwater seepage)	Bq d <sup>-1</sup>	$2.18 \times 10^9 \pm 3.01 \times 10^8$	$2.46 \times 10^9 \pm 3.39 \times 10^8$	
Radon sinks				
<sup>222</sup> Rn evasion to atmosphere (Scenario 1)	Bq d <sup>-1</sup>	$7.38 \times 10^9 \pm 5.25 \times 10^9$	$2.34 \times 10^9 \pm 1.58 \times 10^9$	93% / 75%
<sup>222</sup> Rn evasion to atmosphere (Scenario 2)	Bq d <sup>-1</sup>	$5.52 \times 10^9 \pm 4.33 \times 10^9$	$2.93 \times 10^9 \pm 1.86 \times 10^9$	91% / 79%
<sup>222</sup> Rn evasion to atmosphere (Scenario 3)	Bq d <sup>-1</sup>	$7.25 \times 10^9 \pm 5.85 \times 10^9$	$4.17 \times 10^9 \pm 2.92 \times 10^9$	93% / 84%
<sup>222</sup> Rn outflow from lake opening	Bq d <sup>-1</sup>	0	0	0% / 0%
<sup>222</sup> Rn outflow via barrier	Bq d <sup>-1</sup>	0	$2.69 \times 10^6 \pm 1.42 \times 10^6$	0% / 0.07%
<sup>222</sup> Rn decay	Bq d <sup>-1</sup>	$5.72 \times 10^8 \pm 3.61 \times 10^8$	$7.91 \times 10^8 \pm 3.45 \times 10^8$	8% / 21%
Total Output - Scenario 1	Bq d <sup>-1</sup>	$7.96 \times 10^9 \pm 5.26 \times 10^9$	$3.13 \times 10^9 \pm 1.62 \times 10^9$	
Total Output - Scenario 2	Bq d <sup>-1</sup>	$6.09 \times 10^9 \pm 4.34 \times 10^9$	$3.72 \times 10^9 \pm 1.89 \times 10^9$	
Total Output - Scenario 3	Bq d <sup>-1</sup>	$7.82 \times 10^9 \pm 5.87 \times 10^9$	$4.97 \times 10^9 \pm 2.94 \times 10^9$	

<sup>a</sup> Variable proportions are averaged for the three wind speed scenarios.

<sup>b</sup> Scenario numbers for summer refer to: (1): evasion using mean wind speed during sampling; Scenario (2): evasion using mean wind speed across sampling days; Scenario (3) evasion using mean wind speed from 3-day sampling period + 7 days prior. Scenario numbers for winter refer to (1): evasion using mean wind speed during sampling; Scenario (2): evasion using mean wind speed across sampling days; Scenario (3) evasion using mean wind speed from sampling period.

## **4. Resolving groundwater sources to a coastal lagoon using major ions, nutrients and stable isotopes**

### **4.1 Abstract**

Coastal lagoons are important for ecological, cultural, economic and recreational reasons. Globally, they are subject to significant anthropogenic pressures. Our understanding of the importance of groundwater discharge into coastal lagoons for water and solute budgets is evolving, yet key gaps remain. This study resolves sources of groundwater seepage and estimates nutrient loads from direct groundwater discharge into a large hypertrophic coastal lagoon in New Zealand. We analysed major ions, stable water isotopes and nutrients in lagoon surface water, porewater, groundwater wells and springs. Groundwater and porewater samples split into two distinct groups: (1) inland samples that were  $\text{MgHCO}_3$  dominated with more negative  $\delta^2\text{H}:\delta^{18}\text{O}$  ratios and lower ion concentrations, and (2) permeable barrier samples that were  $\text{NaCl}$  dominated with more positive  $\delta^2\text{H}:\delta^{18}\text{O}$  ratios and higher ion concentrations. Porewater entering the lagoon is sourced from alpine-river and rainfall recharge on the plains. Barrier porewater appears to be sourced from infiltration from the lagoon through the barrier and local rainfall. Despite higher nitrate in deeper groundwater wells, low nitrate in shallow porewater indicates potential denitrification before groundwater discharges to the lagoon. Our observations support efforts to restore and construct wetlands around the lagoon to remove nutrients. However, wetland restoration will need to be carried out by maintaining a balance between enhancing denitrifying conditions while preventing phosphorus release from sediments. Nutrient load calculations revealed that direct groundwater seepage to the lagoon provides ~3% of dissolved inorganic nitrogen and ~30% of dissolved reactive phosphorus compared to river inputs, indicating that groundwater discharge may play an important role in phosphorus transport to the lagoon.

### **4.2 Introduction**

Coastal lagoons are important features, found on coastlines on every continent except Antarctica (Barnes, 1980). These shallow waterbodies range in their degree of connection to the sea, are typically turbid and well mixed, and have a salinity gradient from fresh to close to seawater (Kjerfve, 1986, 1994). Coastal lagoons support rich biological diversity, productive fisheries and extensive wetlands (Costanza et al., 1997) and provide fundamental ecosystem services such as floodwater attenuation and nutrient cycling (Schallenberg et al., 2013). Coastal lagoons are at the nexus of many, often competing, human and ecological needs. As a result, coastal lagoons throughout the world face significant pressure from development, pollution and anthropogenic changes (Beer & Joyce, 2013).

Groundwater discharge into coastal lakes and lagoons has long been overlooked, but it has increasingly been found to be an important component of water and nutrient budgets (Lewandowski et al., 2015; Menció, Casamitjana, Mas-Pla, Coll, Comptee, et al., 2017; Rosenberry et al., 2015; Santos et al., 2021). At some sites where groundwater was found to be a small component of the overall water budget, it was the biggest contributor of nutrient loads and other dissolved species (Santos, Machado, et al., 2008). For effective management of groundwater-derived contaminants in coastal lagoons, the source of the groundwater discharge needs to be identified (Menció, Casamitjana, Mas-Pla, Coll, Comptee, et al., 2017; Young et al., 2008).

The number of studies investigating groundwater sources and hydrological dynamics in coastal lagoons has increased in recent years. There have been studies examining coastal lagoons in the tropics (Young et al., 2008) and Mediterranean (Rocha et al., 2016; Stumpp et al., 2014), however fewer studies have been done in temperate climates in the Southern Hemisphere. A number of studies have specifically examined the role that groundwater plays as a source of nutrients (González-De Zayas et al., 2013; Liefer et al., 2014; McMahon & Santos, 2017; Medina-Gómez & Herrera-Silveira, 2006), dissolved ions (Santos, Machado, et al., 2008) and trace elements (Ganguli et al., 2012) to coastal lagoons. Also, the connectivity between lagoons and sea via the freshwater system underlying barriers remains difficult to quantify (Austin et al., 2013; Bratton et al., 2009; Rapaglia, Di Sipio, et al., 2010; Röper et al., 2012; Schmidt et al., 2011; Tamborski et al., 2019).

A variety of geochemical techniques can characterise groundwater sources including stable water isotopes ( $\delta^{18}\text{O}$  and  $\delta^2\text{H}$ ), radionuclides (namely  $^{222}\text{Rn}$  and Ra isotopes), and major ions (e.g., Bratton et al., 2009; Kong et al., 2019; Petermann, Schubert, et al., 2018). Stable water isotopes offer insights into water sources contributing to submarine groundwater discharge (SGD) because they are simple to sample and the sources may have distinct signatures (Duque, Jessen, et al., 2019). Major ion chemistry can reveal geochemical processes that are relevant at a site and shed light on mixing water sources (Röper et al., 2012; Young et al., 2008). Many of these studies have lumped water samples into representative groups with similar hydrochemical signatures. Techniques for doing this have typically included statistical correlations (e.g., linear regressions or Pearson coefficient correlations (see Santos et al. (2008) or Ji et al. (2013)), or mixing models using end-member mixing analysis (EMMA) (e.g., Moore, 2003; Stumpp et al., 2014; Young et al., 2008). Mixing models often require a high density of samples to determine the chemical signature of each source (Duque, Jessen, et al., 2019) and tracers must be chemically conservative (Moore, 2003).

Analysis of groundwater-derived nutrient transport and nutrient processes in coastal areas has revealed a major role of groundwater nutrients in coastal ecosystems (Andrisoa et al., 2019; Ibáñez et al., 2013; Santos et al., 2021). Nitrogen, phosphorus, carbon and silica concentrations in groundwater are required to estimate nutrient loads to receiving waters based on groundwater

discharge estimates (e.g., Burnett et al., 2007; Ji et al., 2013; Kong et al., 2019; Maher et al., 2019). Several recent studies have examined nutrient processes within nearshore sediments and coastal waterbodies such as denitrification and phosphorus release from sediments (Bernard et al., 2014; Duque, Jessen, et al., 2019; Santos et al., 2014). In coastal aquifers, denitrification often attenuates the nitrogen flux via groundwater pathways (Loveless & Oldham, 2010).

In this study we aim to (1) resolve sources of groundwater seepage to a lagoon and (2) estimate nutrient loads from direct groundwater discharge to the lagoon. We analysed major ion chemistry, nutrients and stable isotopes ( $\delta^{18}\text{O}$  and  $\delta^2\text{H}$ ) around a hypertrophic, temperate climate coastal lagoon in New Zealand including samples from lagoon surface water, porewater on the lagoon margins, groundwater wells and springs. We hypothesise that groundwater seepage comprises a mix of alpine river recharge, rainfall recharge and lagoon water recirculation in shallow sediments. Based on high nutrient concentrations in regional groundwater and rivers (Hayward & Ward, 2009), we also hypothesise that direct groundwater seepage plays an important role releasing nutrients to the lagoon.

## **4.3 Methods**

### **4.3.1 Site Description**

This study focuses on Te Waihora (Lake Ellesmere), a large ( $\sim 150 \text{ km}^2$ ), shallow (mean depth = 1.4 m) coastal lagoon on the east coast of the South Island of New Zealand ( $43^\circ 46' 40.3'' \text{ S } 172^\circ 28' 27.2'' \text{ E}$ ) (Figure 4.1). This culturally significant site is important to a variety of stakeholders for its ecological, economic and recreational values. Local Māori tribe Ngāi Tahu consider Te Waihora a taonga (treasure) and have traditionally referred to the site as Te Kete Ika o Rākaihautū—The Fish Basket of Rākaihautū for its outstanding food and fibre gathering resources. However, the water quality of the lagoon has significantly declined due to pressure from intensive agriculture, deforestation and wetland draining in the surrounding catchment. Te Waihora is hypertrophic with high turbidity, chlorophyll *a* and nutrients, however, the lagoon does not generally exhibit some of the classic characteristics of hypertrophic water bodies like severe oxygen depletion, fish kills or toxic algal blooms (Hayward & Ward, 2009).



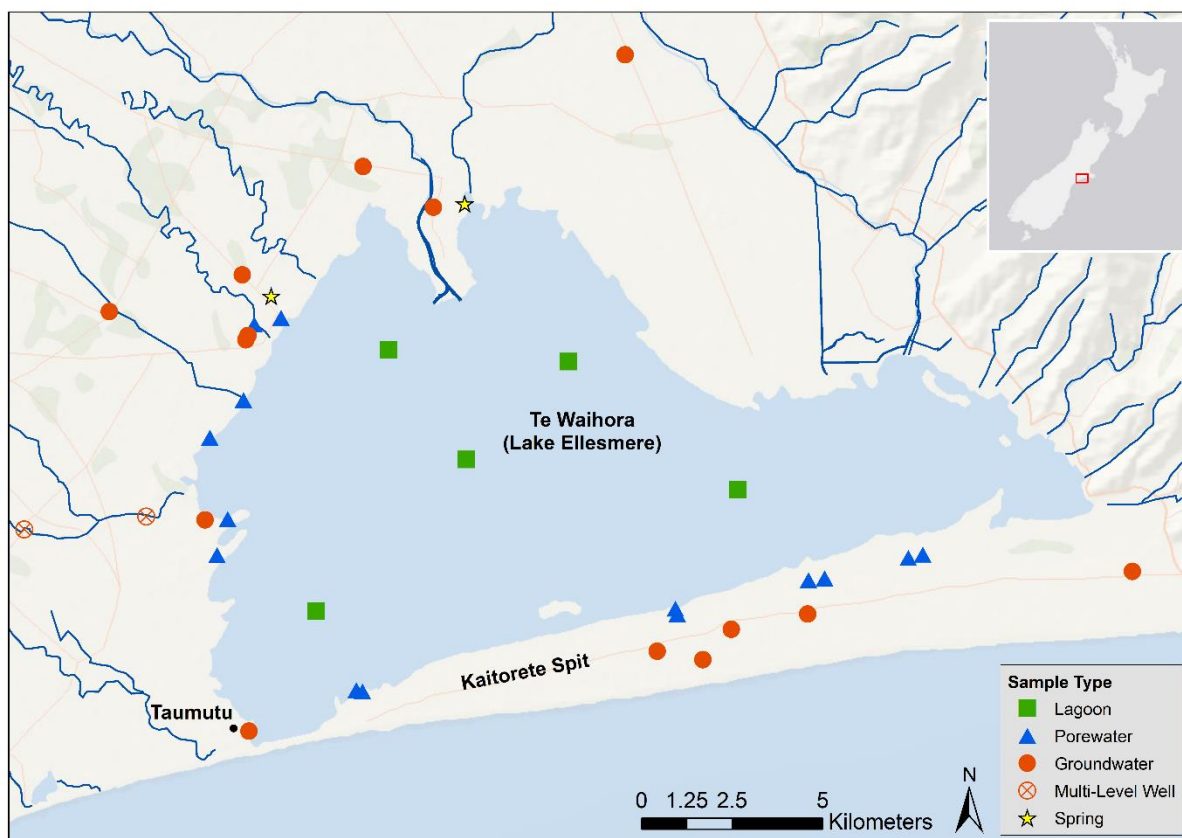


Figure 4.1. Location map of hydrochemistry samples taken in November-December 2020 in and around Te Waihora (Lake Ellesmere). Map base layer credits: Land Information New Zealand and Eagle Technology. Map includes GIS data from Land Information New Zealand (Land Information New Zealand, 2019, 2020).

The geology of the 2560 km<sup>2</sup> Te Waihora catchment is comprised mainly of alluvial sediments eroded from the Southern Alps to the west, which are comprised of greywacke, a marine-derived sedimentary rock dominated by silicates (Brown & Weeber, 1992). The catchment is bordered by two large gravel-bed braided rivers—the Waimakariri River to the north and the Rakaia River to the south, and to the southeast by Banks Peninsula volcanics overtopped by loess. Te Waihora formed in the depression between the alluvial fans of the adjacent braided rivers during interglacial Holocene sea level rise (Bird, 1994), and it has fluctuated between an estuary and an enclosed coastal lake/lagoon (its present state). During the past several thousand years, sand and gravel transported by northward longshore drift formed a barrier that separated Te Waihora from the sea, referred to as Kaitorete Spit (Armon, 1970). The lagoon is considered a “choked” lagoon in terms of Kjerfve’s (1986) lagoon classification and locally as a Waituna-type lagoon (Kirk & Lauder, 2000), with features such as a narrow outlet to the sea; minimal tidal influence; salinity ranging from fresh to brackish; and relatively long water residence times. The lagoon entrance to the sea is mechanically opened to the sea on average 2-6 times per year when the lagoon height reaches set trigger levels. The regional hydrogeology largely consists of an unconfined mixed sand and gravel alluvial aquifer. The system becomes confined

towards the coast where the alluvial gravels are interspersed by semi-confining marine deposits, which is referred to as the Christchurch artesian aquifer system (Brown, 2001; Brown & Weeber, 1992). Here, there are at least five confined aquifers in a stacked formation near the coast. Over 40 rivers, small streams and drains flow into Te Waihora, many of which are spring fed.

While there are various studies investigating groundwater sources in and around Te Waihora in grey literature, there are few relevant published studies. Two previous studies examined the locations of groundwater seepage in the lagoon (Coluccio et al., 2020; Ettema & Moore, 1995), while Coluccio et al. (2021) quantified groundwater discharge to the lagoon using a radon mass balance. Hanson and Abraham (2009) analysed major ion chemistry, stable oxygen isotopes and nutrients along a cross-section of the Canterbury Plains, which intersected with Te Waihora. They found that  $\delta^{18}\text{O}$  is the most reliable tracer on the Canterbury Plains for distinguishing between alpine river recharge and rainfall-based recharge. However, they recommended using a suite of tracers to draw comprehensive conclusions regarding groundwater recharge sources and flow paths (Hanson & Abraham, 2009). Stewart (2012) examined  $\delta^{18}\text{O}$  ratios, age tracers and major ions to determine groundwater sources and flow paths in the Christchurch Aquifer System. Groundwater seepage seems to be a main source of new nutrients to the lagoon, but very limited data sets are available (Larned & Schallenberg, 2006). This study builds on the literature by conducting an in-depth investigation into groundwater sources and their implications in nutrient transport at a site where these processes have been minimally investigated.

#### **4.3.2 Sampling and analysis**

Forty water samples were collected in November-December 2020 from various locations around Te Waihora and consisted of four main sample types: lagoon surface water, porewater on the lagoon margins, groundwater wells and springs (Figure 4.1). Lagoon surface samples ( $n = 5$ ) were taken in five locations spatially distributed across the lagoon on a moderately windy day (mean wind speed = 10.2 m/s). Porewater samples ( $n = 14$ ) were taken with a stainless-steel drive-point 2-m long mini-piezometer screened in the bottom 30 cm (design similar to Coluccio (2018)). The piezometers were installed as close to the edge of the lagoon as possible (max distance from margin = ~750 m) so that shallow groundwater could be sampled (max depth = 0.75 m). Existing groundwater wells at a variety of depths and locations were sampled ( $n = 19$ ), including two multi-level wells. Wells screened in the unconfined surface aquifer to the third confined aquifer were targeted (screened between 0.5-90.5 m below ground). Two springs were sampled: a spring-fed agricultural drain and a spring that emerges in the mudflats on the north margin of the lagoon that has artesian flow at many times of the year, though at the time of sampling, it did not appear to have significant artesian flow.

Most samples were pumped with either peristaltic or submersible pumps. Several groundwater wells were sampled through existing taps, and for one of the springs (SPR1), a bottle was filled directly. All but three samples (GW1, GW8, SPR1) were pumped through a flow cell so that water quality measurements were not exposed to the air. All groundwater samples were taken once water quality parameters stabilised. Wells were purged in excess of three well volumes (Daughney et al., 2006), except for four wells that are continuously pumped (GW4, GW10) or were too deep to practically pump three well volumes (GW6, GW15). Water quality parameters (dissolved oxygen, specific conductivity, temperature, pH, oxidation-reduction potential (ORP)) were measured while the samples were pumped using a YSI Pro Plus Multiparameter Meter (YSI Incorporated, Yellow Springs, OH). Sample colour and smell were noted at time of collection, and samples were refrigerated immediately after collection.

Samples were analysed for major ions, nutrients, stable isotopes and trace metals. Samples for major cation analysis were filtered with 0.45 µm Millipore® mixed cellulose ester filters, preserved with ultra-pure nitric acid and stored at 4°C until analysis. These samples were analysed for  $\text{Ca}^{2+}$ ,  $\text{Mg}^{2+}$ ,  $\text{Na}^+$ ,  $\text{K}^+$ , Fe and Mn on an ICP-OES (Inductively coupled plasma - optical emission spectrometry) at Lincoln University (Lincoln, New Zealand). Major anion analysis ( $\text{Cl}^-$ ,  $\text{SO}_4^{2-}$ ,  $\text{NO}_3^-$ ) was carried out using ion chromatography at University of Canterbury (Christchurch, New Zealand) with refrigerated (4°C) filtered (0.2 µm Millipore®) samples. We used a Metrohm Eco IC (Metrohm AG, Herisau, Switzerland) with a Metrosep A Supp 17-150/4.0 column, 5 mmol/L  $\text{Na}_2\text{CO}_3$  0.3 mmol/L  $\text{NaHCO}_3$  eluent and a flow rate of 0.600 mL/min. Samples were diluted when necessary using deionised water (purified to 0.67 µS/cm). Bicarbonate ( $\text{HCO}_3^-$ ) and carbonate ( $\text{CO}_3^{2-}$ ) ions were determined by measuring total alkalinity by titrating to pH 4 with 1.600 N sulfuric acid using a HACH digital titrator (HACH, Loveland, CO). Samples were analysed for a suite of nutrients at an accredited lab (Hill Laboratories, Hamilton, NZ). Nitrate-N ( $\text{NO}_3^-$ -N) and nitrite-N ( $\text{NO}_2^-$ -N) were determined using automated cadmium reduction and automated colorimetry. Total kjeldahl nitrogen (TKN) and ammoniacal nitrogen ( $\text{NH}_4^+$ -N) were analysed by phenol/hypochlorite colorimetry. Total nitrogen (TN) was calculated ( $\text{TKN} + \text{NO}_3^-$ -N +  $\text{NO}_2^-$ -N). Dissolved reactive phosphorus (DRP) was determined using molybdenum blue colorimetry, and total phosphorus (TP) was analysed by ascorbic acid colorimetry. Stable isotope analysis ( $\delta^{18}\text{O}$  and  $\delta^2\text{H}$ ) was carried out on 38 refrigerated and filtered (0.45 µm Millipore®) samples at the GNS Science Stable Isotope Laboratory (Wellington, NZ) (note: samples SW2 and SW5 were not analysed). Samples were analysed on an Isoprime mass spectrometer for  $\delta^{18}\text{O}$  by water equilibration at 25°C using an Aquaprep device, and for  $\delta^2\text{H}$  by reduction at 1100°C using a Eurovector Chrome HD elemental analyser with analytical precisions of 0.2‰ for  $\delta^{18}\text{O}$  and 2.0‰ for  $\delta^2\text{H}$ . All stable isotope results are reported in terms of deviation from Vienna Standard Mean Ocean Water 2 (VSMOW2) and normalised to internal GNS laboratory standards. Where

results were below detection limits, half the detection limit was used to calculate statistics such as averages, standard deviations and medians.

## **4.4 Results**

### **4.4.1 Field parameters**

The mean values and standard deviations for the parameters measured revealed different sample groups (Table 4.1). Water temperature ranged from 11.3-21.6°C (median = 13.7°C). Electrical conductivity (measured as specific conductivity) ranged from 110.3-34860  $\mu\text{S}/\text{cm}$  (median = 390.6  $\mu\text{S}/\text{cm}$ ). We recorded dissolved oxygen levels between 0.9-103% saturation (median = 44% saturation). The pH of samples ranged from 6.1-8.9 (median = 6.9). ORP values were between -136.0 to 256.3 mV (median = 147.6 mV). During the 5-week sampling period, the ambient air temperature and wind speed ranged from 8-25°C and 0-19 m/s, respectively, and there was 50.5 mm of rainfall (Environment Canterbury, 2020a). The lagoon was on average 0.8 m above mean sea level during the sampling campaign and had last been opened to the sea in mid-August 2020 (Environment Canterbury, 2020a).

Table 4.1. Summary mean and standard deviation of field parameters, major ions, trace metals, nutrients and stable isotopes measured in samples collected in and around Te Waihora.

Parameter (unit)	Inland Groundwater (n = 14)	Inland Porewater (n = 6)	Barrier Groundwater (n = 5)	Barrier Porewater (n = 8)	Springs (n = 2)	Lagoon (n = 5)
Temperature (°C)	13.5 ± 0.7	12.4 ± 1.1	14.7 ± 1.2	13.3 ± 1.5	17.6 ± 5.6	18.5 ± 0.2
Electrical conductivity (µS/cm)	194.6 ± 87.3	295.1 ± 63.1	1461 ± 1422	6432 ± 12020	2843 ± 3308	16330 ± 603
pH (-)	7.52 ± 0.49	6.68 ± 0.25	6.91 ± 0.14	6.25 ± 0.15	7.09 ± 0.23	8.65 ± 0.15
Dissolved Oxygen (% sat)	56.9 ± 34.1	32.3 ± 30.4	36.2 ± 30.6	15.5 ± 13.8	75.3 ± 0.9	98.0 ± 1.6
Redox Potential (mV)	188.7 ± 61.0	62.1 ± 52.4	-12.1 ± 128.3	60.3 ± 63.4	250.5 ± 8.2	234.7 ± 12.8
Ca <sup>2+</sup> (meq/L)	1.04 ± 0.45	1.35 ± 0.38	1.67 ± 1.96	2.49 ± 3.65	2.57 ± 0.47	5.92 ± 0.36
K <sup>+</sup> (meq/L)	0.03 ± 0.01	0.06 ± 0.04	0.41 ± 0.29	1.43 ± 2.30	0.94 ± 1.23	6.37 ± 0.43
Mg <sup>2+</sup> (meq/L)	0.42 ± 0.25	0.77 ± 0.15	2.00 ± 1.74	2.45 ± 1.91	2.92 ± 2.67	6.56 ± 0.10
Na <sup>+</sup> (meq/L)	0.42 ± 0.28	1.06 ± 0.57	13.00 ± 14.11	67.43 ± 130.5	30.04 ± 38.73	190.0 ± 35.09
HCO <sub>3</sub> <sup>-</sup> + CO <sub>3</sub> <sup>2-</sup> (meq/L)	1.10 ± 0.28	1.67 ± 0.54	0.88 ± 0.20	2.08 ± 1.93	1.99 ± 0.64	2.10 ± 0.05
Cl <sup>-</sup> (meq/L)	0.35 ± 0.24	0.78 ± 0.35	13.25 ± 14.58	70.09 ± 140.04	25.96 ± 34.65	174.56 ± 7.54
SO <sub>4</sub> <sup>2-</sup> (meq/L)	0.27 ± 0.39	0.34 ± 0.19	1.08 ± 1.16	5.32 ± 9.95	2.69 ± 2.25	14.99 ± 0.68
Fe (mg/L)	0.025 ± 0.066 <sup>a</sup>	0.918 ± 1.655 <sup>a</sup>	1.051 ± 1.231 <sup>a</sup>	3.968 ± 4.766	0.008 ± 0.009 <sup>a</sup>	<0.003 <sup>b</sup>
Mn (mg/L)	0.016 ± 0.048 <sup>a</sup>	0.139 ± 0.130	0.087 ± 0.096 <sup>a</sup>	0.574 ± 0.829	0.086 ± 0.081	0.001 ± 0.002 <sup>a</sup>
δ <sup>18</sup> O (‰)	-8.78 ± 0.24	-8.56 ± 0.15	-7.46 ± 0.50	-6.60 ± 0.81	-7.42 ± 0.81	-2.30 ± 0.31 <sup>c</sup>
δ <sup>2</sup> H (‰)	-59.32 ± 1.93	-57.92 ± 0.78	-50.58 ± 3.52	-45.41 ± 4.13	-51.08 ± 3.68	-18.84 ± 2.25 <sup>c</sup>
Dissolved Reactive Phosphorus (mg/L)	0.010 ± 0.004 <sup>a</sup>	0.012 ± 0.012 <sup>a</sup>	0.017 ± 0.028	0.092 ± 0.204 <sup>a</sup>	0.006 ± 0.005 <sup>a</sup>	<0.010 <sup>b</sup>
Total P (mg/L)	0.014 ± 0.013 <sup>a</sup>	0.166 ± 0.332	0.077 ± 0.065	0.233 ± 0.319	0.037 ± 0.035	0.186 ± 0.013
Nitrate-N (mg/L)	2.144 ± 3.117	0.068 ± 0.076	0.687 ± 0.700	0.062 ± 0.127 <sup>a</sup>	0.060 ± 0.084 <sup>a</sup>	<0.01 <sup>b</sup>
Nitrite-N (mg/L)	<0.002 <sup>b</sup>	0.006 ± 0.006 <sup>a</sup>	0.005 ± 0.008 <sup>a</sup>	0.007 ± 0.009 <sup>a</sup>	0.003 ± 0.003 <sup>a</sup>	<0.01 <sup>b</sup>
Ammoniacal-N (mg/L)	0.008 ± 0.013 <sup>a</sup>	0.047 ± 0.059 <sup>a</sup>	0.064 ± 0.066 <sup>a</sup>	0.106 ± 0.253 <sup>a</sup>	0.019 ± 0.020 <sup>a</sup>	0.03 ± 0.01 <sup>a</sup>
Total N (mg/L)	2.17 ± 3.10 <sup>a</sup>	0.91 ± 1.25 <sup>a</sup>	0.85 ± 0.71	0.601 ± 0.817	0.48 ± 0.45	3.1 ± 1.6

<sup>a</sup> Where results fell below the detection limit, half the detection limit was used to calculate the average values reported here.

<sup>b</sup> The detection limit is reported for these samples where all results were below detection.

<sup>c</sup> Only three lagoon samples were analysed for  $\delta^{18}\text{O}$  and  $\delta^2\text{H}$ .

#### 4.4.2 Major ions

The average concentrations and standard deviations of major ions are reported in Table 4.1. Of the 40 samples, 92% ( $n = 37$ ) had an ion balance percent difference less than 10% (Figure 4.2). Of the remaining three samples, two had ion balance percent differences of 11 and 13%, while one sample had a 22% difference. These ion balance results are similar to another ion chemistry study in a coastal lagoon (Santos, Machado, et al., 2008) indicating an overall acceptable level of accuracy for these results. The dominant cations were  $\text{Ca}^{2+}$  or  $\text{Na}^+ + \text{K}^+$  (Figure 4.3). The dominant anions were  $\text{HCO}_3^-$  or  $\text{Cl}^-$ , with a small number of samples comprised of a mix between the two. As for overall major ion composition, nearly all samples were either  $\text{MgHCO}_3$  or  $\text{NaCl}$  types, with a small number ( $n = 3$ ) consisting of a mixture between the two (though closer to  $\text{MgHCO}_3$  type).

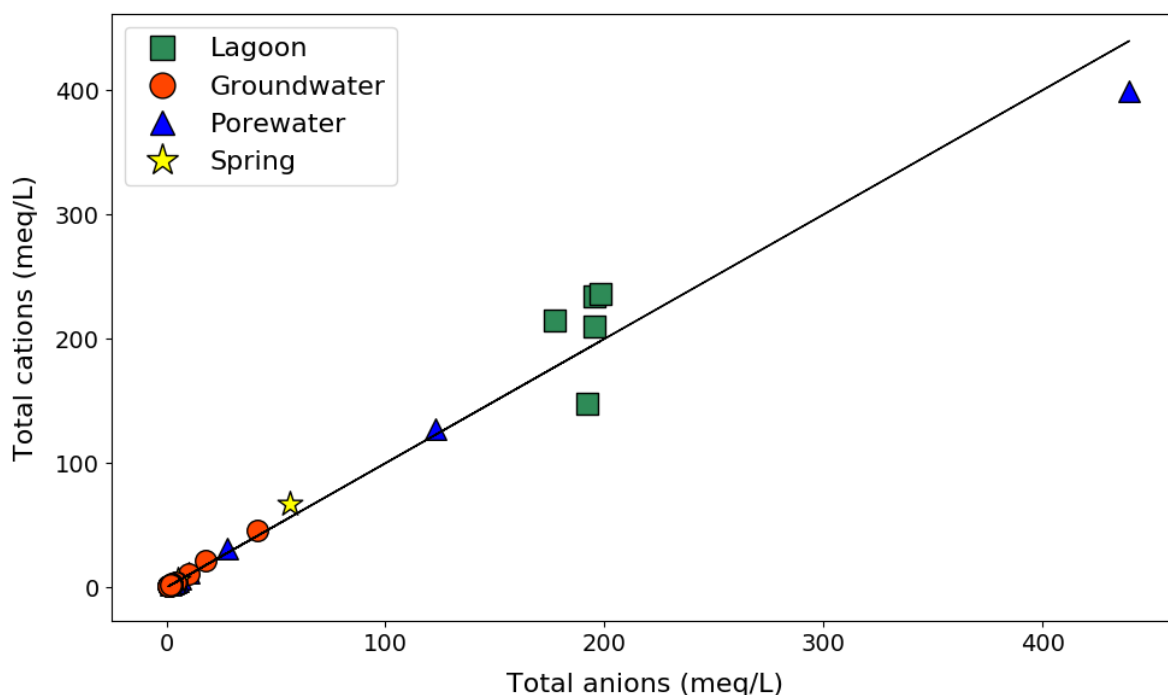


Figure 4.2. Scatter plot of the sum of the anions versus the sum of the cations in the 40 samples taken in and around Te Waihora plotted against a 1:1 line.

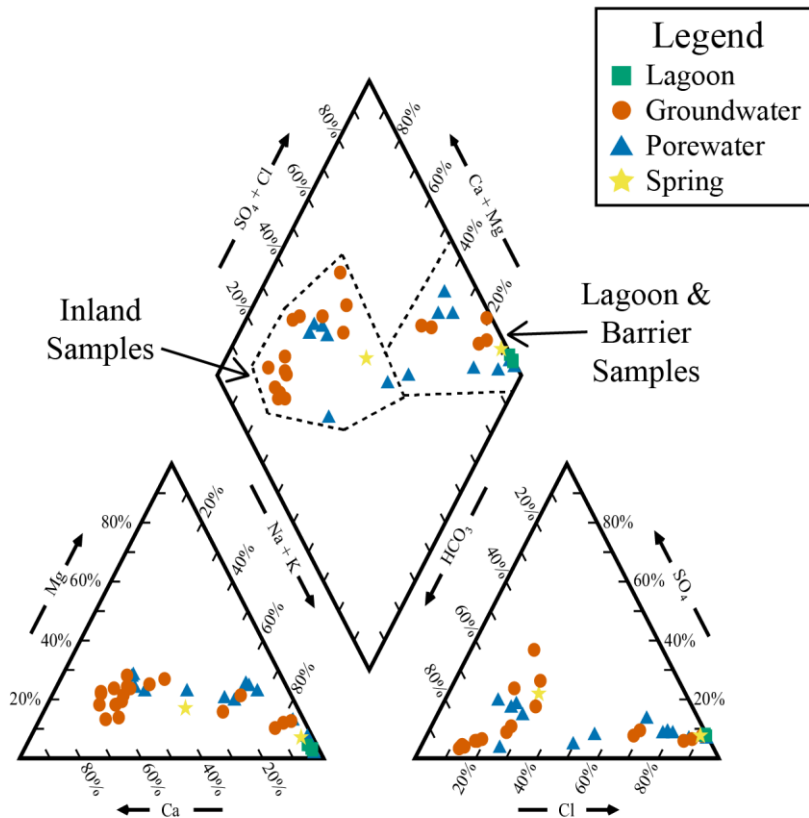


Figure 4.3. Piper diagram showing dominant cations and anions and overall major ion composition in 40 surface and groundwater samples in the study area.

#### 4.4.3 Trace metals

Trace Fe and Mn were above analytical detection limits in 20 and 29 samples, respectively (Table 4.1). Dissolved Fe concentrations ranged from <0.003-13.18 mg/L. Dissolved Mn concentrations ranged from <0.0002-2.47 mg/L. Fe and Mn were overall highest in groundwater wells on the barrier and porewater samples. Mean Fe concentrations were  $1.05 \pm 1.23$  mg/L,  $0.92 \pm 1.65$  mg/L and  $3.97 \pm 4.77$  mg/L in barrier groundwater, inland porewater and barrier porewater, respectively. Mean Mn concentrations were  $0.087 \pm 0.097$  mg/L,  $0.139 \pm 0.130$  mg/L and  $0.574 \pm 0.829$  mg/L, respectively.

#### 4.4.4 Nutrients

TN was on average highest in the inland groundwater samples ( $2.17 \pm 3.10$  mg/L), but the lagoon had the highest median at 2.3 mg/L (Table 4.1). Nitrate-N (also referred to here as nitrate) was highest in the inland groundwater wells ( $2.14 \pm 3.11$  mg/L) with the remainder of sample types on average between 0.06-0.69 mg/L and all lagoon samples below detection. Nitrite-N (also referred to here as nitrite) was below detection in inland groundwater and the lagoon and was most often measured



above detection in porewater samples. Porewater and groundwater wells on the barrier had the highest  $\text{NH}_4^+$  concentrations while the inland groundwater was the lowest. TP was highest in porewater samples on the barrier with slightly lower TP concentrations in the lagoon and in barrier groundwater, while all inland samples were much lower. Overall, inland groundwater samples had the highest median DRP concentration (0.011 mg/L), while the barrier porewater had several high readings, including one sample as high as 0.59 mg/L. All lagoon samples were below detection for DRP.

#### **4.4.5 Stable Isotopes**

$\delta^{18}\text{O}$  ranged from -9.07 to -2.10‰ (median = -8.31‰) (Table 4.1), and  $\delta^2\text{H}$  ranged from -61.9 to -17.4‰ (median = -56.5‰) (Figure 4.4). Samples from inland groundwater wells had the most negative  $\delta^{18}\text{O}$  ratios (most between -8.4 to -9.0‰). Samples from groundwater wells on the barrier had less negative  $\delta^{18}\text{O}$  ratios (~7.0‰). Inland porewater samples had  $\delta^{18}\text{O}$  values between -8.74 and -8.35‰, while barrier porewater samples were less negative (between -7.33 to -4.89‰). This compares to lagoon  $\delta^{18}\text{O}$  ratios that were significantly less negative than all other samples (-2.1 to -2.7‰).

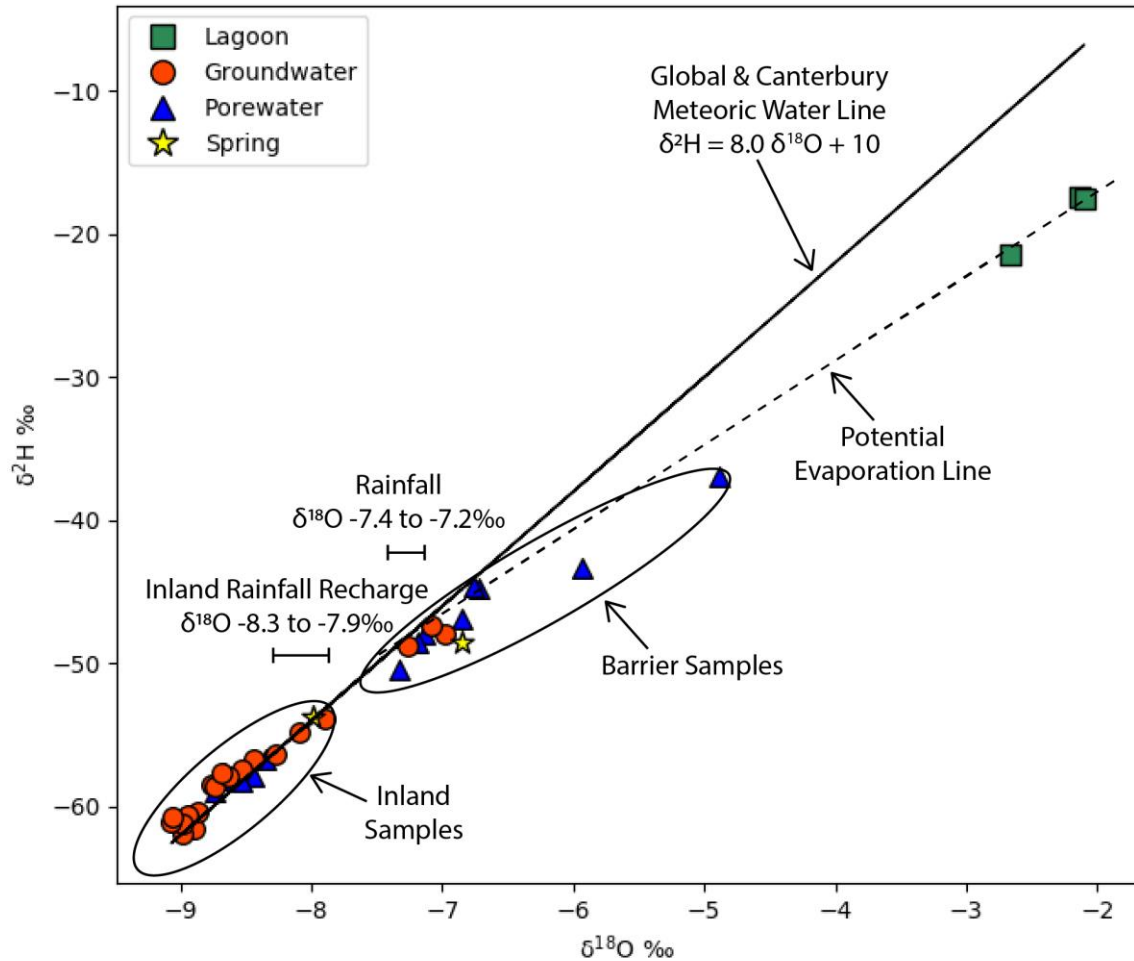


Figure 4.4.  $\delta^{18}\text{O}$  versus  $\delta^2\text{H}$  values for 38 samples in and around Te Waihora. The Global and Local meteoric water line is plotted (Stewart & Morgenstern, 2001), as well as a potential evaporation line. Inland rainfall recharge isotope ratios are from Hanson & Abraham (2009). Rainfall isotope ratios are from Stewart (2012).

## 4.5 Discussion

### 4.5.1 Groundwater sources to the lagoon

The major ion chemistry revealed relatively clear distinction of water types based on sample locations. Groundwater from both inland wells and on the barrier had more defined hydrochemical facies, while porewater samples showed more mixed signatures. The lagoon samples had a strong NaCl signature, as did all porewater and groundwater samples taken on the barrier (Figure 4.3 and Figure 4.5). This is likely due to the influence of seawater, particularly in the lagoon samples affected by mixing via the ocean outlet, wave overtopping and salt spray (Spigel, 2009). Similar  $\text{Na}^+$  and  $\text{Cl}^-$  dominance has been found in other coastal lagoons in Spain and Turkey where mixing of fresh and

sea water is a significant driver of lagoon ion chemistry (Menció, Casamitjana, Mas-Pla, Coll, Comptee, et al., 2017; Stumpp et al., 2014). The Te Waihora surface water is strongly dominated by  $\text{Na}^+$  and  $\text{Cl}^-$ , and the Na:Cl ratios of the lagoon samples plot close to the seawater dilution line with a Na:Cl ratio of 0.86 (Mæller, 1990) (Figure 4.5), indicating that the  $\text{Na}^+$  and  $\text{Cl}^-$  are sourced from seawater as opposed to weathering (Rosen, 2001). In contrast, previous investigations in Germany and Brazil have found more evidence of geological drivers influencing ion chemistry in lagoon and barrier samples, such as carbonate mineral dissolution resulting in higher  $\text{HCO}_3^-$ ,  $\text{Ca}^{2+}$  and  $\text{Mg}^{2+}$  compositions (Röper et al., 2012; Santos, Machado, et al., 2008; Seibert et al., 2018).

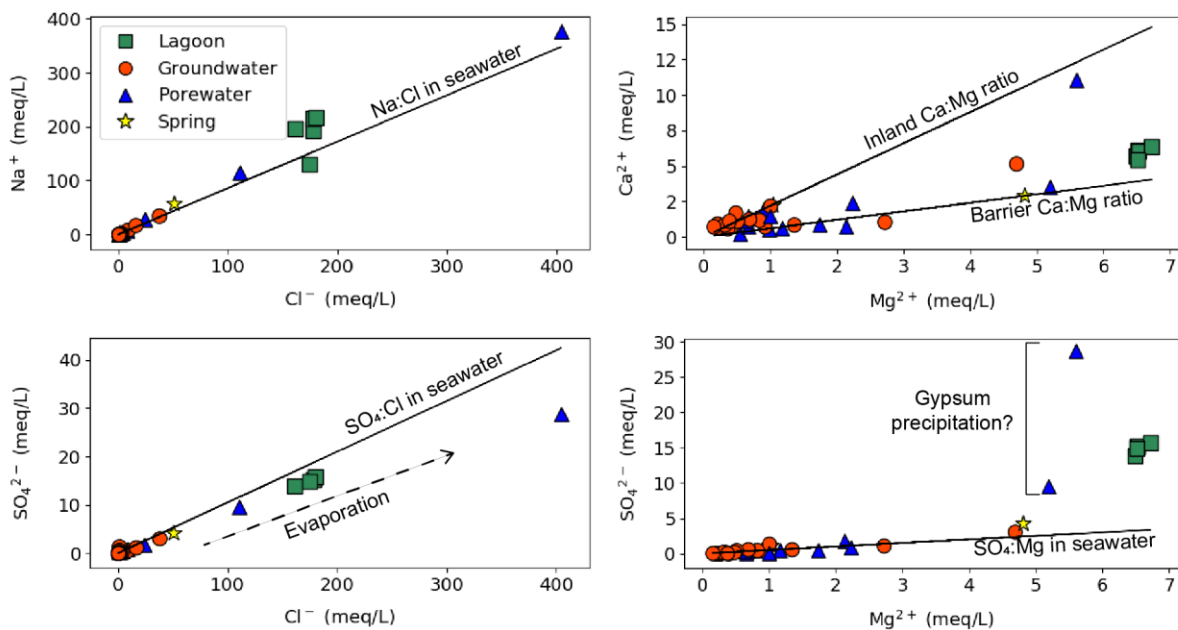


Figure 4.5. Plots of key major ion ratios sampled at Te Waihora with seawater dilution lines and slopes representing major groups of samples.

In general, groundwater wells on the barrier also had high  $\text{Cl}^-$ ,  $\text{Na}^+$  and  $\text{K}^+$ ; low  $\text{HCO}_3^-$  and  $\text{Ca}^{2+}$ ; and less negative  $\delta^{18}\text{O}$ . This reflects stronger influence from coastal rainfall with salt spray influence, representing a lens of locally recharged groundwater, as well as seepage from the lagoon (Hanson & Abraham, 2009). Both lagoon samples and groundwater from the barrier had higher  $\text{SO}_4^{2-}$  concentrations, which also correlated with higher  $\text{Cl}^-$  concentrations (Figure 4.5). The sulfate is most likely sourced from seawater given there are no significant geological sources of sulfate nearby such as pyrite, gypsum or anhydrite (Rosen, 2001). There may also be some input of  $\text{SO}_4^{2-}$  from gypsum in fertiliser applications (Hem, 1985). The lagoon samples and two porewater samples on the barrier had reduced  $\text{SO}_4^{2-}$  when compared to the  $\text{SO}_4$ :Cl seawater concentration dilution line (Figure 4.5), which may be explained by gypsum precipitation as a result of evaporation (Menció, Casamitjana, Mas-Pla,

Coll, Comptee, et al., 2017). This group of samples plots above the  $\text{SO}_4\text{:Mg}$  seawater concentration dilution line (Figure 4.5), implying gypsum precipitation (Rosen, 2001).

In contrast to the lagoon, inland samples were  $\text{MgHCO}_3$  type and largely dominated by  $\text{Ca}^{2+}$  and  $\text{HCO}_3^-$  ions (Figure 4.3). The  $\text{MgHCO}_3$  signature corresponds with data from groundwater sampled elsewhere from the greywacke-derived alluvial gravel aquifers of the Canterbury Plains, which have mostly  $\text{HCO}_3^-$  type groundwater (Hayward, 2002; Vincent, 2005). Most  $\text{HCO}_3^-$  in this location is sourced from interactions between dissolved atmospheric  $\text{CO}_2$  and organic matter in soil that results in  $\text{HCO}_3^-$  ions dissolved in groundwater (Rosen, 2001). Most groundwater in New Zealand is relatively young and rarely evolves past the  $\text{HCO}_3^-$  phase in the Cheboratev sequence (Freeze & Cherry, 1979) because of a lack of soluble minerals (Rosen, 2001). The  $\text{Ca}^{2+}$  sources in Canterbury are mainly from carbonate cement, pebbles and shells, which are common in the coastal aquifer system (Hayward, 2002; Rosen, 2001). The chemistry of the inland samples in this study suggests an inland source, in contrast to the lagoon and barrier samples, which showed evidence of seawater influence (Rosen, 2001). Hayward (2002) noted that even as groundwater approaches the coast in this area,  $\text{HCO}_3^-$  remains the dominant anion except where there is obvious saltwater influence.

In general, the inland samples had lower  $\text{Ca}^{2+}$ ,  $\text{K}^+$ ,  $\text{Mg}^{2+}$ ,  $\text{SO}_4^{2-}$  and significantly lower  $\text{Na}^+$  and  $\text{Cl}^-$  compared to the lagoon and barrier samples, aligning with results from Hanson and Abraham (2009). Most ion concentrations reduced with depth, reflecting a greater influence of low-ion alpine river recharge and more rainfall recharge at shallower depths (Hanson & Abraham, 2009; Hayward, 2002). Previous studies have shown  $\text{Ca:Mg}$  ratios to be higher in alpine river-sourced groundwater on the Canterbury Plains, whereas rainfall-recharged groundwater had lower  $\text{Ca:Mg}$  ratios (Hanson & Abraham, 2009). Local river water and rainfall have low  $\text{Mg}^{2+}$  concentrations, and  $\text{Mg}^{2+}$  has a proportionally greater increase than  $\text{Ca}^{2+}$  when groundwater reacts with soil and aquifer sediments (Hanson & Abraham, 2009). This is evident in the inland samples from the current study, which had a higher  $\text{Ca:Mg}$  ratio (median ratio = 2.2, max ratio = 4.9) than the barrier samples (median ratio = 0.6) (Figure 4.5), indicating an influence of alpine river recharge in inland groundwater. However it is worth noting that the inland  $\text{Ca:Mg}$  ratios found here are on the low end of the range compared to those in Hanson and Abraham (2009) who found that the  $\text{Ca:Mg}$  ratio was a more useful tracer closest to the recharge source and may be less helpful for groundwater near the coast.

Overall,  $\delta^{18}\text{O}$  and  $\delta^2\text{H}$  distinguished water sources as demonstrated in previous studies in China, Europe and Brazil (e.g., Luo et al., 2018; Rapaglia, Di Sipio, et al., 2010; Schmidt et al., 2011) and specifically on the Canterbury Plains (e.g., Blackstock, 2011; Dench & Morgan, 2020; Stewart, 2012; Vincent, 2005). Similar to the major ions, the  $\delta^{18}\text{O}$  versus  $\delta^2\text{H}$  ratios fit into clear groups based on sample locations and types (Figure 4.4). Samples from inland groundwater wells had the most negative  $\delta^{18}\text{O}$  ratios, reaching -9.1‰. This is in line with Blackstock (2011) and Stewart (2012) who

found alpine river recharge to have  $\delta^{18}\text{O}$  ratios below  $-8.8\text{‰}$ . Shallower inland wells had less negative  $\delta^{18}\text{O}$  ratios and may reflect a mix of alpine river recharge and rainfall recharge (Stewart, 2012). It is worth noting that there may be some potential masking of stable isotope recharge sources because alpine-sourced water is used for irrigation on the Canterbury Plains (Close et al., 1995; Dench & Morgan, 2020).

On the opposite end of the local meteoric water line (Figure 4.4) were the lagoon samples, which were significantly more positive than all other samples ( $\sim 2\text{‰}$ ). The lagoon  $\delta^{18}\text{O}$  ratios deviate strongly from the meteoric water line plotted in Figure 4.4, indicating that the heavier oxygen isotopes have been enriched due to evaporation from the large open surface of the lagoon (Schwartz & Zhang, 2003). Röper et al. (2012), Cartwright et al. (2019) and Lopez et al. (2020) also found isotope ratios strongly influenced by evaporation of surface waters in barrier islands, rivers and estuaries in Germany, Australia and the U.S., respectively. The evaporation effect in the current study may have also been enhanced due to sampling in summer (i.e., temperature effects) and because of strong winds at the site (Craig & Gordon, 1965; Stewart & Morgenstern, 2001).

Water sampled on the barrier was in between the lagoon and inland groundwater samples in terms of  $\delta^2\text{H}:\delta^{18}\text{O}$  ratios (Figure 4.4). Samples from groundwater wells in general had the most negative  $\delta^{18}\text{O}$  ratios ( $\sim 7.0\text{‰}$ ) amongst the barrier samples, while porewater samples ranged more widely from  $-7.3$  to  $-4.9\text{‰}$ . All of the barrier  $\delta^{18}\text{O}$  ratios were more positive than the range of ratios ( $\sim 8.3$  to  $7.9\text{‰}$ ) previously found in rainfall-recharged groundwater on the Canterbury Plains (Hanson & Abraham, 2009), suggesting locally specific hydrological processes on the barrier. Barrier groundwater had similar  $\delta^{18}\text{O}$  ratios to local rainfall samples reported in Stewart (2012), which were  $-7.4$  to  $-7.2\text{‰}$ . As the range of barrier samples becomes more positive in terms of  $\delta^{18}\text{O}$ , they plot increasingly below the local meteoric water line (Figure 4.4) indicating isotopic enrichment from evaporation (Mazor, 1991).

In this study, we use the porewater samples at the lagoon margins as proxies for groundwater seepage into the lagoon. The chemistry of the porewater samples separates out two groups: the samples on the north and west margins of the lagoon (referred to here as “inland porewater”) and the samples on the barrier (referred to here as “barrier porewater”). Overall, the inland porewater was more chemically similar to inland groundwater samples, and on the barrier, porewater was chemically similar to barrier groundwater. These distinct groups are visible in the Piper plot (Figure 4.3) and  $\delta^2\text{H}:\delta^{18}\text{O}$  plot (Figure 4.4). Previous studies also distinguished groups of samples in other coastal lagoons and lakes using similar hydrochemical and stable isotopic tracers (Menció, Casamitjana, Mas-Pla, Coll, Comptee, et al., 2017; Sánchez-Martos et al., 2014; Santos, Machado, et al., 2008; Young et al., 2008).

Combining  $\delta^{18}\text{O}$  and  $\text{Cl}^-$  may provide further insight into recharge sources for porewater samples (Figure 4.6) (Duque, Jessen, et al., 2019; Han et al., 2019; Luo et al., 2018). Inland  $\delta^{18}\text{O}$  ratios suggest that the deeper groundwater wells are likely sourced primarily from alpine recharge, whereas shallow

inland groundwater is likely sourced from rainfall recharge on the plains (Stewart, 2012). This is also reflected in the increased  $\text{Cl}^-$  concentrations (10-100 mg/L) in the shallower groundwater and porewater, which corresponds to typical ranges in inland rainfall-derived recharge (Hayward, 2002). In contrast, the barrier samples plotted closer to the coastal rainfall recharge  $\delta^{18}\text{O}$  signature (Figure 4.6), indicating a different water source than the inland samples. This aligns with Schmidt et al. (2011) who found groundwater on the barrier of a Brazilian lagoon to be mostly recharged from precipitation rather than lagoon infiltration.

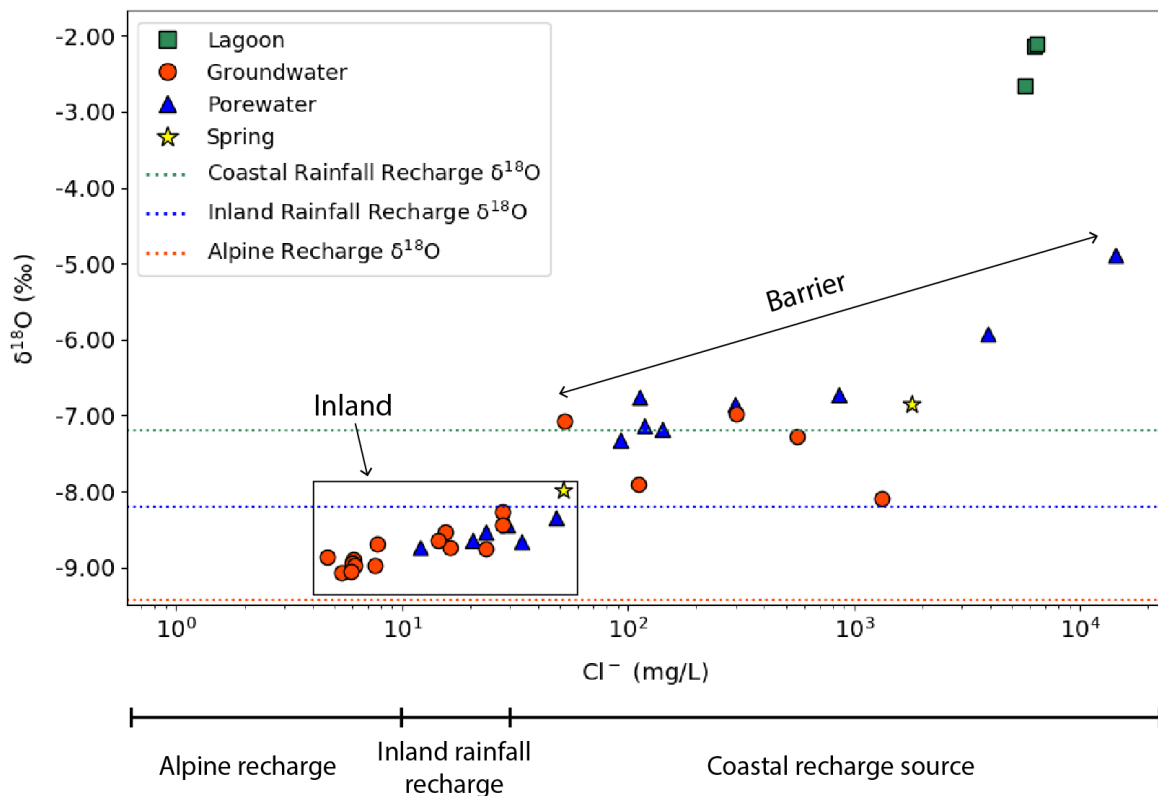


Figure 4.6. Chloride vs.  $\delta^{18}\text{O}$  for the four sample types.  $\delta^{18}\text{O}$  ratios from the literature are plotted as horizontal lines for coastal rainfall recharge (Stewart, 2012), inland rainfall recharge (Stewart, 2012) and alpine recharge (Stewart et al., 1983).

Despite a previous study showing freshwater inputs along the lagoon side of the barrier that may have been groundwater discharge (Coluccio et al., 2020), the major ion and stable isotope composition of the barrier porewater most likely reflects a combination of seepage from the lagoon and rainfall-recharged groundwater on the barrier (Hanson & Abraham, 2009). Barrier groundwater and porewater samples were chemically more similar to the lagoon than inland groundwater (Blackstock, 2011; Vincent, 2005). This provides supportive evidence that the general direction of shallow groundwater

flow underneath the barrier is from the lagoon towards the sea. During sampling in November-December 2020, the lagoon was on average 0.8 metres above mean sea level, which would have resulted in seepage through the barrier from the lagoon towards the sea (Horrell, 1992).

#### **4.5.2 Implications of groundwater sources for nutrient transport**

Te Waihora is a hypertrophic lagoon with significant water quality issues. Analysing groundwater-derived nutrient inputs is a key part of gaining a holistic understanding of drivers of water quality (Schallenberg et al., 2010). Inland groundwater wells had the highest  $\text{NO}_3^-$ -N concentrations (4.9-9.3 mg/L), similar to other sites on the Canterbury Plains (Hanson & Abraham, 2009; Hayward, 2002). In contrast, both inland and barrier porewater samples had low  $\text{NO}_3^-$ -N concentrations (mean = 0.06 mg/L), demonstrating a trend of decreasing  $\text{NO}_3^-$ -N concentrations near the lagoon (Hanson & Abraham, 2009; Rutter & Rutter, 2019). Porewater observations imply denitrifying conditions around the lagoon margins with increased Fe, Mn,  $\text{NO}_2^-$ -N and  $\text{NH}_4^+$  (Figure 4.7) (Close et al., 2001; Dahiru et al., 2020), and denitrification has been confirmed in the lagoon bed sediments (Crawshaw et al., 2019). Organic matter deposition causing anoxic conditions on the margins of lagoons and other coastal waterbodies can provide the ideal setting for denitrification (Burgin & Hamilton, 2007). Bratton et al. (2009) highlights that denitrification of groundwater in nearshore sediments before it discharges offshore is not often accounted for in models or nutrient budgets. Yet, it may serve as an important natural bioremediation pathway for nitrogen-rich SGD (Bratton et al., 2009). The results here align with a recent global review that found the main N species in SGD to be ammonium and dissolved organic nitrogen (Santos et al., 2021).

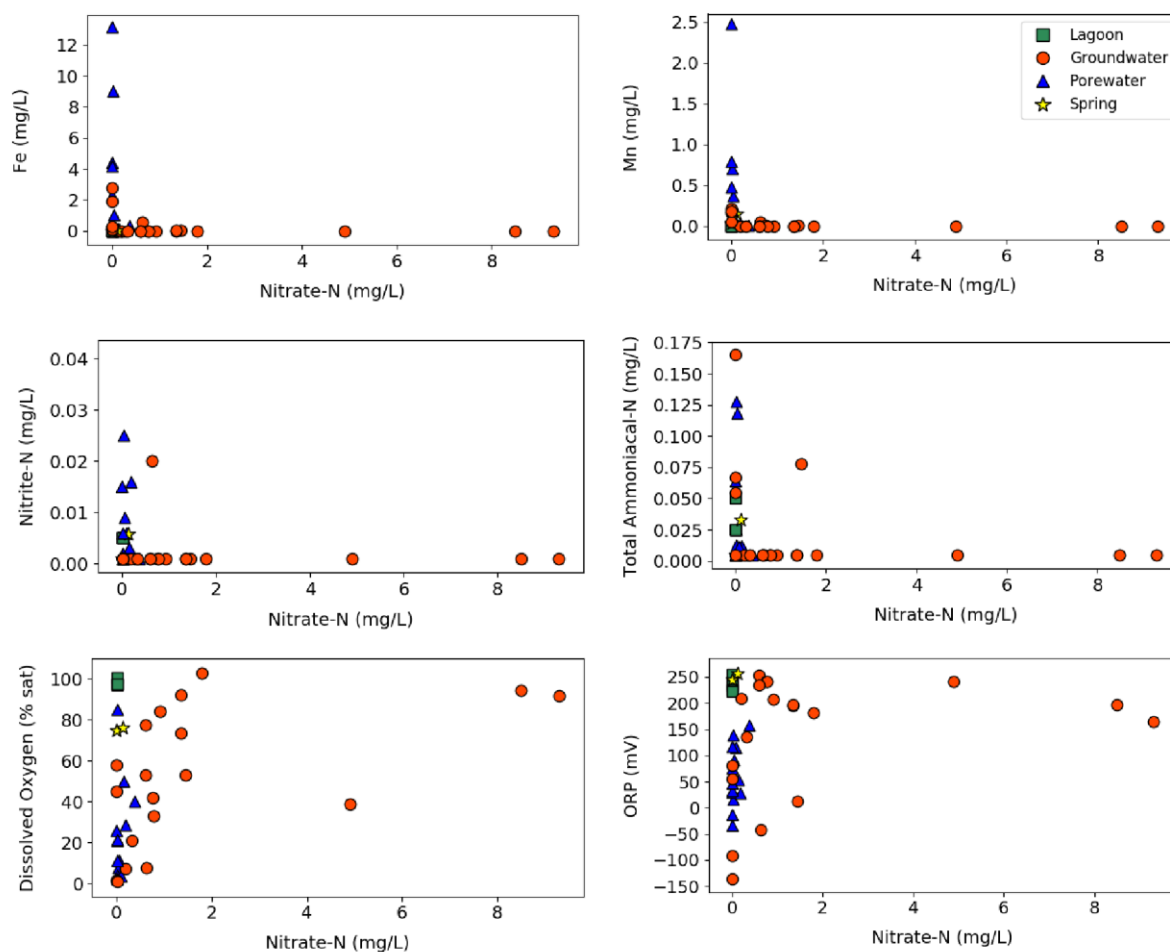


Figure 4.7. Plots of Fe, Mn, nitrite, ammonia, dissolved oxygen and oxidation reduction potential (ORP) vs. nitrate concentrations in lagoon margin porewater. Note, one (high concentration) outlier was excluded from the ammonia plot to improve plot display.

Reactive phosphorus results did not display trends as clear as the nitrogen. Overall, inland groundwater wells had the highest median DRP (0.011 mg/L). These values are similar to those in Hayward (2002), who reviewed ~15 years of groundwater monitoring data in the neighbouring Christchurch-West Melton catchment. However the DRP results from the groundwater wells in the current study are higher than the median found in Hanson and Abraham (2009) of 0.004 mg/L in the Te Waihora catchment. While inland groundwater had higher median DRP, samples from porewater and groundwater wells on the barrier in the current study had the highest maximum DRP concentrations (0.590 and 0.066 mg/L, respectively). Given anoxic conditions in nearshore sediments (i.e., low dissolved oxygen and higher dissolved Fe, Mn,  $\text{NH}_4^+$  and  $\text{NO}_2^-$ -N concentrations), it is possible that phosphorus is being released to groundwater at the lagoon margins (Kazmierczak et al., 2020). Mobilisation of phosphorus may also be enhanced in more saline anoxic barrier porewater where higher  $\text{SO}_4^{2-}$  concentrations were observed. The sulfides may combine with Fe in the



sediments, making Fe less able to bind to phosphate ( $\text{PO}_4^{3-}$ ), and thereby making phosphorus more bioavailable (Hartzell & Jordan, 2012).

Examining the ratios of nitrogen to phosphorus can be useful for shedding light on nutrient limitations for phytoplankton production in receiving water bodies (Ptacnik et al., 2010). When TN:TP ratios from samples in this study are plotted against the 16:1 Redfield N:P ratio (Redfield, 1934, 1958), it appears that most samples are phosphorus limited (Figure 4.8). This corresponds to analysis of long-term regional groundwater monitoring data that also found most groundwater to be phosphorus limited (Hayward, 2002). The main exception in the current study was four porewater samples, three of which were from the barrier. Santos et al. (2021) found that most groundwater discharging on the coast has higher concentrations of nitrogen relative to phosphorus. In Te Waihora, both TN and TP concentrations are relatively high compared to other coastal lakes in Canterbury and put the lagoon into the hypertrophic Trophic Lake Index category (Hayward & Ward, 2009).

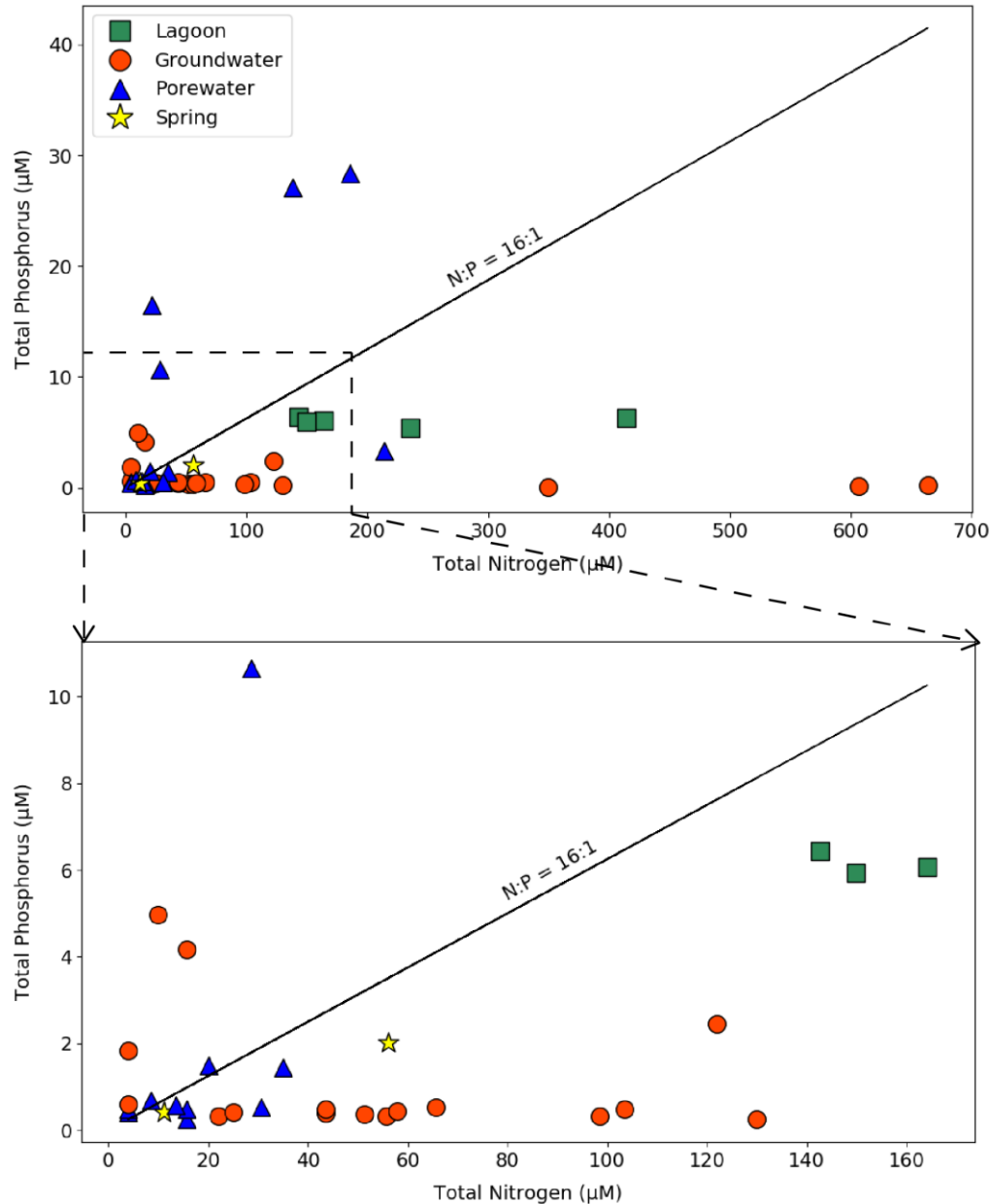


Figure 4.8. Total nitrogen vs. total phosphorus ratios in porewater, groundwater well, lagoon and spring samples at Te Waihora. The plots include the 16:1 N:P Redfield ratio. Top panel: Full dataset. Bottom panel: Zoomed inset.

High nitrogen concentrations appear to drive algal growth in Te Waihora, as algal blooms have been linked to sudden increased N fluxes from rivers (Schallenberg & Crawshaw, 2017). However, previous work has shown that phytoplankton in Te Waihora are predominantly limited by nitrogen (MacKenzie, 2016). Measurement of denitrification rates in the lagoon have shown that nitrate is quickly processed by phytoplankton (Crawshaw et al., 2019). There is also evidence of phosphorus production in the lagoon via the release of phosphorus bound to sediments under anoxic conditions (Schallenberg & Crawshaw, 2017). As a result, the measured N:P ratios in the lagoon (between 22-

65) (Figure 4.8) were relatively low compared to N:P ratios in SGD across 169 studies (mean = 259, range 1-12,100) (Santos et al., 2021). However, Te Waihora being nitrogen limited fits in the context of most coastal waterbodies being nitrogen limited (Burnett et al., 2007). Light availability, which is a function of sediment suspension, also plays an important role in controlling phytoplankton and biomass growth (Larned & Schallenberg, 2006). Visual clarity in the shallow, wind-affected lagoon has decreased in recent decades largely due to the removal of macrophytes in a large storm in the late 1960s (Hayward & Ward, 2009).

The nutrient observations shed light on nitrogen and phosphorus loads to the lagoon (Figure 4.9). In some cases where groundwater inflow was a small proportion of water budgets, the nutrient and ion load contribution from groundwater has been significant due to the lack of other sources and high concentrations in groundwater (Luo et al., 2018; Santos, Machado, et al., 2008). In some cases, nutrient inputs to coastal lagoons have been underestimated because groundwater was not considered (Schallenberg et al., 2010). Here, we use the mean DIN (dissolved inorganic nitrogen, i.e.,  $\text{NO}_3^-$ -N +  $\text{NO}_2^-$ -N +  $\text{NH}_4^+$ ) and DRP concentrations in the inland porewater samples (0.121 mg/L and 0.012 mg/L, respectively) to represent nutrient concentrations in groundwater seepage to the lagoon. For DIN in particular, using this value (as opposed to the higher average DIN in inland groundwater wells) takes into account possible nutrient processing on the margins before groundwater enters the lagoon. This approach prevents an over-estimation of nitrogen loads (Robinson et al., 2018; Rocha et al., 2016). Using groundwater discharge estimates from the radon mass balances in Coluccio et al. (2021), this results in an average annual DIN load of 28.6 T (tonnes) and DRP load of 2.8 T.

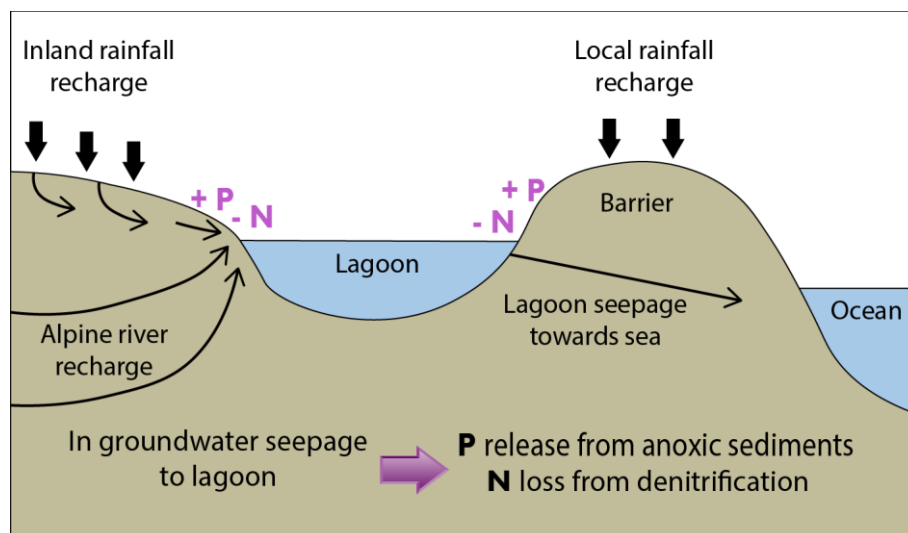


Figure 4.9. Conceptual diagram illustrating groundwater sources and nutrient processes in seepage to Te Waihora. Results of this study indicate inland porewater is sourced from alpine river recharge and inland rainfall recharge. Porewater on the barrier appears to be sourced from local rainfall recharge on the barrier and mixing from lagoon surface water. Porewater on the lagoon margins had low nitrate

concentrations and showed evidence of potential denitrifying conditions, while porewater had elevated levels of phosphorus possibly due to release from anoxic nearshore sediments.

When compared to estimated nutrient loads from tributaries (Larned & Schallenberg, 2006), groundwater inputs comprise approximately 3% of DIN and 30% of DRP. This highlights that groundwater seepage may be an important contributor of phosphorus to Te Waihora, while the nitrogen contribution may be relatively small. A ~30% phosphorus contribution from groundwater discharge (as a proportion of river DRP load) is much higher than estimates in previous studies (Hayward & Ward, 2009; Larned & Schallenberg, 2006). Notably, previous studies relied on a limited number of groundwater samples, which did not target shallow groundwater on the lagoon margins, as well as earlier seepage estimates that were lower than those in Coluccio et al. (2021). Given the affinity of phosphorus to bind with sediment, it is possible that this phosphorus load is an over-estimate. Also, while the groundwater discharge rate in Coluccio et al. (2021) used to calculate the nutrient loads includes both winter and summer estimates, we have only used nutrient concentrations from one sampling campaign (late spring), so it is possible that our flux estimates vary as a result of seasonal changes in concentrations in the groundwater endmember. It is also likely that groundwater discharge rates to the lagoon would fluctuate over time due to short-term seasonal effects and long-term impacts such as climate change, which would impact nutrient load estimations. Assuming the low DIN concentrations in porewater are representative of direct groundwater seepage into the lagoon, this highlights the importance of managing surface water inputs of nutrients to Te Waihora. Also, the potential denitrifying capacity of wetlands around the lagoon margins provides support for current efforts to restore and construct wetlands around the lagoon. Wetland restoration will need to be carried out by maintaining a balance between enhancing denitrifying conditions while preventing phosphorus release from sediments.

## 4.6 Conclusion

There has been increasing interest in recent years in delineating the source waters of groundwater seepage to coastal lagoons. Hydrochemistry and stable isotope analysis revealed two distinct water types in groundwater around the lagoon. Inland groundwater was dominated by  $\text{Ca}^{2+}$  and  $\text{HCO}_3^-$ , and had lower ion concentrations and more negative  $\delta^2\text{H}:\delta^{18}\text{O}$  ratios, reflecting a combination of alpine-river recharge and rainfall recharge from the plains. Groundwater on the barrier, which was NaCl type and had high ion concentrations and more positive  $\delta^2\text{H}:\delta^{18}\text{O}$  ratios, is a mix of seepage from lagoon surface water and locally recharged rainfall. The general flow direction of shallow groundwater underlying the barrier is towards the sea. Nutrient analysis implied potential denitrification occurring

in the nearshore sediments around the lagoon due to low  $\text{NO}_3^-$ -N concentrations and the presence of dissolved Fe, Mn,  $\text{NO}_2^-$ -N and  $\text{NH}_4^+$  associated with P release in anoxic sediments. Groundwater seepage to the lagoon seems to be a minor contributor of inorganic nitrogen compared to rivers, but groundwater may play an important role in phosphorus transport.

**Data availability:** The data set for this paper is available in an online Figshare repository:

DOI: 10.6084/m9.figshare.14411975.v1

## **5. Synthesis and Conclusions**

### **5.1 Study motivation and objectives**

This thesis set out to deepen the understanding of groundwater processes in a coastal lagoon. The main motivation was that groundwater input to coastal water bodies has frequently been discounted as an important component of water and nutrient budgets. Its contribution to water balances has often been assumed to be negligible, largely because groundwater seepage is difficult to measure. Further, coastal wetlands, lagoons and estuaries are significant natural features that provide vital habitat and food resources, have considerable cultural value, are important recreational sites, and are home to some of the world's most developed coastal communities. Ongoing research has shown that groundwater discharge plays important roles in coastal biogeochemical processes.

This thesis involved an in-depth study of groundwater processes in a large, nutrient-rich coastal lagoon in New Zealand: Te Waihora (Lake Ellesmere). This chapter synthesises the findings of this study, highlights implications for management and outlines future research directions.

### **5.2 Key study findings and contributions**

#### **5.2.1 Mapping the spatial distribution of groundwater seepage in a lagoon**

In Chapter 2, I explored how groundwater seepage to a coastal lagoon is distributed across the lagoon bed. I tested whether the traditional conceptual models of seepage distribution—placing most seepage near the margins—held true for a geologically heterogeneous lagoon underlain by a confined aquifer system. To investigate this question, I carried out an airborne thermal infrared imaging survey and physicochemical spatial surveys by boat in two seasons.

The main groundwater discharge locations were near the margins of the lagoon. I found evidence of diffuse seepage, as well as point-source seepage (i.e., springs) on mudflats and on the lagoon shore. Signs of groundwater seepage were concentrated on the northern and western sides of the lagoon. Given the artesian aquifers under the lagoon, I conducted a second, more comprehensive spatial survey with a high-density sampling grid. However, I found no significant signs of freshwater inputs away from the lagoon shore. Interestingly, I did find new evidence of freshwater along the lagoon-barrier interface, which I hypothesised is either sourced from upwelling inland-sourced groundwater from underneath the lagoon or seepage from the surface aquifer on the mixed sand and gravel barrier. Overall, the main controls on groundwater discharge patterns appear to be the regional groundwater

flow direction, and the hydraulic gradient between adjacent and underlying groundwater and the lagoon.

This study demonstrates a unique combination of remote sensing and in-situ techniques for investigating groundwater discharge to coastal areas. Thermal infrared imaging in particular has only recently had an increase in use in hydrological studies due to the availability of less expensive cameras. While there is still room for further work on the methodology, in Chapter 2, I attempted to address a gap in the literature by detailing the procedures used to process and analyse this type of large dataset.

### **5.2.2 Quantifying groundwater seepage to a lagoon**

In Chapter 3, I set out to test the hypothesis that groundwater seepage is only a minor component of Te Waihora's water budget, as estimated in an earlier study. The prior estimates were based on point-source seepage meter measurements in limited areas of the lagoon. In contrast, I used a broad-scale method—a radon ( $^{222}\text{Rn}$ ) mass balance—to estimate total groundwater inputs through the lagoon bed. I calculated radon mass balances in two seasons and carried out detailed uncertainty analysis.

The mass balance results showed that groundwater seepage to the lagoon was 1-2 orders of magnitude greater than previous estimates. Discharge estimates ranged from  $5.2 \pm 5.8 \text{ m}^3/\text{s}$  to  $18.7 \pm 19.6 \text{ m}^3/\text{s}$  during summer and  $0.9 \pm 2.2 \text{ m}^3/\text{s}$  to  $8.1 \pm 10.5 \text{ m}^3/\text{s}$  during winter. Wind-driven radon evasion to the atmosphere was the most influential variable in the model. Higher wind speeds during the summer survey resulted in seepage estimates 3.5 times greater than in winter. The in-depth uncertainty analysis of each variable helped in understanding how the radon mass balance model operated for the case study site from a conceptual perspective. It is also important to recognise that errors in system conceptualisation will affect estimates produced in models, such as mass balances. It is key to establish a well-reasoned conceptual model prior to building an analytical or numeric model and iteratively improve the conceptual model in parallel to refining the analytical or numeric one. Incorrect conceptualisation may lead to misrepresentations of fundamental underpinnings of models such as the geology or groundwater flow paths.

The radon mass balance uncertainty analysis also revealed which parameters were the most sensitive: namely atmospheric evasion, as well as lagoon surface area and volume; the radon in groundwater endmember; and the average radon concentration in the lagoon surface water. After reviewing published radon mass balance papers, it became clear that detailed uncertainty analyses on these models were rarely done, or at least rarely reported. Chapter 3 provides an example of carrying out in-depth uncertainty analyses on radon mass balance seepage estimates.

### 5.2.3 Identifying groundwater seepage sources and their nutrient transport implications in a lagoon

Chapter 4 detailed a geochemical investigation into sources of groundwater seepage to a lagoon and their role in transporting nutrients. Here, I tested the hypothesis that deep groundwater upwelling contributes to seepage on the northern and western margins of the lagoon, as well as along the lagoon-barrier interface. In terms of nutrients, I expected groundwater to be a more significant vector of nitrogen and phosphorus than the small proportions previous studies had estimated. I carried out a sampling campaign around Te Waihora, analysing water from the lagoon surface water, porewater (shallow nearshore groundwater), existing groundwater wells and springs.

Groundwater seepage largely split into two groups: inland samples with low ion concentrations and more negative  $\delta^{18}\text{O}$  and  $\delta^2\text{H}$  ratios, and samples from the permeable barrier with higher ion concentrations and more positive  $\delta^{18}\text{O}$  and  $\delta^2\text{H}$  ratios. Inland samples were dominated by  $\text{Ca}^{2+}$  and  $\text{HCO}_3^-$  ions and had mean  $\delta^{18}\text{O}$  ratios less than  $-8.5\text{‰}$ . Barrier samples were comprised mainly of  $\text{Na}^+$  and  $\text{Cl}^-$  ions and had mean  $\delta^{18}\text{O}$  ratios of  $-7.5\text{‰}$  for groundwater wells and  $-6.6\text{‰}$  for porewater. The ion and stable isotope chemistry imply that inland seepage is sourced primarily from alpine river recharge and inland rainfall recharge, while barrier porewater is comprised of mainly mixing with lagoon surface water and localised rainfall recharge on the barrier. The study did not find evidence in the barrier porewater of freshwater inputs from upwelling artesian groundwater from under the lagoon.

In regard to groundwater seepage as a source of nutrients to the lagoon, analysis of porewater samples showed evidence of potential denitrification on the lagoon margins attenuating nitrogen inputs. In contrast, dissolved reactive phosphorus was elevated in porewater, suggesting phosphorus mobilisation may be occurring in nearshore anoxic groundwater. Previous work estimated surface tributaries to be the largest sources of new nitrogen and phosphorus to the lagoon. I estimated 28.6 tonnes of dissolved inorganic nitrogen (DIN) and 2.8 tonnes of dissolved reactive phosphorus (DRP) are delivered to the lagoon annually via groundwater seepage. When this is put into the context of river inputs, seepage-derived nitrogen inputs are small—at 3% of river DIN inputs, but the phosphorus load is significant—at 30% of river DRP inputs.

Chapter 4 demonstrated a successful case study examining groundwater sources to a large, nutrient-rich coastal water body. These types of studies have increased in recent years as interest in resolving groundwater flow paths, transport times, source areas and solute loads has increased. While techniques for answering these questions have improved, these remain difficult questions to resolve, and demonstrating successful use of tools, such as the tracers used here, is valuable for the research community and practitioners.



### 5.3 Local insights and management implications

This thesis provides valuable contributions to the body of work in New Zealand. Research on groundwater discharge to coastal areas in New Zealand has been considerably underexplored compared to other areas globally. This is important in New Zealand for a variety of reasons, including the often short transport times of groundwater to the coast, the significant proportion of coastline relative to the country's land mass, and not least, the significant and complex water resource issues facing the country. From a coastal hydrology and geomorphology perspective, this thesis serves as an in-depth study of groundwater processes in a Waituna-type coastal lagoon. This sub-classification of lagoon is common in New Zealand, but some of their features are rare worldwide, such as their mixed sand and gravel barriers. Understanding how they operate from a hydrological perspective is crucial to restoration and improving management of these lagoons, many of which hold significant cultural and ecological value yet have suffered from serious water quality degradation.

Globally, coastal lagoon management is complex because these sites are at the nexus of many ecological values and services, as well as human interests. Given the increasingly recognised role that groundwater discharge plays in biogeochemical processes on the coast, improving our hydrological understanding of coastal lagoons is key to their effective management. The findings from this thesis highlight some important implications for coastal lagoon management. Data collected across the three studies presented here consistently highlighted temporal and spatial heterogeneity in lagoon characteristics, such as small-scale variability in nearshore geology; dynamic interactions of fluctuating shallow groundwater and lagoon levels on the lagoon margins; and variations in salinity seasonally and spatially within the lagoon. While individual lagoon characteristics will vary, the findings of heterogeneity in lagoon conditions are supported in the literature (e.g., Duque et al., 2018; Liefer et al., 2014; Rodellas et al., 2020). This highlights that adequate lagoon management may need to account for spatial and temporal variability rather than treating these systems as homogeneous or static (Benedetti-Cecchi et al., 2001). In the case of Te Waihora, much of the previous data collection had been at the point scale, so the results of this thesis such as the heterogeneous conditions described above; groundwater discharge in previously unidentified areas of the lagoon; and significantly greater seepage estimates than previous studies, show that broad-scale techniques are valuable for providing rich information about large, complex lagoons.

In terms of managing nutrient inputs to lagoons, Chapter 4 highlighted the role that nearshore sediments can play in transporting and processing nutrients. Coastal sediments high in organic matter are well-known potential sites for denitrification (Burgin & Hamilton, 2007), and to reduce nitrogen inputs to coastal waters, wetland restoration and construction is being pursued worldwide. However, given at least an estimated 33% of global wetlands had disappeared by 2009 (Hu et al., 2107), there is still much progress to be made to repair past damage. The potential denitrifying capacity of nearshore

lagoon sediments observed in this study supports the use of wetlands to reduce nitrogen inputs to coastal waters. However, these findings complicate the picture, as the same sediments were observed to be potentially releasing soil-bound phosphorus to groundwater. This is a relatively well-recognised complexity of wetland restoration where conditions such as pH must be carefully managed to balance nitrogen removal with phosphorus release (Duff et al., 2009). In many cases, addressing legacy phosphorus (i.e., phosphorus bound to soils) at the shores or in the beds of lagoons, is an important component of management.

## **5.4 Directions for future research**

The studies in this thesis have highlighted several potential avenues for future research. In terms of method development, Chapter 2 signalled the need for clearer and more practical guidance on processing thermal infrared imaging datasets, particularly datasets that are large (e.g., 1000s of images); are over open water or on shorelines with indistinct features; and contain imagery of diffuse (as opposed to point-source) groundwater seepage. Chapter 3 highlighted some of the shortcomings of using Gaussian error propagation to calculate uncertainties for radon mass balances. Researchers and practitioners would benefit from clearer examples of different uncertainty calculation approaches being used for radon mass balances, while appreciating that in-depth uncertainty analysis can be complex and site specific. Approaches such as Monte Carlo analysis, which has been applied extensively in other types of hydrological models for uncertainty analysis (e.g., Fu & Gómez-Hernández, 2009; Shi et al., 2014), may be worthwhile to apply in a radon mass balance context.

Gaps remain in our understanding of groundwater processes in coastal lagoons. There is still limited knowledge of the temporal fluctuations in groundwater-lagoon interactions and their drivers. The influence of factors such as fluctuating adjacent groundwater levels, sea level rise and tides has been minimally explored, so there are opportunities for additional studies examining the impacts of these temporal drivers. While numerical modelling approaches have been widely used in other hydrogeological contexts, there appears to have been limited use of them for studying groundwater processes in coastal lagoons. Given the complexity, dynamic nature and large size of many coastal lagoons, testing the impacts of factors such as openings to the sea, sea level rise, tides and barrier seepage may be more feasible by way of modelling than direct observations. The collective understanding of the drivers and significance of porewater exchange (i.e., hyporheic exchange) in lagoon beds remains limited (Rodellas et al., 2020). There is scope for further studies that can successfully demonstrate quantifying porewater exchange versus net groundwater input to lagoons. In particular, there would be great benefit in developing streamlined approaches for doing so. Further, there is a real need for evolving techniques used in research into practical tools for hydrology and hydrogeology practitioners. Groundwater contributions to water and nutrient budgets will continue to

be poorly understood and discounted at local and regional levels if characterising and quantifying them remains in the “too difficult” category for practicing scientists and water managers.

There are also still questions regarding the local hydrology of Te Waihora. Further investigation would be worthwhile into the contribution of groundwater inputs from Banks Peninsula (to the east of the lagoon) in terms of quantity and solute load. There is also scope to further investigate the freshwater signal along the barrier to determine the source and quantity of this seepage. Direct sampling of porewater in the bed of the lagoon could also shed light on a number of questions including porewater exchange fluxes and the chemistry of groundwater seepage. There is also room to further explore the hydrogeology of the barrier, examining questions such as the extent of the freshwater lens underneath the barrier, and the hydrological connections between the barrier, lagoon and sea.

This thesis contributes to the body of literature in several ways. The case study site is relatively unique compared to features of the majority of coastal lagoons where groundwater discharge has been studied: Mediterranean and tropical climates; smaller surface areas; and few surface tributaries. In contrast, Te Waihora is a large lagoon (~150 km<sup>2</sup>) on a gravel coastline situated in a temperate climate with many (>40) surface inflows and a managed outlet to the sea. Further, while radon mass balances have become more common in the past 10-15 years to estimate groundwater discharge to surface water, the study presented here incorporates features of a dynamic and complex site in terms of its hydrological and geomorphic characteristics, including openings to the ocean, seepage through the permeable barrier and variable wind speeds. In many other studies where radon mass balances were applied, either the sites were less complex or they were simplified in the models. This thesis demonstrates how these complexities can be explored in relation to groundwater discharging to coastal lagoons, a key component in their management and restoration.

## References

- Ahmed, M. H., El Leithy, B. M., Thompson, J. R., Flower, R. J., Ramdani, M., Ayache, F., & Hassan, S. M. (2009). Application of remote sensing to site characterisation and environmental change analysis of North African coastal lagoons. *Hydrobiologia*, 622, 147–171.  
<https://doi.org/10.1007/s10750-008-9682-8>
- Alcolea, A., Contreras, S., Hunink, J. E., García-Aróstegui, J. L., & Jiménez-Martínez, J. (2019). Hydrogeological modelling for the watershed management of the Mar Menor coastal lagoon (Spain). *Science of the Total Environment*, 663, 901–914.  
<https://doi.org/10.1016/j.scitotenv.2019.01.375>
- Allan, M., Hamilton, D. P., & Muraoka, K. (2018). *A coupled hydrodynamic-ecological model to test management options for restoration of lakes Onoke and Wairarapa* (ERI Report No. 111).  
[https://www.waikato.ac.nz/\\_\\_data/assets/pdf\\_file/0005/411944/Wairarapa\\_Allan\\_et\\_al\\_release\\_Report\\_No\\_111.pdf](https://www.waikato.ac.nz/__data/assets/pdf_file/0005/411944/Wairarapa_Allan_et_al_release_Report_No_111.pdf)
- Alongi, D. M. (1998). *Coastal Ecosystem Processes*. CRC Press.
- Andrisoa, A., Stieglitz, T. C., Rodellas, V., & Raimbault, P. (2019). Primary production in coastal lagoons supported by groundwater discharge and porewater fluxes inferred from nitrogen and carbon isotope signatures. *Marine Chemistry*, 210, 48–60.  
<https://doi.org/10.1016/j.marchem.2019.03.003>
- Armon, J. W. (1970). *Recent shorelines between Banks Peninsula and Coopers Lagoon*. University of Canterbury. <https://ir.canterbury.ac.nz/handle/10092/4306>
- Atkins, M. L., Santos, I. R., Ruiz-Halpern, S., & Maher, D. T. (2013). Carbon dioxide dynamics driven by groundwater discharge in a coastal floodplain creek. *Journal of Hydrology*, 493, 30–42. <https://doi.org/10.1016/j.jhydrol.2013.04.008>
- Austin, M. J., Masselink, G., McCall, R. T., & Poate, T. G. (2013). Groundwater dynamics in coastal gravel barriers backed by freshwater lagoons and the potential for saline intrusion: Two cases from the UK. *Journal of Marine Systems*, 123–124, 19–32.  
<https://doi.org/10.1016/j.jmarsys.2013.04.004>
- Barnes, R. S. K. (1980). *Coastal Lagoons*. Cambridge University Press.
- Barwell, V. K., & Lee, D. R. (1981). Determination of horizontal-to-vertical hydraulic conductivity ratios from seepage measurements on lake beds. *Water Resources Research*, 17(3), 565–570.
- Bateman, H. (1910). The solution of a system of differential equations occurring in the theory of radioactive transformations. *Proceedings of the Cambridge Philosophical Society, Mathematical and Physical Sciences*, 15, 423–427.
- Baudron, P., Cockenpot, S., Lopez-Castejon, F., Radakovitch, O., Gilabert, J., Mayer, A., Garcia-Arostegui, J. L., Martinez-Vicente, D., Leduc, C., & Claude, C. (2015). Combining radon, short-lived radium isotopes and hydrodynamic modeling to assess submarine groundwater discharge from an anthropized semiarid watershed to a Mediterranean lagoon (Mar Menor, SE Spain). *Journal of Hydrology*, 525, 55–71. <https://doi.org/10.1016/j.jhydrol.2015.03.015>
- Beer, N. A., & Joyce, C. B. (2013). North Atlantic coastal lagoons: Conservation, management and research challenges in the twenty-first century. *Hydrobiologia*, 701, 1–11.  
<https://doi.org/10.1007/s10750-012-1325-4>
- Bejannin, S., van Beek, P., Stieglitz, T., Souhaut, M., & Tamborski, J. (2017). Combining airborne thermal infrared images and radium isotopes to study submarine groundwater discharge along the French Mediterranean coastline. *Journal of Hydrology: Regional Studies*, 13, 72–90.  
<https://doi.org/10.1016/j.ejrh.2017.08.001>
- Benedetti-Cecchi, L., Rindi, F., Bertocci, I., Bulleri, F., & Cinelli, F. (2001). Spatial variation in development of epibenthic assemblages in a coastal lagoon. *Estuarine, Coastal and Shelf Science*, 52, 659–668. <https://doi.org/10.1006/ecss.2001.0775>
- Bernard, R. J., Mortazavi, B., Wang, L., Ortmann, A. C., MacIntyre, H., & Burnett, W. C. (2014). Benthic nutrient fluxes and limited denitrification in a sub-tropical groundwater-influenced coastal lagoon. *Marine Ecology Progress Series*, 504, 13–26.  
<https://doi.org/10.3354/meps10783>
- Berry, N., & Webster-Brown, J. (2012). *A summer hydrological budget for Lake Forsyth/Wairewa: Preliminary findings* (WCFM Report 2012-004).

- <http://www.waterways.ac.nz/documents/Technical%20reports/WCFM%20TR%202012-004%20Lake%20Forsyth%20Hydrologic%20Budget.pdf>
- Bird, E. C. F. (1982). Changes on barriers and spits enclosing coastal lagoons. *Oceanologica Acta*, 45-53.
- Bird, E. C. F. (1994). Physical Setting and Geomorphology of Coastal Lagoons. In B. Kjerfve (Ed.), *Coastal Lagoon Processes*. Elsevier.
- Blackstock, J. (2011). *Isotope study of moisture sources, recharge areas, and groundwater flow paths within the Christchurch Groundwater System*. University of Canterbury. <https://ir.canterbury.ac.nz/handle/10092/7042>
- Blume, T., Krause, S., Meinikmann, K., & Lewandowski, J. (2013). Upscaling lacustrine groundwater discharge rates by fiber-optic distributed temperature sensing. *Water Resources Research*, 49, 7929–7944. <https://doi.org/10.1002/2012WR013215>
- Bokuniewicz, H., & Pavlik, B. (1990). Groundwater seepage along a barrier island. *Biogeochemistry*, 10(3), 257-276. <https://doi.org/10.1007/BF00003147>
- Borges, A. V., Delille, B., Schiettecatte, L.-S., Gazeau, F., Abril, G., & Frankignoulle, M. (2004). Gas transfer velocities of CO<sub>2</sub> in three European estuaries (Randers Fjord, Scheldt, and Thames). *Limnology and Oceanography*, 49(5), 1630-1641. <https://doi.org/10.4319/lo.2004.49.5.1630>
- Bradski, G. (2000). The OpenCV Library. *Dr. Dobbs's Journal of Software Tools*.
- Bratton, J. F., Böhlke, J. K., Krantz, D. E., & Tobias, C. R. (2009). Flow and geochemistry of groundwater beneath a back-barrier lagoon: The subterranean estuary at Chincoteague Bay, Maryland, USA. *Marine Chemistry*, 113, 78–92. <https://doi.org/10.1016/j.marchem.2009.01.004>
- Brown, L. J. (2001). Canterbury. In M. R. Rosen & P. A. White (Eds.), *Groundwaters of New Zealand* (pp. 441-459). New Zealand Hydrological Society Inc.
- Brown, L. J., & Weeber, J. H. (1992). *Geology of the Christchurch urban area*. Institute of Geological & Nuclear Sciences.
- Burgin, A. J., & Hamilton, S. K. (2007). Have we overemphasized the role of denitrification in aquatic ecosystems? A review of nitrate removal pathways. *Frontiers in Ecology and the Environment*, 5(2), 89-96. [https://doi.org/10.1890/1540-9295\(2007\)5\[89:HWOTRO\]2.0.CO;2](https://doi.org/10.1890/1540-9295(2007)5[89:HWOTRO]2.0.CO;2)
- Burnett, W. C., Aggarwal, P. K., Aureli, A., Bokuniewicz, H., Cable, J. E., Charette, M. A., Kontar, E., Krupa, S., Kulkarni, K. M., Loveless, A., Moore, W. S., Oberdorfer, J. A., Oliveira, J., Ozyurt, N., Povinec, P., Privitera, A. M. G., Rajar, R., Ramessur, R. T., Scholten, J., Stieglitz, T., Taniguchi, M., & Turner, J. V. (2006). Quantifying submarine groundwater discharge in the coastal zone via multiple methods. *Science of the Total Environment*, 367, 498-543. <https://doi.org/10.1016/j.scitotenv.2006.05.009>
- Burnett, W. C., Bokuniewicz, H., Huettel, M., Moore, W. S., & Taniguchi, M. (2003). Groundwater and pore water inputs to the coastal zone. *Biogeochemistry*, 66(1/2), 3-33. <https://doi.org/10.1023/B:BI0G.0000006066.21240.53>
- Burnett, W. C., & Dulaiova, H. (2003). Estimating the dynamics of groundwater input into the coastal zone via continuous radon-222 measurements. *Journal of Environmental Radioactivity*, 69, 21–35. [https://doi.org/10.1016/S0265-931X\(03\)00084-5](https://doi.org/10.1016/S0265-931X(03)00084-5)
- Burnett, W. C., Kim, G., & Lane-Smith, D. (2001). A continuous monitor for assessment of <sup>222</sup>Rn in the coastal ocean. *Journal of Radioanalytical and Nuclear Chemistry*, 249(1), 167–172. <https://doi.org/10.1023/A:1013217821419>
- Burnett, W. C., Wattayakorn, G., Taniguchi, M., Dulaiova, H., Sojisuporn, P., Rungsupa, S., & Ishitobi, T. (2007). Groundwater-derived nutrient inputs to the Upper Gulf of Thailand. *Continental Shelf Research*, 27, 176–190. <https://doi.org/10.1016/j.csr.2006.09.006>
- Cable, J. E., Martin, J. B., Swarzenski, P. W., Lindenberg, M. K., & Steward, J. (2004). Advection within shallow pore waters of a coastal lagoon, Florida. *Ground Water*, 42(7), 1011–1020.
- Cartwright, I., Morgenstern, U., & Hofmann, H. (2019). Concentration versus streamflow trends of major ions and tritium in headwater streams as indicators of changing water stores. *Hydrological Processes*, 34, 485–505. <https://doi.org/10.1002/hyp.13600>
- Charette, M. A., & Allen, M. C. (2006). Precision ground water sampling in coastal aquifers using a direct-push, shielded-screen well-point system. *Ground Water Monitoring & Remediation*, 26(2), 87-93. <https://doi.org/10.1111/j.1745-6592.2006.00076.x>

- Cherkauer, D. S., & Nader, D. C. (1989). Distribution of groundwater seepage to large surface-water bodies: The effect of hydraulic heterogeneities. *Journal of Hydrology*, 109, 151-165.
- Chikita, K. A., Iwasaka, W., Al Mamun, A., Ohmori, K., & Itoh, Y. (2012). The role of groundwater outflow in the water cycle of a coastal lagoon sporadically opening to the ocean. *Journal of Hydrology*, 464–465, 423–430. <https://doi.org/10.1016/j.jhydrol.2012.07.035>
- Chikita, K. A., Umgiesser, G., Uyebara, H., Iwasaka, W., Al Mamun, A., Hossain, M. M., & Sakata, Y. (2015). Water and heat budgets in a coastal lagoon controlled by groundwater outflow to the ocean. *Limnology*, 16, 149–157. <https://doi.org/10.1007/s10201-015-0449-4>
- Clark, A. (2015). *Pillow (PIL Fork) Documentation*. <https://buildmedia.readthedocs.org/media/pdf/pillow/latest/pillow.pdf>
- Close, M. E., Rosen, M. R., & Smith, V. R. (2001). Fate and transport of nitrates and pesticides in New Zealand's aquifers. In M. R. Rosen & P. A. White (Eds.), *Groundwaters of New Zealand* (pp. 185-220). New Zealand Hydrological Society.
- Close, M. E., Tod, J. L., & Tod, G. J. (1995). Effect of recharge variations on regional groundwater quality in mid-Canterbury, New Zealand. *Journal of Hydrology (New Zealand)*, 33(1), 1-16.
- Cole, J. J., Bade, D. L., Bastviken, D., Pace, M. L., & Van de Bogert, M. (2010). Multiple approaches to estimating air-water gas exchange in small lakes. *Limnology and Oceanography: Methods*, 8, 285–293. <https://doi.org/10.4319/lom.2010.8.285>
- Cole, J. J., & Caraco, N. F. (1998). Atmospheric exchange of carbon dioxide in a low-wind oligotrophic lake measured by the addition of SF<sub>6</sub>. *Limnology and Oceanography*, 43(4), 647-656. <https://doi.org/10.4319/lo.1998.43.4.0647>
- Coluccio, K. (2018). *A comparison of methods for estimating groundwater-surface water interactions in braided rivers*. University of Canterbury. <http://hdl.handle.net/10092/15390>
- Coluccio, K., & Morgan, L. K. (2019). A review of methods for measuring groundwater–surface water exchange in braided rivers. *Hydrology and Earth System Sciences*, 23(10), 4397-4417. <https://doi.org/10.5194/hess-23-4397-2019>
- Coluccio, K., Santos, I., Jeffrey, L. C., Katurji, M., Coluccio, S., & Morgan, L. K. (2020). Mapping groundwater discharge to a coastal lagoon using combined spatial airborne thermal imaging, radon (<sup>222</sup>Rn) and multiple physicochemical variables. *Hydrological Processes*, 34(24), 4592-4608. <https://doi.org/10.1002/hyp.13903>
- Coluccio, K., Santos, I. R., Jeffrey, L. C., & Morgan, L. K. (2021). Groundwater discharge rates and uncertainties in a coastal lagoon using a radon mass balance *Journal of Hydrology*, 598. <https://doi.org/10.1016/j.jhydrol.2021.126436>
- Coluccio, S., & Coluccio, K. (2020). *loochlabs/temperature\_parser: Official (Version 1.0)*. Zenodo. <https://doi.org/10.5281/zenodo.3905347>
- Conant, B., Robinson, C. E., Hinton, M. J., & Russell, H. A. J. (2019). A framework for conceptualizing groundwater-surface water interactions and identifying potential impacts on water quality, water quantity, and ecosystems. *Journal of Hydrology*, 544, 609–627. <https://doi.org/10.1016/j.jhydrol.2019.04.050>
- Cook, P. G., & Herczeg, A. L. (2000). *Environmental Tracers in Subsurface Hydrology*. Kluwer Academic Publishers.
- Cook, P. G., Rodellas, V., Andrisoa, A., & Stieglitz, T. C. (2018). Exchange across the sediment-water interface quantified from porewater radon profiles. *Journal of Hydrology*, 559, 873–883. <https://doi.org/10.1016/j.jhydrol.2018.02.070>
- Corbett, D. R., Burnett, W. C., Cable, P. H., & Clark, S. B. (1997). Radon tracing of groundwater input into Par Pond, Savannah River Site. *Journal of Hydrology*, 203(1), 209-227. [https://doi.org/10.1016/S0022-1694\(97\)00103-0](https://doi.org/10.1016/S0022-1694(97)00103-0)
- Corbett, D. R., Burnett, W. C., Cable, P. H., & Clark, S. B. (1998). A multiple approach to the determination of radon fluxes from sediments. *Journal of Radioanalytical and Nuclear Chemistry*, 236(1-2), 247-252. <https://doi.org/10.1007/BF02386351>
- Correia, M. J., Costa, J. L., Chainho, P., Félix, P. M., Chaves, M. L., Medeiros, J. P., Silva, G., Azeda, C., Tavares, P., Costa, A., Costa, A. M., Bernardo, J., Cabral, H. N., Costa, M. J., & Cancela da Fonseca, L. (2012). Inter-annual variations of macrobenthic communities over three decades in a land-locked coastal lagoon (Santo André, SW Portugal). *Estuarine, Coastal and Shelf Science*, 110, 168-175. <https://doi.org/10.1016/j.ecss.2012.04.028>

- Costanza, R., d'Arge, R., de Groot, R., Farber, S., Grasso, M., Hannon, B., Limburg, K., Naeem, S., O'Neill, R. V., Paruelo, J., G., R. R., Sutton, P., & van den Belt, M. (1997). The value of the world's ecosystem services and natural capital. *Nature*, 387(6630), 253-260. <https://doi.org/10.1038/387253a0>
- Craig, H., & Gordon, L. I. (1965). Deuterium and oxygen-18 variations in the ocean and the marine atmosphere. In E. Tongiorgi (Ed.), *Stable Isotopes in Oceanographic Studies and Paleotemperatures* (pp. 9-130). CNR-Laboratorio di Geologia Nucleare.
- Crawshaw, J. A., Schallenberg, M., Savage, C., & Van Hale, R. (2019). Hierarchy of factors controls denitrification rates in temperate intermittently closed and open coastal lakes/lagoons (ICOLLS). *Aquatic Ecology*, 53, 719–744. <https://doi.org/10.1007/s10452-019-09721-4>
- Crivelli, A. J. (1995). Are fish introductions a threat to endemic freshwater fishes in the northern Mediterranean region? *Biological Conservation*, 72, 311-319. [https://doi.org/10.1016/0006-3207\(94\)00092-5](https://doi.org/10.1016/0006-3207(94)00092-5)
- Crusius, J., & Wanninkhof, R. (2003). Gas transfer velocities measured at low wind speed over a lake. *Limnology and Oceanography*, 48(3), 1010-1017. <https://doi.org/10.4319/lo.2003.48.3.1010>
- Dahiru, M., Bakar, N. K. A., Yus Off, I., Low, K. H., & Mohd, M. N. (2020). Assessment of denitrification potential for coastal and inland sites using groundwater and soil analysis: The multivariate approach. *Environmental Monitoring and Assessment*, 192(294). <https://doi.org/10.1007/s10661-020-08276-4>
- Danish, M., Tripathy, G. R., & Rahaman, W. (2020). Submarine groundwater discharge to a tropical coastal lagoon (Chilika Lagoon, India): An estimation using Sr isotopes. *Marine Chemistry*, 224. <https://doi.org/10.1016/j.marchem.2020.103816>
- Daughney, C., Jones, A., Baker, T., Hanson, C., Davidson, P., Zemansky, G., Reeves, R., & Thompson, M. (2006). *A National Protocol for State of the Environment Groundwater Sampling in New Zealand* Ministry for the Environment. <https://environment.govt.nz/publications/a-national-protocol-for-state-of-the-environment-groundwater-sampling-in-new-zealand/>
- David, M., Bailly-Comte, V., Munaron, D., Fiandrino, A., & Stieglitz, T. C. (2019). Groundwater discharge to coastal streams – A significant pathway for nitrogen inputs to a hypertrophic Mediterranean coastal lagoon. *Science of the Total Environment*. <https://doi.org/10.1016/j.scitotenv.2019.04.233>
- Dench, W. E., & Morgan, L. K. (2020). Unintended consequences to groundwater from improved irrigation efficiency: Lessons from the Hinds-Rangitata Plain, New Zealand. *Agricultural Water Management*, 245, 28 February 2021(106530). <https://doi.org/10.1016/j.agwat.2020.106530>
- Dimova, N. T., Burnett, W. C., Chanton, J. P., & Corbett, J. E. (2013). Application of radon-222 to investigate groundwater discharge into small shallow lakes. *Journal of Hydrology*, 486, 112–122. <https://doi.org/10.1016/j.jhydrol.2013.01.043>
- Duff, J. H., Carpenter, K. D., Snyder, D. T., Lee, K. K., Avanzino, R. J., & Triska, F. J. (2009). Phosphorus and nitrogen legacy in a restoration wetland, Upper Klamath Lake, Oregon. *Wetlands*, 29(2), 735–746. <https://doi.org/10.1672/08-129.1>
- Dulaiova, H., & Burnett, W. C. (2006). Radon loss across the water-air interface (Gulf of Thailand) estimated experimentally from  $^{222}\text{Rn}$ - $^{224}\text{Ra}$ . *Geophysical Research Letters*, 33(5). <https://doi.org/10.1029/2005GL025023>
- Dulaiova, H., Burnett, W. C., Wattayakorn, G., & Sojisuporn, P. (2006). Are groundwater inputs into river-dominated areas important? The Chao Phraya River: Gulf of Thailand. *Limnology and Oceanography*, 51(5), 2232-2247. <https://doi.org/10.4319/lo.2006.51.5.2232>
- Dulaiova, H., Peterson, R., Burnett, W. C., & Lane-Smith, D. (2005). A multi-detector continuous monitor for assessment of  $^{222}\text{Rn}$  in the coastal ocean. *Journal of Radioanalytical and Nuclear Chemistry*, 263(2), 361–365. <https://doi.org/10.1007/s10967-005-0063-8>
- Duque, C., Haider, K., Sebok, E., Sonnenborg, T. O., & Engesgaard, P. (2018). A conceptual model for groundwater discharge to a coastal brackish lagoon based on seepage measurements (Ringkøbing Fjord, Denmark). *Hydrological Processes*, 32(22), 3352–3364. <https://doi.org/10.1002/hyp.13264>

- Duque, C., Jessen, S., Tirado-Conde, J., Karan, S., & Engesgaard, P. (2019). Application of stable isotopes of water to study coupled submarine groundwater discharge and nutrient delivery. *Water*, 11(1842). <https://doi.org/10.3390/w11091842>
- Duque, C., Knee, K. L., Russoniello, C. J., Sherif, M., Abu Risha, U. A., Sturchio, N. C., & Michael, H. A. (2019). Hydrogeological processes and near shore spatial variability of radium and radon isotopes for the characterization of submarine groundwater discharge. *Journal of Hydrology*, 579. <https://doi.org/10.1016/j.jhydrol.2019.124192>
- Duque, C., Müller, S., Sebok, E., Haider, K., & Engesgaard, P. (2016). Estimating groundwater discharge to surface waters using heat as a tracer in low flux environments: The role of thermal conductivity. *Hydrological Processes*, 30, 383–395. <https://doi.org/10.1002/hyp.10568>
- Duque, C., Russoniello, C. J., & Rosenberry, D. O. (2020). History and evolution of seepage meters for quantifying flow between groundwater and surface water: Part 2 – Marine settings and submarine groundwater discharge. *Earth-Science Reviews*, 204. <https://doi.org/10.1016/j.earscirev.2020.103168>
- Enke, C. G. (2000). *The Art & Science of Chemical Analysis*. Wiley.
- Environment Canterbury. (2020a). *Monitoring Data*.
- Environment Canterbury. (2020b). *State of Environment Monitoring - Surface Water Quality*.
- Ettema, M., & Moore, C. R. (1995). *Seepage in Lake Ellesmere* (U95/18). Canterbury Regional Council.
- Evans, T. B., & Wilson, A. M. (2017). Submarine groundwater discharge and solute transport under a transgressive barrier island. *Journal of Hydrology*, 547, 97–110. <https://doi.org/10.1016/j.jhydrol.2017.01.028>
- Félix, P. M., Correia, M. J., Chainho, P., Costa, J. L., Chaves, M. L., Cruz, T., Castro, J. J., Mirra, C., Domingos, I., Silva, A. C. F., & Cancela da Fonseca, L. (2015). Impact of freshwater inputs on the spatial structure of benthic macroinvertebrate communities in two landlocked coastal lagoons. *Hydrobiologia*, 758, 197–209. <https://doi.org/10.1007/s10750-015-2290-5>
- Ferri, R., Pierdicca, N., & Talice, S. (2000). Mapping sea surface temperature from aircraft using a multi-angle technique: An experiment over the Orbetello Lagoon. *International Journal of Remote Sensing*, 21(16), 3003–3024. <https://doi.org/10.1080/01431160050144929>
- FitzGerald, D. M., Fenster, M. S., Argow, B. A., & Buynevich, I. V. (2008). Coastal impacts due to sea-level rise. *Annual Review of Earth and Planetary Sciences*, 36, 601–647. <https://doi.org/10.1146/annurev.earth.35.031306.140139>
- Freeze, R. A., & Cherry, J. A. (1979). *Groundwater*. Prentice-Hall.
- Fu, J., & Gómez-Hernández, J. (2009). Uncertainty assessment and data worth in groundwater flow and mass transport modeling using a blocking Markov chain Monte Carlo method. *Journal of Hydrology*, 364, 328–341. <https://doi.org/10.1016/j.jhydrol.2008.11.014>
- Fujita, M., Ide, Y., Sato, D., Kench, P. S., Kuwahara, Y., Yokoki, H., & Kayanne, H. (2014). Heavy metal contamination of coastal lagoon sediments: Fongafale Islet, Funafuti Atoll, Tuvalu. *Chemosphere*, 95, 628–634. <https://doi.org/10.1016/j.chemosphere.2013.10.023>
- Ganguli, P. M., Conaway, C. H., Swarzenski, P. W., Izbicki, J. A., & Flegal, A. R. (2012). Mercury speciation and transport via submarine groundwater discharge at a Southern California coastal lagoon system. *Environmental Science & Technology*, 46, 1480–1488. <https://doi.org/10.1021/es202783u>
- Garcia-Solsona, E., Masqué, P., Garcia-Orellana, J., Rapaglia, J., Beck, A. J., Cochran, J. K., Bokuniewicz, H. J., Zaggia, L., & Collavini, F. (2008). Estimating submarine groundwater discharge around Isola La Cura, northern Venice Lagoon (Italy), by using the radium quartet. *Marine Chemistry*, 109, 292–306. <https://doi.org/10.1016/j.marchem.2008.02.007>
- Gattacceca, J. C., Mayer, A., Cucco, A., Claude, C., Radakovitch, O., Vallet-Coulomb, C., & Hamelin, B. (2011). Submarine groundwater discharge in a subsiding coastal lowland: A <sup>226</sup>Ra and <sup>222</sup>Rn investigation in the Southern Venice lagoon. *Applied Geochemistry*, 26, 907–920. <https://doi.org/10.1016/j.apgeochem.2011.03.001>
- Gedan, K. B., Kirwan, M. L., Wolanski, E., Barbier, E. B., & Silliman, B. R. (2011). The present and future role of coastal wetland vegetation in protecting shorelines: Answering recent



- challenges to the paradigm. *Climatic Change*, 106, 7-29. <https://doi.org/10.1007/s10584-010-0003-7>
- Genereux, D., & Bandopadhyay, I. (2001). Numerical investigation of lake bed seepage patterns: Effects of porous medium and lake properties. *Journal of Hydrology*, 241, 286-303. [https://doi.org/10.1016/S0022-1694\(00\)00380-2](https://doi.org/10.1016/S0022-1694(00)00380-2)
- Gerbeaux, P., & Ward, J. C. (1991). Factors affecting water clarity in Lake Ellesmere, New Zealand. *New Zealand Journal of Marine and Freshwater Research*, 25(3), 289-296. <https://doi.org/10.1080/00288330.1991.9516481>
- Gibbs, M., Clayton, J., & Wells, R. (2005). *Further Investigation of Direct Groundwater Seepage to Lake Taupo* (Environment Waikato Technical Report 2005/34). <https://www.waikatoregion.govt.nz/services/publications/tr200534/>
- Gönenç, I. E., & Wolflin, J. P. (2004). *Coastal Lagoons: Ecosystem Processes and Modeling for Sustainable Use and Development*. CRC Press.
- González-De Zayas, R., Merino-Ibarra, M., Soto-Jiménez, M. F., & Castillo-Sandoval, F. S. (2013). Biogeochemical responses to nutrient inputs in a Cuban coastal lagoon: Runoff, anthropogenic, and groundwater sources. *Environmental Monitoring and Assessment*, 185, 10101–10114. <https://doi.org/10.1007/s10661-013-3316-y>
- Guérin, J., & Wourms, C. (2016). *Waituna Lagoon project: Mapping groundwater seepage areas and determining the age and chemical characteristics of groundwater seeps to Waituna Lagoon* (Unpublished). Environment Southland, University of Otago.
- Haider, K., Engesgaard, P., Sonnenborg, T. O., & Kirkegaard, C. (2015). Numerical modeling of salinity distribution and submarine groundwater discharge to a coastal lagoon in Denmark based on airborne electromagnetic data. *Hydrogeology Journal*, 23, 217–233. <https://doi.org/10.1007/s10040-014-1195-0>
- Hall, R. J. (2003). *Hydrological implications of a lake level control weir for Wainono Lagoon, South Canterbury* (DOC Science Internal Series 127). <https://www.doc.govt.nz/globalassets/documents/science-and-technical/dsis127.pdf>
- Han, Z., Shi, X., Jia, K., Sun, B., Zhao, S., & Fu, C. (2019). Determining the discharge and recharge relationships between lake and groundwater in Lake Hulun using hydrogen and oxygen isotopes and chloride ions. *Water*, 11(264). <https://doi.org/10.3390/w11020264>
- Hanson, C., & Abraham, P. (2009). *Depth and spatial variation in groundwater chemistry - Central Canterbury Plains* (Report No. R09/39). Environment Canterbury. <https://natlib.govt.nz/records/21242540?search%5Bpath%5D=items&search%5Btext%5D=Abraham%2C+Phil>
- Hart, D. E. (2007). River-mouth lagoon dynamics on mixed sand and gravel barrier coasts. *Journal of Coastal Research* (Special Issue 50: The International Coastal Symposium (ICS 2007)), 927-931.
- Hartzell, J. L., & Jordan, T. E. (2012). Shifts in the relative availability of phosphorus and nitrogen along estuarine salinity gradients. *Biogeochemistry*, 107(1/3), 489-500. <https://doi.org/10.1007/s10533-010-9548-9>
- Harvey, F. E., Rudolph, D. L., & Frape, S. K. (2000). Estimating Ground Water Flux into Large Lakes: Application in the Hamilton Harbor, Western Lake Ontario. *Ground Water*, 38(4). <https://doi.org/10.1111/j.1745-6584.2000.tb00248.x>
- Hayward, S., & Ward, J. C. (2009). Water quality in the Ellesmere catchment. In K. F. D. Hughey & K. J. W. Taylor (Eds.), *Te Waihora/Lake Ellesmere: State of the lake and future management*. EOS Ecology. <https://researcharchive.lincoln.ac.nz/handle/10182/4776>
- Hayward, S. A. (2002). *Christchurch-West Melton Groundwater Quality: A review of groundwater quality monitoring data from January 1986 to March 2002* (Report No. U02/47). Environment Canterbury.
- Hem, J. D. (1985). *Study and Interpretation of the Chemical Characteristics of Natural Water* (3rd ed.). U.S. Geological Survey. <https://pubs.usgs.gov/wsp/wsp2254/pdf/wsp2254a.pdf>
- Herrera-Silveira, J. (1996). Salinity and nutrients in a tropical coastal lagoon with groundwater discharges to the Gulf of Mexico. *Hydrobiologia*, 321, 165-176. <https://doi.org/10.1007/BF00023172>

- Herrera-Silveira, J. (1998). Nutrient-phytoplankton production relationships in a groundwater-influenced tropical coastal lagoon. *Aquatic Ecosystem Health & Management*, 1(3-4), 373-385. <https://doi.org/10.1080/14634989808656931>
- Herrera-Silveira, J. A., Medina-Gomez, I., & Colli, R. (2002). Trophic status based on nutrient concentration scales and primary producers community of tropical coastal lagoons influenced by groundwater discharges. *Hydrobiologia*, 475/476, 91–98. <https://doi.org/10.1023/A:1020344721021>
- Horrell, G. (1992). *Lake Ellesmere water balance model: Variable analysis and evaluation*. University of New South Wales. <http://docs.niwa.co.nz/library/public/Horrellthesis.pdf>
- Hu, S., Niu, Z., Chen, Y., Li, L., & Zhang, H. (2107). Global wetlands: Potential distribution, wetland loss, and status. *Science of the Total Environment*, 586, 319-327. <https://doi.org/10.1016/j.scitotenv.2017.02.001>
- Hughey, K. F. D., & Taylor, K. J. W. (2009). *Te Waihora/Lake Ellesmere: State of the Lake and Future Management*. EOS Ecology. <https://researcharchive.lincoln.ac.nz/handle/10182/4776>
- Hugman, R., Stigter, T., & Costa, L. M., J. P. (2017). Modeling nitrate-contaminated groundwater discharge to the Ria Formosa coastal lagoon (Algarve, Portugal). *Procedia Earth and Planetary Science*, 17, 650-653. <https://doi.org/10.1016/j.proeps.2016.12.174>
- Hume, T., Gerbeaux, P., Hart, D., Kettles, H., & Neale, D. (2016). *A classification of New Zealand's coastal hydrosystems* (HAM2016-062). National Institute of Water & Atmospheric Research, Ltd. <https://www.mfe.govt.nz/sites/default/files/media/Marine/a-classification-of-nz-coastal-hydrosystems.pdf>
- Ibáñez, J. S. P., Leote, C., & Rocha, C. (2013). Seasonal enhancement of submarine groundwater discharge (SGD)-derived nitrate loading into the Ria Formosa coastal lagoon assessed by 1-D modeling of benthic NO<sub>3</sub><sup>-</sup> profiles. *Estuarine, Coastal and Shelf Science*, 132, 56-64. <https://doi.org/10.1016/j.ecss.2012.04.015>
- Inpasihardjo, P. (1988). *Application of a mathematical model of seepage in a coastal barrier*. University of Newcastle upon Tyne.
- Irwin, J., & Main, W. d. (1989). *Lake Ellesmere Bathymetry 1:25,000*
- Jeffrey, L. C., Maher, D. T., Santos, I. R., Calla, M., Reading, M. J., Holloway, C., & Tait, D. R. (2018). The spatial and temporal drivers of pCO<sub>2</sub>, pCH<sub>4</sub> and gas transfer velocity within a subtropical estuary. *Estuarine, Coastal and Shelf Science*, 208, 83–95. <https://doi.org/10.1016/j.ecss.2018.04.022>
- Jeffrey, L. C., McMahon, A., Maher, D. T., Tait, D. R., & Santos, I. R. (2016). Groundwater, acid and carbon dioxide dynamics along a coastal wetland, lake and estuary continuum. *Estuaries and Coasts*, 39(5), 1325-1344. <https://doi.org/10.1007/s12237-016-0099-8>
- Jenkins, B. (2016). *Sustainability analysis of five lakes in the Wellington Region: Lake Wairarapa, Lake Onoke, Lake Pounui, Lake Waitawa and Lake Kohangatera* (WCFM Report 2015-005). <http://www.waterways.ac.nz/documents/Technical%20reports/WCFM%20TR%202015-005%20Sustainability%20analysis%20of%20five%20lakes%20in%20the%20Wellington%20Region.pdf>
- Ji, T., Du, J., Moore, W. S., Zhang, G., Su, N., & Zhang, J. (2013). Nutrient inputs to a lagoon through submarine groundwater discharge: The case of Laoye Lagoon, Hainan, China. *Journal of Marine Systems*, 111–112, 253–262. <https://doi.org/10.1016/j.jmarsys.2012.11.007>
- Johannes, R. E., & Hearn, C. J. (1985). The effect of submarine groundwater discharge on nutrient and salinity regimes in a coastal lagoon off Perth, Western Australia. *Estuarine, Coastal and Shelf Science*, 21, 789-800. [https://doi.org/10.1016/0272-7714\(85\)90073-3](https://doi.org/10.1016/0272-7714(85)90073-3)
- Johannesson, K. H., Chevis, D. A., Burdige, D. J., Cable, J. E., Martin, J. B., & Roy, M. (2011). Submarine groundwater discharge is an important net source of light and middle REEs to coastal waters of the Indian River Lagoon, Florida, USA. *Geochimica et Cosmochimica Acta*, 75, 825–843. <https://doi.org/10.1016/j.gca.2010.11.005>
- Johnson, A. G., Glenn, C. R., Burnett, W. C., Peterson, R. N., & Lucey, P. G. (2008). Aerial infrared imaging reveals large nutrient-rich groundwater inputs to the ocean. *Geophysical Research Letters*, 35(15). <https://doi.org/10.1029/2008GL034574>

- Kalbus, E., Reinstorf, F., & Schirmer, M. (2006). Measuring methods for groundwater–surface water interactions: A review. *Hydrology and Earth System Sciences*, 10, 873–887. <https://doi.org/10.5194/hess-10-873-2006>
- Kazmierczak, J., Postma, D., Müller, S., Jessen, S., Nilsson, B., Czekaj, J., & Engesgaard, P. (2020). Groundwater-controlled phosphorus release and transport from sandy aquifer into lake. *Limnology and Oceanography*, 65, 2188–2204. <https://doi.org/10.1002/lno.11447>
- Kennish, M. J., & Paerl, H. W. (2010). Coastal Lagoons: Critical Habitats of Environmental Change. In M. J. Kennish & H. W. Paerl (Eds.), *Coastal Lagoons: Critical Habitats of Environmental Change*. CRC Press (Taylor & Francis Group).
- Kirk, R. M., & Lauder, G. A. (2000). *Significant coastal lagoon systems in the South Island, New Zealand: Coastal processes and lagoon mouth closure* (Science for Conservation, Issue. Department of Conservation). <https://www.doc.govt.nz/globalassets/documents/science-and-technical/sfc146.pdf>
- Kitto, S. G. (2010). *The Environmental History of Te Waihora – Lake Ellesmere*. University of Canterbury.
- Kjerfve, B. (1986). Comparative oceanography of coastal lagoons. In D. A. Wolfe (Ed.), *Estuarine Variability* (pp. 63-81). Academic Press.
- Kjerfve, B. (1994). Coastal Lagoons. In B. Kjerfve (Ed.), *Coastal Lagoon Processes*. Elsevier.
- Kluge, T., von Rohden, C., Sonntag, P., Lorenz, S., Wieser, M., Aeschbach-Hertig, W., & Ilmberger, J. (2012). Localising and quantifying groundwater inflow into lakes using high-precision  $^{222}\text{Rn}$  profiles. *Journal of Hydrology*, 450–451, 70-81. <https://doi.org/10.1016/j.jhydrol.2012.05.026>
- Knapp, M. A., Geeraert, N., Kim, K., & Knee, K. L. (2020). Submarine groundwater discharge (SGD) to coastal waters of Saipan (Commonwealth of the Northern Mariana Islands, USA): Implications for nitrogen sources, transport and ecological effects. *Water*, 12(3029). <https://doi.org/10.3390/w12113029>
- Kong, F., Sha, Z., Luo, X., Du, J., Jiao, J. J., Moore, W. S., Yang, Y., & Su, W. (2019). Evaluation of lacustrine groundwater discharge and associated nutrients, trace elements and DIC loadings into Qinghai Lake in Qinghai-Tibetan Plateau, using radium isotopes and hydrological methods. *Chemical Geology*, 510, 31-46. <https://doi.org/10.1016/j.chemgeo.2019.01.020>
- La Jeunesse, I., & Elliot, M. (2004). Anthropogenic regulation of the phosphorus balance in the Thau catchment–coastal lagoon system (Mediterranean Sea, France) over 24 years. *Marine Pollution Bulletin*, 48, 679–687. <https://doi.org/10.1016/j.marpolbul.2003.10.011>
- LaBaugh, J. W., & Rosenberry, D. O. (2008). Introduction and Characteristics of Flow. In D. O. Rosenberry & J. W. LaBaugh (Eds.), *Field Techniques for Estimating Water Fluxes Between Surface Water and Ground Water: U.S. Geological Survey Techniques and Methods 4–D2*. U.S. Geological Survey. <https://pubs.usgs.gov/tm/04d02/>
- Land Information New Zealand. (2019). *NZ River Name Polygons (Pilot)* Retrieved 18 Aug 2021, from <https://data.linz.govt.nz/layer/103631-nz-river-name-polygons-pilot/>
- Land Information New Zealand. (2020). *NZ River Centrelines (Topo, 1:250k)* Retrieved 18 Aug 2021, from <https://data.linz.govt.nz/layer/50182-nz-river-centrelines-topo-1250k/>
- Larned, S. T., Gooseff, M. N., Packman, A. I., Rugel, K., & Wondzell, S. M. (2015). Groundwater–surface-water interactions: Current research directions. *Freshwater Science*, 34(1), 92–98. <https://doi.org/10.1086/679491>
- Larned, S. T., Hicks, D. M., Schmidt, J., Davey, A. J. H., Dey, K., Scarsbrook, M., Arscott, D. B., & Woods, R. A. (2008). The Selwyn River of New Zealand: A benchmark system for alluvial plain rivers. *River Research and Applications*, 24(1), 1-21. <https://doi.org/10.1002/rra.1054>
- Larned, S. T., & Schallenberg, M. (2006). *Constraints on phytoplankton production in Lake Ellesmere/Te Waihora* (Report No. U06/38). Environment Canterbury. <https://citeseerx.ist.psu.edu/viewdoc/download?doi=10.1.1.799.7330&rep=rep1&type=pdf>
- Lee, D. R. (1977). A device for measuring seepage flux in lakes and estuaries. *Limnology and Oceanography*, 22(1), 140-147. <https://doi.org/10.4319/lo.1977.22.1.0140>
- Lee, E., Kang, K., Hyun, S. P., Lee, K.-Y., Yoon, H., Kim, S. H., Kim, Y., Xu, Z., Kim, D., Koh, D.-C., & Ha, K. (2016). Submarine groundwater discharge revealed by aerial thermal infrared

- imagery: A case study on Jeju Island, Korea. *Hydrological Processes*, 30, 3494–3506. <https://doi.org/10.1002/hyp.10868>
- Lee, J. M., & Kim, G. (2006). A simple and rapid method for analyzing radon in coastal and ground waters using a radon-in-air monitor. *Journal of Environmental Radioactivity*, 89, 219–228. <https://doi.org/10.1016/j.jenvrad.2006.05.006>
- Leote, C., Ibáñez, J. S., & Rocha, C. (2008). Submarine groundwater discharge as a nitrogen source to the Ria Formosa studied with seepage meters. *Biogeochemistry*, 88(2), 185–194. <https://doi.org/10.1007/s10533-008-9204-9>
- Lewandowski, J., Meinikmann, K., & Krause, S. (2020). Groundwater–surface water interactions: Recent advances and interdisciplinary challenges. *Water*, 12(296). <https://doi.org/10.3390/w12010296>
- Lewandowski, J., Meinikmann, K., Nützmann, G., & Rosenberry, D. O. (2015). Groundwater – the disregarded component in lake water and nutrient budgets. Part 2: effects of groundwater on nutrients. *Hydrological Processes*, 29, 2922–2955. <https://doi.org/10.1002/hyp.10384>
- Lewandowski, J., Meinikmann, K., Ruhtz, T., Pöschke, F., & Kirillin, G. (2013). Localization of lacustrine groundwater discharge (LGD) by airborne measurement of thermal infrared radiation. *Remote Sensing of Environment*, 138, 119–125. <https://doi.org/10.1016/j.rse.2013.07.005>
- Liefer, J. D., MacIntyre, H. L., Su, N., & Burnett, W. C. (2014). Seasonal alternation between groundwater discharge and benthic coupling as nutrient sources in a shallow coastal lagoon. *Estuaries and Coasts*, 37, 925–940. <https://doi.org/10.1007/s12237-013-9739-4>
- Lineham, I. W. (1983). *Eutrophication of Lake Ellesmere: A study of phytoplankton*. University of Canterbury. <https://ir.canterbury.ac.nz/handle/10092/4760>
- Lopez, C. V., Murgulet, D., & Santos, I. R. (2020). Radioactive and stable isotope measurements reveal saline submarine groundwater discharge in a semiarid estuary. *Journal of Hydrology*, 590. <https://doi.org/10.1016/j.jhydrol.2020.125395>
- Lotze, H. K., Lenihan, H. S., Bourque, B. J., Bradbury, R. H., Cooke, R. G., Kay, M. C., Kidwell, S. M., Kirby, M. X., Peterson, C. H., & Jackson, J. B. C. (2006). Depletion, Degradation, and Recovery Potential of Estuaries and Coastal Seas. *Science*, 312(5781), 1806–1809. <https://doi.org/10.1126/science.1128035>
- Loveless, A. M., & Oldham, C. E. (2010). Natural attenuation of nitrogen in groundwater discharging through a sandy beach. *Biogeochemistry*, 98(1/3), 75–87. <https://doi.org/10.1007/S10533-009-9377-X>
- Lovett, A., Cameron, S., Reeves, R., Meijer, E., Verhagen, F., van der Raaij, R., Westerhoff, R., Moridnejad, M., & Morgenstern, U. (2015). *Characterisation of groundwater-surface water interaction at three case study sites within the Upper Waikato River Catchment using temperature sensing and hydrochemistry techniques* (GNS Science Report 2014/64). Institute of Geological and Nuclear Sciences Limited (GNS). [http://shop.gns.cri.nz/sr\\_2014-064-pdf/](http://shop.gns.cri.nz/sr_2014-064-pdf/)
- Luo, X., Kuang, X., Jiao, J. J., Liang, S., Mao, R., Zhang, X., & Li, H. (2018). Evaluation of lacustrine groundwater discharge, hydrologic partitioning, and nutrient budgets in a proglacial lake in the Qinghai–Tibet Plateau: Using <sup>222</sup>Rn and stable isotopes. *Hydrology and Earth System Sciences*, 22, 5579–5598. <https://doi.org/10.5194/hess-22-5579-2018>
- MacIntyre, S., Wanninkhof, R., & Chanton, J. P. (1995). Trace gas exchange across the air-water interface in freshwater and coastal marine environments. In P. A. Matson & R. C. Harriss (Eds.), *Biogenic Trace Gases: Measuring Emissions from Soil and Water* (1st ed.). John Wiley & Sons, Incorporated.
- MacKenzie, E. M. (2016). *The role of nutrients and light in the growth of phytoplankton in Te Waihora/Lake Ellesmere, New Zealand*. University of Canterbury. <https://ir.canterbury.ac.nz/handle/10092/12889>
- Macklin, P. A., Suryaputra, I. G. N. A., Maher, D. T., & Santos, I. R. (2018). Carbon dioxide dynamics in a lake and a reservoir on a tropical island (Bali, Indonesia). *PLoS One*, 13(6), e0198678. <https://doi.org/10.1371/journal.pone.0198678>
- Mæller, D. (1990). The Na/Cl ratio in rainwater and the seasalt chloride cycle. *Tellus B: Chemical and Physical Meteorology*, 42(3), 254–262. <https://doi.org/10.3402/tellusb.v42i3.15216>

- Maher, D. T., Call, M., Macklin, P., Webb, J. R., & Santos, I. R. (2019). Hydrological versus biological drivers of nutrient and carbon dioxide dynamics in a coastal lagoon. *Estuaries and Coasts*. <https://doi.org/10.1007/s12237-019-00532-2>
- Manzoni, S., Maneas, G., Scaini, A., Psiloglou, B. E., Destouni, G., & Lyon, S. W. (2020). Understanding coastal wetland conditions and futures by closing their hydrologic balance: The case of the Gialova lagoon, Greece. *Hydrology and Earth System Sciences*, 24(7), 3557-3571. <https://doi.org/10.5194/hess-24-3557-2020>
- Martens, C. S., Kipphut, G. W., & Klump, J. V. (1980). Sediment-water chemical exchange in the coastal zone traced by in situ radon-222 flux measurements. *Science*, 208(4441), 285-288. <https://doi.org/10.1126/science.208.4441.285>
- Martin, J. B., Cable, J. E., Jaeger, J., Hartl, K., & Smith, C. G. (2006). Thermal and chemical evidence for rapid water exchange across the sediment-water interface by bioirrigation in the Indian River Lagoon, Florida. *Limnology and Oceanography*, 51(3), 1332-1341. <https://doi.org/10.4319/lo.2006.51.3.1332>
- Mateus, M., Almeida, D., Simonson, W., Felgueiras, M., Banza, P., & Batty, L. (2016). Conflictive uses of coastal areas: A case study in a southern European coastal lagoon (Ria de Alvor, Portugal). *Ocean & Coastal Management*, 132, 90-100. <https://doi.org/10.1016/j.ocecoaman.2016.08.016>
- Mazor, E. (1991). *Applied Chemical and Isotopic Groundwater Hydrology*. John Wiley & Sons.
- McBride, M. S., & Pfannkuch, H. O. (1975). The distribution of seepage within lakebeds. *U.S. Geological Survey Journal of Research*, 3(5), 505-512.
- McMahon, A., & Santos, I. R. (2017). Nitrogen enrichment and speciation in a coral reef lagoon driven by groundwater inputs of bird guano. *Journal of Geophysical Research: Oceans*, 122, 7218-7236. <https://doi.org/10.1002/2017JC012929>
- Medina-Gómez, I., & Herrera-Silveira, J. A. (2006). Primary production dynamics in a pristine groundwater influenced coastal lagoon of the Yucatan Peninsula. *Continental Shelf Research*, 26, 971-986. <https://doi.org/10.1016/j.csr.2006.03.003>
- Meinikmann, K., Lewandowski, J., & Nützmann, G. (2013). Lacustrine groundwater discharge: Combined determination of volumes and spatial patterns. *Journal of Hydrology*, 502, 202-211. <https://doi.org/10.1016/j.jhydrol.2013.08.021>
- Menció, A., Casamitjana, X., Mas-Pla, J., Coll, N., Compte, J., Martinoy, M., Pascual, J., & Quintana, X. D. (2017). Groundwater dependence of coastal lagoons: The case of La Pletera salt marshes (NE Catalonia). *Journal of Hydrology*, 552, 793-806. <https://doi.org/10.1016/j.jhydrol.2017.07.034>
- Menció, A., Casamitjana, X., Mas-Pla, J., Coll, N., Compte, J., Martinoy, M., Pascual, J., & Quintana, X. D. (2017). Groundwater dependence of coastal lagoons: The case of La Pletera salt marshes (NE Catalonia). *Journal of Hydrology*, 552, 793-806. <https://doi.org/10.1016/j.jhydrol.2017.07.034>
- Mitsch, W. J., & Gosselink, J. G. (2000). The value of wetlands: Importance of scale and landscape setting. *Ecological Economics*, 35, 25-33. [https://doi.org/10.1016/S0921-8009\(00\)00165-8](https://doi.org/10.1016/S0921-8009(00)00165-8)
- Moore, W. S. (2003). Sources and fluxes of submarine groundwater discharge delineated by radium isotopes. *Biogeochemistry*, 66(No. 1/2, Submarine Groundwater Discharge), 75-93. <https://doi.org/10.1023/B:BIOG.0000006065.77764.a0>
- Moore, W. S. (2007). Seasonal distribution and flux of radium isotopes on the southeastern U.S. continental shelf. *Journal of Geophysical Research*, 112(C10013). <https://doi.org/10.1029/2007JC004199>
- Mudge, S. M., Icely, J. D., & Newton, A. (2008). Residence times in a hypersaline lagoon: Using salinity as a tracer. *Estuarine, Coastal and Shelf Science*, 77, 278-284. <https://doi.org/10.1016/j.ecss.2007.09.032>
- Mullinger, N. J., Pates, J. M., Binley, A. M., & Crook, N. P. (2009). Controls on the spatial and temporal variability of <sup>222</sup>Rn in riparian groundwater in a lowland Chalk catchment. *Journal of Hydrology*, 376(1), 58-69. <https://doi.org/10.1016/j.jhydrol.2009.07.015>
- Mundy, E., Gleeson, T., Roberts, M., Baraer, M., & McKenzie, J. M. (2017). Thermal imagery of groundwater seeps: Possibilities and limitations. *Groundwater*, 55(2), 160-170. <https://doi.org/10.1111/gwat.12451>

- Nichols, M. M., & Boon, J. D. (1994). Sediment Transport Processes in Coastal Lagoons. In B. Kjerfve (Ed.), *Coastal Lagoon Processes*. Elsevier.
- Nielsen, L., Jørgensen, N. O., & Gelting, P. (2007). Mapping of the freshwater lens in a coastal aquifer on the Keta Barrier (Ghana) by transient electromagnetic soundings. *Journal of Applied Geophysics*, 62, 1–15. <https://doi.org/10.1016/j.jappgeo.2006.07.002>
- Oliphant, T. E. (2006). *A guide to NumPy*. Trelgol Publishing.
- Ortega-Arbulú, A., Pichler, M., Vuillemin, A., & Orsi, W. D. (2019). Effects of organic matter and low oxygen on the mycobenthos in a coastal lagoon. *Environmental Microbiology*, 21(1), 374–388. <https://doi.org/10.1111/1462-2920.14469>
- Peng, T.-H., Takahashi, T., & Broecker, W. S. (1974). Surface radon measurements in the North Pacific Ocean station Papa. *Journal of Geophysical Research*, 79(12), 1772–1780. <https://doi.org/10.1029/JC079i012p01772>
- Perkins, A. K., Santos, I. R., Sadat-Noori, M., & Maher, D. T. (2015). Groundwater seepage as a driver of CO<sub>2</sub> evasion in a coastal lake (Lake Ainsworth, NSW, Australia). *Environmental Earth Sciences*, 74(1). <https://doi.org/10.1007/s12665-015-4082-7>
- Petermann, E., Knöller, K., Rocha, C., Scholten, J., Stollberg, R., Weiß, H., & Schubert, M. (2018). Coupling endmember mixing analysis and isotope mass balancing (222-Rn) for differentiation of fresh and recirculated submarine groundwater discharge into Knysna Estuary, South Africa. *Journal of Geophysical Research: Oceans*, 123, 952–970. <https://doi.org/10.1002/2017JC013008>
- Petermann, E., Schubert, M., Gibson, J. J., Knöller, K., Pannier, T., & Weiß, H. (2018). Determination of groundwater discharge rates and water residence time of groundwater-fed lakes by stable isotopes of water (18O, 2H) and radon (222Rn) mass balances. *Hydrological Processes*, 32, 805–816. <https://doi.org/10.1002/hyp.11456>
- Peterson, R. N., Burnett, W. C., Dimova, N., & Santos, I. R. (2009). Comparison of measurement methods for radium-226 on manganese-fiber. *Limnology and Oceanography: Methods*, 7, 196–205. <https://doi.org/10.4319/lom.2009.7.196>
- Precht, E., Franke, U., Polerecky, L., & Huettel, M. (2004). Oxygen dynamics in permeable sediments with wave-driven pore water exchange. *Limnology and Oceanography*, 49(3), 693–705. <https://doi.org/10.4319/lo.2004.49.3.0693>
- Ptacnik, R., Andersen, T., & Tamminen, T. (2010). Performance of the Redfield Ratio and a family of nutrient limitation indicators as thresholds for phytoplankton N vs. P limitation. *Ecosystems*, 13(8), 1201–1214. <https://doi.org/10.1007/S10021-010-9380-Z>
- Rapaglia, J., Di Sipio, E., Bokuniewicz, H., Zuppi, G. M., Zaggia, L., Galgaro, A., & Beck, A. (2010). Groundwater connections under a barrier beach: A case study in the Venice Lagoon. *Continental Shelf Research*, 30, 119–126. <https://doi.org/10.1016/j.csr.2009.10.001>
- Rapaglia, J., Ferrarin, C., Zaggia, L., Moore, W. S., Umgiesser, G., Garcia-Solsona, E., Garcia-Orellana, J., & Masqué, P. (2010). Investigation of residence time and groundwater flux in Venice Lagoon: Comparing radium isotope and hydrodynamical models. *Journal of Environmental Radioactivity*, 101, 571–581. <https://doi.org/10.1016/j.jenvrad.2009.08.010>
- Rautio, A. B., Korkka-Niemi, K. I., & Salonen, V.-P. (2018). Thermal infrared remote sensing in assessing groundwater and surface-water resources related to Hannukainen mining development site, northern Finland. *Hydrogeology Journal*, 26, 163–183. <https://doi.org/10.1007/s10040-017-1630-0>
- Redfield, A. C. (1934). On the proportions of organic derivatives in sea water and their relation to the composition of plankton. In *James Johnstone Memorial Volume* (pp. 176–192). University Press of Liverpool.
- Redfield, A. C. (1958). The biological control of chemical factors in the environment. *American Scientist*, 46(3), 205–221.
- Rissmann, C., Wilson, K., & Hughes, B. (2012). *Waituna Catchment Groundwater Resource* (2012–04). Environment Southland. [https://www.es.govt.nz/Document%20Library/Research%20and%20reports/Groundwater%20reports/waituna\\_technical\\_report\\_2012.pdf](https://www.es.govt.nz/Document%20Library/Research%20and%20reports/Groundwater%20reports/waituna_technical_report_2012.pdf)
- Robinson, C. E., Xin, P., Santos, I. R., Charette, M. A., Ling, L., & Barry, D. A. (2018). Groundwater dynamics in subterranean estuaries of coastal unconfined aquifers: Controls on submarine

- groundwater discharge and chemical inputs to the ocean. *Advances in Water Resources*, 115, 315–331. <https://doi.org/10.1016/j.advwatres.2017.10.041>
- Rocha, C., Veiga-Pires, C., Scholten, J., Knoeller, K., Gröcke, D. R., Carvalho, L., Anibal, J., & Wilson, J. (2016). Assessing land–ocean connectivity via submarine groundwater discharge (SGD) in the Ria Formosa Lagoon (Portugal): Combining radon measurements and stable isotope hydrology. *Hydrology and Earth System Sciences*, 20, 3077–3098. <https://doi.org/10.5194/hess-20-3077-2016>
- Rodellas, V., Cook, P. G., McCallum, J., Andrisoa, A., Meuléa, S., & Stieglitz, T. C. (2020). Temporal variations in porewater fluxes to a coastal lagoon driven by wind waves and changes in lagoon water depths. *Journal of Hydrology*, 581. <https://doi.org/10.1016/j.jhydrol.2019.124363>
- Rodellas, V., Stieglitz, T. C., Andrisoa, A., Cook, P. G., Raimbault, P., Tamborski, J. J., van Beek, P., & Radakovitch, O. (2018). Groundwater-driven nutrient inputs to coastal lagoons: The relevance of lagoon water recirculation as a conveyor of dissolved nutrients. *Science of the Total Environment*, 642, 764–780. <https://doi.org/10.1016/j.scitotenv.2018.06.095>
- Rodellas, V., Stieglitz, T. C., Tamborski, J. J., van Beek, P., Andrisoa, A., & Cook, P. G. (2021). Conceptual uncertainties in groundwater and porewater fluxes estimated by radon and radium mass balances. *Limnology and Oceanography*, 9999(2021), 1–19. <https://doi.org/10.1002/lno.11678>
- Röper, T., Kröger, K. F., Meyer, H., Sültenfuss, J., Greskowiak, J., & Massmann, G. (2012). Groundwater ages, recharge conditions and hydrochemical evolution of a barrier island freshwater lens (Spiekeroog, Northern Germany). *Journal of Hydrology*, 454–455, 173–186. <https://doi.org/10.1016/j.jhydrol.2012.06.011>
- Rosen, M. R. (2001). Hydrochemistry of New Zealand's aquifers. In M. R. Rosen & P. A. White (Eds.), *Groundwaters of New Zealand* (pp. 77–110). New Zealand Hydrological Society Inc.
- Rosenberry, D. O., Duque, C., & Lee, D. R. (2020). History and evolution of seepage meters for quantifying flow between groundwater and surface water: Part 1 – Freshwater settings. *Earth-Science Reviews*, 204. <https://doi.org/10.1016/j.earscirev.2020.103167>
- Rosenberry, D. O., Lewandowski, J., Meinikmann, K., & Nützmänn, G. (2015). Groundwater - the disregarded component in lake water and nutrient budgets. Part 1: Effects of groundwater on hydrology. *Hydrological Processes*, 29, 2895–2921. <https://doi.org/10.1002/hyp.10403>
- Rosenberry, D. O., Sheibley, R. W., Cox, S. E., Simonds, F. W., & Naftz, D. L. (2013). Temporal variability of exchange between groundwater and surface water based on high-frequency direct measurements of seepage at the sediment-water interface. *Water Resources Research*, 49, 2975–2986. <https://doi.org/10.1002/wrcr.20198>
- Rosenberry, D. O., Toran, L., & Nyquist, J. E. (2010). Effect of surficial disturbance on exchange between groundwater and surface water in nearshore margins. *Water Resources Research*, 46(W06518). <https://doi.org/10.1029/2009WR008755>
- Rudnick, S., Lewandowski, J., & Nützmänn, G. (2015). Investigating groundwater-lake interactions by hydraulic heads and a water balance. *Groundwater*, 53(2), 227–237. <https://doi.org/10.1111/gwat.12208>
- Rutter, K., & Rutter, H. (2019). An assessment of nitrate trends in groundwater across Canterbury: results from a Science Fair project. *Journal of Hydrology (NZ)*, 58(2), 65–80.
- Sadat-Noori, M., Santos, I. R., Sanders, C. J., Sanders, L. M., & Maher, D. T. (2015). Groundwater discharge into an estuary using spatially distributed radon time series and radium isotopes. *Journal of Hydrology*, 528, 703–719. <https://doi.org/10.1016/j.jhydrol.2015.06.056>
- Sadat-Noori, M., Santos, I. R., Tait, D. R., McMahon, A., Kadel, S., & Maher, D. T. (2016). Intermittently Closed and Open Lakes and/or Lagoons (ICOLLS) as groundwater-dominated coastal systems: Evidence from seasonal radon observations. *Journal of Hydrology*, 535, 612–624. <https://doi.org/10.1016/j.jhydrol.2016.01.080>
- Sánchez-Martos, F., Gisbert-Gallego, J., & Molina-Sánchez, L. (2014). Groundwater–wetlands interaction in coastal lagoon of Almería (SE Spain). *Environmental Earth Sciences*, 71, 67–76. <https://doi.org/10.1007/s12665-013-2695-2>

- Santos, I. R., Bryan, K. R., Pilditch, C. A., & Tait, D. R. (2014). Influence of porewater exchange on nutrient dynamics in two New Zealand estuarine intertidal flats. *Marine Chemistry*, 167, 57–70. <https://doi.org/10.1016/j.marchem.2014.04.006>
- Santos, I. R., Chen, X., Lecher, A. L., Sawyer, A. H., Moosdorf, N., Rodellas, V., Tamborski, J., Cho, H., Dimova, N., Sugimoto, R., Bonaglia, S., Li, H., Hajati, M., & Li, L. (2021). Submarine groundwater discharge impacts on coastal nutrient biogeochemistry. *Nature Reviews Earth and Environment*. <https://doi.org/10.1038/s43017-021-00152-0>
- Santos, I. R., Eyre, B. D., & Huettel, M. (2012). The driving forces of porewater and groundwater flow in permeable coastal sediments: A review. *Estuarine, Coastal and Shelf Science*, 98, 1–15. <https://doi.org/10.1016/j.ecss.2011.10.024>
- Santos, I. R., Machado, M. I., Niencheski, L. F., Burnett, W., Milani, I. B., Andrade, C. F. F., Peterson, R. N., Chanton, J., & Baisch, P. (2008). Major ion chemistry in a freshwater coastal lagoon from southern Brazil (Mangueira Lagoon): Influence of groundwater inputs. *Aquatic Geochemistry*, 14, 133–146. <https://doi.org/10.1007/s10498-008-9029-0>
- Santos, I. R., Niencheski, F., Burnett, W., Peterson, R., Chanton, J., Andrade, C. F. F., Milani, I. B., Schmidt, A., & Knoeller, K. (2008). Tracing anthropogenically driven groundwater discharge into a coastal lagoon from southern Brazil. *Journal of Hydrology*, 353, 275–293. <https://doi.org/10.1016/j.jhydrol.2008.02.010>
- Schallenberg, M., & Crawshaw, J. A. (2017). *In-lake nutrient processing in Te Waihora/Lake Ellesmere*. University of Otago. <https://tewaihora.org/wp-content/uploads/2019/07/Otago-InLake-Nutrient-Processing-Report-Final-web-compressed.pdf>
- Schallenberg, M., de Winton, M. D., Verburg, P., Kelly, D. J., Hamill, K. D., & Hamilton, D. P. (2013). Ecosystem services of lakes. In J. R. Dymond (Ed.), *Ecosystem services in New Zealand – conditions and trends*. Manaaki Whenua Press.
- Schallenberg, M., Larned, S. T., Hayward, S., & Arbuckle, C. (2010). Contrasting effects of managed opening regimes on water quality in two intermittently closed and open coastal lakes. *Estuarine, Coastal and Shelf Science*, 86, 587–597. <https://doi.org/10.1016/j.ecss.2009.11.001>
- Schmidt, A., Gibson, J. J., Santos, I. R., Schubert, M., Tattier, K., & Weiss, H. (2010). The contribution of groundwater discharge to the overall water budget of two typical Boreal lakes in Alberta/Canada estimated from a radon mass balance. *Hydrology and Earth System Sciences*, 14, 79–89. <https://doi.org/10.5194/hess-14-79-2010>
- Schmidt, A., Santos, I. R., Burnett, W. C., Niencheski, F., & Knöller, K. (2011). Groundwater sources in a permeable coastal barrier: Evidence from stable isotopes. *Journal of Hydrology*, 406, 66–72. <https://doi.org/10.1016/j.jhydrol.2011.06.001>
- Schubert, M., Paschke, A., Bednorz, D., Bürkin, W., & Stieglitz, T. (2012). Kinetics of the water/air phase transition of radon and its implication on detection of radon-in-water concentrations: Practical assessment of different on-site radon extraction methods. *Environmental Science & Technology*, 46, 8945–8951. <https://doi.org/10.1021/es3019463>
- Schubert, M., Paschke, A., Lieberman, E., & Burnett, W. C. (2012). Air-water partitioning of  $^{222}\text{Rn}$  and its dependence on water temperature and salinity. *Environmental Science & Technology*, 46, 3905–3911. <https://doi.org/10.1021/es204680n>
- Schubert, M., Petermann, E., Stollberg, R., Gebel, M., Scholten, J., Knöller, K., Lorz, C., Glück, F., Riemann, K., & Weiß, H. (2019). Improved approach for the investigation of submarine groundwater discharge by means of radon mapping and radon mass balancing. *Water*, 11(749). <https://doi.org/10.3390/w11040749>
- Schwartz, F. W., & Zhang, H. (2003). *Fundamentals of Ground Water*. John Wiley & Sons, Inc.
- Sebestyen, S. D., & Schneider, R. L. (2001). Dynamic temporal patterns of nearshore seepage flux in a headwater Adirondack lake. *Journal of Hydrology*, 247, 137–150. [https://doi.org/10.1016/S0022-1694\(01\)00377-8](https://doi.org/10.1016/S0022-1694(01)00377-8)
- Seibert, S. L., Holt, T., Reckhardt, A., Ahrens, J., Beck, M., Pollmann, T., Giani, L., Waska, H., Böttcher, M. E., Greskowiak, J., & Massmann, G. (2018). Hydrochemical evolution of a freshwater lens below a barrier island (Spiekeroog, Germany): The role of carbonate mineral reactions, cation exchange and redox processes. *Applied Geochemistry*, 92, 196–208. <https://doi.org/10.1016/j.apgeochem.2018.03.001>



- Shi, X., Ye, M., Curtis, G. P., Miller, G. L., Meyer, P. D., Kohler, M., Yabusaki, S., & Wu, J. (2014). Assessment of parametric uncertainty for groundwater reactive transport modeling. *Water Resources Research*, 50(5), 4416–4439. <https://doi.org/10.1002/2013WR013755>
- Sibson, R. (1981). A brief description of natural neighbor interpolation. In V. Barnett (Ed.), *Interpreting Multivariate Data* (pp. 21–36). Wiley.
- Smith, C. G., Cable, J. E., Martin, J. B., & Roy, M. (2008). Evaluating the source and seasonality of submarine groundwater discharge using a radon-222 pore water transport model. *Earth and Planetary Science Letters*, 273, 312–322. <https://doi.org/10.1016/j.epsl.2008.06.043>
- Smith, M. B. (2003). *The hydrogeology and hydraulics of artesian springs in Canterbury*. University of Canterbury. <https://ir.canterbury.ac.nz/handle/10092/7890>
- Spigel, R. (2009). *Salinity balance model for Lake Ellesmere/Te Waihora and results from salinity – temperature surveys* (CHC2009-174). National Institute of Water & Atmospheric Research Ltd. <https://api.ecan.govt.nz/TrimPublicAPI/documents/download/2302389>
- Stewart, M., & Morgenstern, U. (2001). Age and source of groundwater from isotope tracers. In M. R. Rosen & P. A. White (Eds.), *Groundwaters of New Zealand* (pp. 161–183). New Zealand Hydrological Society.
- Stewart, M. K. (2012). A 40-year record of carbon-14 and tritium in the Christchurch groundwater system, New Zealand: Dating of young samples with carbon-14. *Journal of Hydrology*, 430–431, 50–68. <https://doi.org/10.1016/j.jhydrol.2012.01.046>
- Stewart, M. K., Cox, M. A., James, M. R., & Lyon, G. L. (1983). *Deuterium in New Zealand rivers and streams* (Report No. INS-R-320). Institute of Nuclear Sciences (DSIR), New Zealand. [https://inis.iaea.org/collection/NCLCollectionStore/\\_Public/16/070/16070830.pdf?r=1](https://inis.iaea.org/collection/NCLCollectionStore/_Public/16/070/16070830.pdf?r=1)
- Stieglitz, T. (2005). Submarine groundwater discharge into the near-shore zone of the Great Barrier Reef, Australia. *Marine Pollution Bulletin*, 51(51–59). <https://doi.org/10.1016/j.marpolbul.2004.10.055>
- Stieglitz, T. C., van Beek, P., Souhaut, M., & Cook, P. G. (2013). Karstic groundwater discharge and seawater recirculation through sediments in shallow coastal Mediterranean lagoons, determined from water, salt and radon budgets. *Marine Chemistry*, 156, 73–84. <https://doi.org/10.1016/j.marchem.2013.05.005>
- Stumpp, C., Ekdal, A., Gönenc, I. E., & Maloszewski, P. (2014). Hydrological dynamics of water sources in a Mediterranean lagoon. *Hydrology and Earth System Sciences*, 18, 4825–4837. <https://doi.org/10.5194/hess-18-4825-2014>
- Su, N., Burnett, W. C., MacIntyre, H. L., Liefer, J. D., Peterson, R. N., & Viso, R. (2014). Natural radon and radium isotopes for assessing groundwater discharge into Little Lagoon, AL: Implications for harmful algal blooms. *Estuaries and Coasts*, 37, 893–910. <https://doi.org/10.1007/s12237-013-9734-9>
- Tait, D. R., Santos, I. R., Erler, D. V., Befus, K. M., Cardenas, M. B., & Eyre, B. D. (2013). Estimating submarine groundwater discharge in a South Pacific coral reef lagoon using different radioisotope and geophysical approaches. *Marine Chemistry*, 156, 49–60. <https://doi.org/10.1016/j.marchem.2013.03.004>
- Tamborski, J., van Beek, P., Rodellas, V., Monnin, C., Bergsma, E., Stieglitz, T., Heilbrun, C., Cochran, J. K., Charbonnier, C., Anschutz, P., Bejannin, S., & Beck, A. (2019). Temporal variability of lagoon–sea water exchange and seawater circulation through a Mediterranean barrier beach. *Limnology and Oceanography*, 64, 2059–2080. <https://doi.org/10.1002/lno.11169>
- Tamborski, J. J., Rogers, A. D., Bokuniewicz, H. J., Cochran, J. K., & Young, C. R. (2015). Identification and quantification of diffuse fresh submarine groundwater discharge via airborne thermal infrared remote sensing. *Remote Sensing of Environment*, 171, 202–217. <https://doi.org/10.1016/j.rse.2015.10.010>
- Taniguchi, M., Dulai, H., Burnett, K. M., Santos, I. R., Sugimoto, R., Stieglitz, T., Kim, G., Moosdorf, N., & Burnett, W. C. (2019). Submarine groundwater discharge: Updates on its measurement techniques, geophysical drivers, magnitudes, and effects. *Frontiers in Environmental Science*, 7(141). <https://doi.org/10.3389/fenvs.2019.00141>
- Tellinghuisen, J. (2001). Statistical error propagation. *Journal of Physical Chemistry A*, 105, 3917–3921. <https://doi.org/10.1021/jp003484u>

- Tirado-Conde, J., Engesgaard, P., Karan, S., Müller, S., & Duque, C. (2019). Evaluation of temperature profiling and seepage meter methods for quantifying submarine groundwater discharge to coastal lagoons: Impacts of saltwater intrusion and the associated thermal regime. *Water*, 11(1648). <https://doi.org/10.3390/w11081648>
- Tommasone, F. P., De Francesco, S., Cuoco, E., Verrengia, G., Santoro, D., & Tedesco, D. (2011). Radon hazard in shallow groundwaters II: Dry season fracture drainage and alluvial fan upwelling. *Science of the Total Environment*, 409(18), 3352–3363. <https://doi.org/10.1016/j.scitotenv.2011.05.039>
- Trigg, M. A., Cook, P. G., & Brunner, P. (2014). Groundwater fluxes in a shallow seasonal wetland pond: The effect of bathymetric uncertainty on predicted water and solute balances. *Journal of Hydrology*, 517, 901–912. <https://doi.org/10.1016/j.jhydrol.2014.06.020>
- Tuccimei, P., Salvati, R., Capelli, G., Delitala, M. C., & Primavera, P. (2005). Groundwater fluxes into a submerged sinkhole area, Central Italy, using radon and water chemistry. *Applied Geochemistry*, 20, 1831–1847. <https://doi.org/10.1016/j.apgeochem.2005.04.006>
- Ünlü, S., & B., A. (2017). Evaluation of sediment contamination by monoaromatic hydrocarbons in the coastal lagoons of Gulf of Saros, NE Aegean Sea. *Marine Pollution Bulletin*, 118, 442–446. <https://doi.org/10.1016/j.marpolbul.2017.03.033>
- Vainu, M., Terasmaa, J., Vaasma, T., & Vandel, E. (2014, 11–13 September, 2014). *Groundwater seepage patterns in a closed-basin lake before and after an increase in groundwater pumping rates from an unconfined aquifer in the Kurtna Kame Field, Estonia*. 2nd International Conference - Water resources and wetlands, Tulcea, Romania. <http://www.limnology.ro/water2014/proceedings.html>
- Valentine, E. M. (1988). *Estimates of seepage flow through Kaitorete Spit: Report to the North Canterbury Catchment Board*.
- Viezzoli, A., Tosi, L., Teatini, P., & Silvestri, S. (2010). Surface water–groundwater exchange in transitional coastal environments by airborne electromagnetics: The Venice Lagoon example. *Geophysical Research Letters*, 37(1). <https://doi.org/10.1029/2009GL041572>
- Vincent, C. (2005). *Hydrogeology of the Upper Selwyn Catchment*. University of Canterbury. <https://ir.canterbury.ac.nz/handle/10092/1137>
- Volpi, C. M. (2014). *An Investigation of Coastal Groundwater Discharge and Associated Nutrient Inputs Using Electrical Resistivity, Temperature, and Geochemical Tracers in Pescadero Lagoon, California*. San Jose State University. [http://scholarworks.sjsu.edu/etd\\_theses/4443](http://scholarworks.sjsu.edu/etd_theses/4443)
- Wang, X., & Du, J. (2016). Submarine groundwater discharge into typical tropical lagoons: A case study in eastern Hainan Island, China. *Geochemistry, Geophysics, Geosystems*, 17, 4366–4382. <https://doi.org/10.1002/2016GC006502>
- Williams, H. (2010). *Groundwater resources in the Te Waihora/Lake Ellesmere catchment: Management issues and options* (R10/05). Environment Canterbury. <http://citeseerx.ist.psu.edu/viewdoc/download?doi=10.1.1.799.6725&rep=rep1&type=pdf>
- Winter, T. C., Harvey, J. W., Franke, O. L., & Alley, W. M. (1998). *Ground Water and Surface Water: A Single Resource* (US Geological Survey Circular 1139) (Circular, Issue). <https://doi.org/10.3133/cir1139>
- Woessner, W. W. (2000). Stream and fluvial plain ground water interactions: Rescaling hydrogeologic thought *Ground Water*, 38(3), 423–429. <https://doi.org/10.1111/j.1745-6584.2000.tb00228.x>
- Young, M. B., Gonnea, M. E., Fong, D. A., Moore, W. S., Herrera-Silveira, J., & Paytan, A. (2008). Characterizing sources of groundwater to a tropical coastal lagoon in a karstic area using radium isotopes and water chemistry. *Marine Chemistry*, 109, 377–394. <https://doi.org/10.1016/j.marchem.2007.07.010>
- Zappa, C. J., Raymond, P. A., Terray, E. A., & McGillis, W. R. (2003). Variation in surface turbulence and the gas transfer velocity over a tidal cycle in a macro-tidal estuary. *Estuaries*, 26(6), 1401–1415. <https://doi.org/10.1007/BF02803649>